Mechanical Properties of Random Discontinuous Fiber Composites Manufactured from Wetlay Process

by

Yunkai Lu

Thesis submitted to the Faculty of the Virginia Polytechnic Institute and State University
in partial fulfillment of the requirements for the degree of

Master of Science
in
Engineering Mechanics

A. C. Loos, Chairman
M. W. Hyer
R. C. Batra

August 6, 2002
Blacksburg, Virginia

Key Words: wetlay process, random, discontinuous, fiber reinforced composite, micromechanics, molding cycle

Mechanical Properties of Random Discontinuous Fiber Composites Manufactured from Wetlay Process

Yunkai Lu

(Abstract)

The random discontinuous fiber composite has uniform properties in all directions. The wetlay process is an efficient method to manufacture random discontinuous thermoplastic preform sheets that can be molded into random composite plaques in the hot-press. Investigations were done on the molding parameters that included the set-point mold pressure, set-point mold temperature and cooling methods. The fibers used in the study included glass and carbon fiber. Polypropylene (PP) and Polyethylene Terephthalate (PET) were used as the matrix.

Glass/PP and Glass/PET plaques that had fiber volume fractions ranging from 0.05 to 0.50 at an increment of 0.05 were molded. Both tensile and flexural tests were conducted. The test results showed a common pattern, i.e., the modulus and strength of the composite increased with the fiber volume fraction to a maximum and then started to descend. The test results were analyzed to find out the optimal fiber volume fraction that yielded the maximum modulus or strength. Carbon/PET composites plaques were also molded to compare their properties with Glass/PET composite at similar fiber volume fractions. Micrographs were taken of selected specimens to examine the internal structure of the material.

Existing micromechanics models that predict the tensile modulus or strength of random fiber composites were examined. Predictions from some of the models were compared with test data.

Acknowledgments

I would like to thank my advisor, Professor A. C. Loos for giving me the opportunity to join in this project and providing his guidance for my study and research. Also, I want to thank professor R. C. Batra and M. W. Hyer for being my committee members.

The help of Joe Price-O'Brien, manager of the Virginia Tech – DuPont Random Wetlay Composites Laboratory is much appreciated. My thanks also go to Bob Simonds and George Lough for their help and expertise during the mechanical testing. I would also like to thank Joe Thompson for his help during my earlier time here and Robert Stephane for providing part of the Carbon/PET data.

Finally, I would like to take this opportunity to thank my parents for always supporting me with their love.

Table of Contents

List of Figures

List of Tables

Chapter 1. Introduction

Fiber-reinforced composites have very high strength to weight and stiffness to weight ratios. Other significant benefits of composites are excellent durability and corrosion resistance, good fatigue behavior and dimensional stability. Commonly used reinforcing fiber materials include metals, ceramics, glasses and carbon. The fiber can be in continuous or discontinuous forms. This investigation focuses on randomly distributed, discontinuous fiber reinforced composites manufactured from the wetlay process.

Fibers play the role of reinforcement in the composite. The performance of the composite is determined by factors such as fiber length (aspect ratio), fiber orientation, the matrix's ability to adhere to the fibers and processing condition, etc. The detailed discussions about the properties of fiber-reinforced composites can be found in a lot of literature such as reference [1,2,3]. They are used a lot in construction, aerospace applications, biomedical and automotive industry. Typical uses of fiber-reinforced composites also include some of the most advanced sports equipments such as a racing bicycle frame and body parts of race cars.

While there are a lot of traditional ways to make the fiber reinforced composites, such as injection molding, a method introduced in this study is called wetlay process. The idea was proposed by inventor Gregory P. Weeks in his patent [4]. It provides a way to make composite of highly homogeneous distribution of the glass fiber and the

thermoplastic resin matrix. In this method the glass fiber and the resin fibers are dispersed in water to form a slurry. The slurry is deposited on a wire screen and then dewatered and dried by passing an oven before a preform sheet is obtained.

Layers of the preform thermoplastic sheets made from the wetlay process are heated to above the melting temperature of the resin under pressure in a hot press mold where the resin is melted. Then the mold is cooled down and a random fiber reinforced composite plaque is produced.

The hot press molding machine is programmed to work by computer code. There are many parameters that affect the molding process. For instance, a high pressure is the prerequisite to make a well-consolidated composite plaque. But a much too high mold pressure will cause excessive resin flow and leakage. One way to determine the optimal molding parameters is to make composite plaques under different molding conditions. The plaques can then be tested and the results will show under what kind of molding parameters the highest mechanical properties can be achieved. The molding parameters that can be varied include set-point mold pressure, set-point mold temperature and cooling methods.

One significant difference between the properties of random discontinuous fiber composite and those of unidirectional continuous fiber reinforced composite is that the modulus or strength of the former reaches a maximum as the fiber volume fraction increases and then starts to decrease. For the latter, the modulus and strength increase with the fiber volume fraction. The fiber volume fraction at which the highest modulus or strength is achieved is of great interest for the random fiber composites. This optimal fiber volume fraction varies for different types of composites. For a certain type of composite, the value is usually different for modulus and strength. The tensile and flexural tests are conducted to determine this optimal fiber volume fraction.

Because of the widely use of fiber reinforced composites, people want to have some theoretical base level of their mechanical properties with which testing data can be compared. Models on random fiber composite were reviewed in this study. Comparisons were made between the predictions from the models and test data.

Chapter 2. Literature Review

There have been many micromechanical theories and models developed to predict the strength and stiffness of fiber-reinforced composites. Most of the work has focused on continuous, unidirectional composites. Theoretical models such as the Halpin-Tsai [7, 8] model have been developed and are able to accurately predict the strength or stiffness of continuous fiber composites.

In the present study, random, discontinuous fiber composites are investigated. A few micromechanical models have been established for discontinuous fiber composites.

2.1 Halpin-Tsai Equation

The Halpin-Tsai equations [7,8] use the mechanical properties of the fiber and the matrix to calculate the properties of the composite. The equation can be expressed in a common form

$$\frac{P}{P_m} = \frac{1 + \zeta \eta V_f}{1 - \eta V_f} \tag{2.1}$$

where

$$\eta = \frac{\frac{P_f}{P_m} - 1}{\frac{P_f}{P_m} + 1} \tag{2.2}$$

Here, P represents any one of the composite moduli listed in Table 2.1 [9]. P_f and P_m are the corresponding moduli of the fiber and matrix respectively. ζ is a parameter that depends on the particular elastic property being considered.

Table 2.1. Traditional Halpin-Tsai parameters for short-fiber composites

P	P_f	P_m	ζ	Comments
E_{11}	E_f	E_m	$2(l/d)$	Longitudinal modulus
E_{22}	E_f	E_m	2	Transverse modulus
G_{12}	G_f	G_m	1	Longitudinal shear modulus

Note: (l/d) is the fiber aspect ratio.

Based on the predictions of E_{11} and E_{22}, theories were proposed to estimate the moduli of the random fiber composite that used the same fiber/resin and had the same fiber volume fraction. The models are shown in Section 2.3.

Nielson [10] modified the Halpin-Tsai model in order to predict the modulus and strength of random, discontinuous fiber composites as follows

$$E_c = E_m\left(\frac{1 + A\eta V_f}{1 - \eta\psi V_f}\right) \tag{2.3}$$

$$T_c = T_m\left(\frac{1 + A\eta^* V_f}{1 - \eta^*\psi V_f}\right) \tag{2.4}$$

where

$$\psi = 1 + \left(\frac{1 - \phi_{\max}}{\phi_{\max}^2}\right)V_f \tag{2.5}$$

$$A = K - 1 = 2l / d \tag{2.6}$$

$$K = 1 + 2l / d \tag{2.7}$$

$$\eta = \frac{E_f / E_m - 1}{E_f / E_m + A} \tag{2.8}$$

$$\eta^* = \frac{T_f / T_m - 1}{T_f / T_m + A} \tag{2.9}$$

Here E_c, E_f and E_m are the moduli of the composite, fiber and matrix, respectively. T_c, T_f and T_m are the strength of the composite, fiber and matrix, respectively. Eq. (2.5) and Eq. (2.6) include the parameter $\phi_{\max}$, which is the maximum packing fraction of the reinforcement. For random packing of fibers, $\phi_{\max} = 0.82$. Finally, l / d is the fiber aspect ratio.

2.2 Shear-Lag Model

The shear lag model [11] is a commonly used micromechanics model for oriented short-fiber composites. It is often used to predict the longitudinal modulus E_{11}. The model considers a single fiber of length l and radius r_f encapsulated in a concentric cylindrical shell of matrix having radius *R*. The following expression is obtained for the longitudinal modulus

$$E_{11} = \eta_l V_f E_f + (1 - V_f) E_m \tag{2.10}$$

where

$$\eta_l = 1 - \frac{\tanh(\frac{\beta l}{2})}{\frac{\beta l}{2}} \tag{2.11}$$

and

$$\beta = (\frac{H}{\pi r_f^2 E_f})^{\frac{1}{2}} \tag{2.12}$$

$$H = \frac{2\pi G_m}{\ln(\frac{R}{r_f})} \tag{2.13}$$

$$R = r_f \sqrt{\frac{K_R}{V_f}} \tag{2.14}$$

Here, E_f and E_m are the moduli of the fiber and matrix, respectively. G_m is the shear modulus of the matrix and η_l is a length-dependent efficiency factor. In Eq. (2.14), K_R is a constant and is usually chosen to be one of the values in Table 2.2. Different choices of K_R give a slightly different value of η_l, and, therefore a slightly different value of E_{11}. Larger values of K_R yield lower values of E_{11}. A modified shear model for discontinuous composites can be found in reference [12].

Table 2.2. Different choices of K_R for shear lag model [9]

Fiber Packing	K_R
Cox	$2\pi / \sqrt{3} = 3.628$
Composite Cylinders	1
Hexagonal	$\pi / 2\sqrt{3} = 0.907$
Square	$\pi / 4 = 0.785$

2.3 Theories for Random Fiber Composites Based on the Calculated Properties of Unidirectional Fiber-Reinforced Composites

It has been shown that the mechanical properties of the reinforcement fiber and the matrix can be used to calculate the properties of the unidirectional composite. This naturally leads to one question—can the properties of the random fiber composite also be calculated from the properties of the corresponding unidirectional composites?

The in-plane modulus of a random fiber composite was proposed by Cox [11] to be

$$E = \frac{1}{3} E_{11} \tag{2.15}$$

and by Loewenstein [13] to be

$$E = \frac{3}{8} E_{11} \tag{2.16}$$

and by Tsai and Pagano [14] to be

$$E = \frac{3}{8} E_{11} + \frac{5}{8} E_{22} \tag{2.17}$$

Although Eq.(2.15) to Eq. (2.17) have very simple forms, the predictions are only good at very low fiber volume fractions. At high fiber volume fractions, the predicted modulus is much higher than measured. Blumentritt [15] explained that this was caused by the increase in concentration of defects within the composite as the fiber content increases.

2.4 Fiber Efficiency Factor Approach

Blumentritt and Cooper [15] proposed a method to calculate the ultimate strength and the Young's modulus of the composite in the plane of the fibers. Their results are summarized below

$$\sigma_{uc} = K_{\sigma}\sigma_{uf}V_f + \sigma_m^{'}(1-V_f) \tag{2.18}$$

$$E_c = K_E E_f V_f + E_m(1-V_f) \tag{2.19}$$

where, σ_{uc} is the ultimate strength of the composite, K_{σ} is the fiber efficiency factor for strength, σ_{uf} is the ultimate strength of the fiber, V_f is the fiber volume fraction, $\sigma_m^{'}$ is the matrix stress at the fracture strain of the composite, E_c is the modulus of the composite, K_E is the fiber efficiency factor for modulus, E_f is the modulus of the fiber and E_m is the matrix modulus.

Blumentritt and Cooper [15] measured the mechanical properties of discontinuous fiber reinforced thermoplastics fabricated using six types of reinforcement fiber and five types of thermoplastics matrix resin. The fibers used were Dupont type 702 nylon 6/6, Dupont type 73 poly (ethylene terephthalate), Kuralon poly (vinyl alcohol), Owens-Cornings type 801 E-glass, Dupont Kevlar-49, and Union Carbide Thornel 300 graphite. The poly (vinyl alcohol) fibers were 5 mm in length and the glass fibers were 6.3 mm in length. The other fibers were all 9.5 mm in length. The five thermoplastics used were Dupont Surlyn 1558 type 30 ionomer, Dupont Alathon 7140 high-density polyethylene, Huels grade L-1901 nylon 12, General Electric Lexan

105-111 polycarbonate and Dupont Lucite 47 poly (methyl methacrylate) (PMMA). All together thirty different combinations of fiber/resin were tried.

The specimens in their study were made by a hand lay-up process and then compression molded. The molded panels had a thickness of about 1 mm. Tensile tests were conducted at an elongation rate of 5.1 mm/min to determine K_E and K_σ.

From the measurements, K_E had a range of 0.44 to 0.06, while K_σ had a range of 0.25 to 0. The average fiber efficiency factors were 0.19 for modulus and 0.11 for strength.

Average values of 0.43 and 0.25 for K_E and K_σ, respectively were reported for similar composites with unidirectional fiber orientation [16]. They concluded that for similar materials, the fiber efficiency factor of unidirectional fiber composites was approximately twice that of random-in-plane composites.

2.5 Christensen and Waals' Model

Christensen and Waals [17] examined the behavior of a composite system with a three-dimensional random fiber orientation. Both fiber orientation and fiber-matrix interaction effects were considered. For low fiber volume fractions, the modulus of the 3-D composite was estimated to be

$$E_{3-D} \approx \frac{c}{6} E_f + [1 + (1 + \nu_m)c] E_m \qquad (2.20)$$

where, c < 0.2 and ν_m is the Poisson's ratio of the matrix. c is the volume

concentration of the fiber phase, which is equivalent to the fiber volume fraction.

For a state of plane stress, the modulus is given as

$$E \approx \frac{c}{3} E_f + (1+c) E_m \qquad (2.21)$$

where, c < 0.2.

Comparisons were made between the predictions given by Eq.(2.21) and data reported by Lee [18]. It was found that at low fiber volume fractions, predictions from Eq.(2.21) were within a range of 0 ~ +15% higher than the test data. The difference between the prediction and test data was attributed to "partially ineffective bonds and/or end effects for the chopped fibers".

2.6 Approximation Model by Manera

Manera [19] proposed approximate equations to predict the elastic properties of randomly oriented short fiber-glass composites. The invariant properties of composites defined by Tsai and Pagano [20] were used along with Puck's micromechanic formulation [19]. Manera made a few assumptions and simplified Puck invariants equations. The assumptions included high fiber aspect ratio (>300), two-dimensional random distribution of fibers and treatment of randomly oriented discontinuous fiber composites as laminates with an infinite number layers oriented in all directions. The approximate equations can be expressed as

$$\overline{E} = V_f \left(\frac{16}{45} E_f + 2E_m\right) + \frac{8}{9} E_m \qquad (2.22)$$

$$\overline{G} = V_f(\frac{2}{15}E_f + \frac{3}{4}E_m) + \frac{1}{3}E_m \quad (2.23)$$

$$\overline{\nu} = \frac{1}{3} \quad (2.24)$$

where, V_f is the fiber volume fraction, ν_m is the Poisson's ratio of the matrix, E_m is the modulus of the matrix, E_f is the modulus of the fiber, $\overline{E}$ and $\overline{G}$ are the tensile (flexural) and shear moduli of the composite, respectively and $\overline{\nu}$ is Poisson's ratio of the composite.

It can be seen from Eq.(2.22)-Eq.(2.24) that $\overline{E}$, $\overline{\nu}$, and $\overline{G}$ satisfy the relationship $\overline{G} = \frac{\overline{E}}{2(1+\overline{\nu})}$. In order to get adequate precision in the results, Manera chose V_f to be within the range $0.1 \le V_f \le 0.4$ and E_m within the range $2GPa \le E_m \le 4GPa$.

Predictions of composite modulus by Eq.(2.22) were compared with test data [19]. The constituent properties of the composites in the tests were 5 cm chopped glass fiber with $E_f = 73GPa$, $\nu_f = 0.25$ and polyester resin with $E_m = 2.25GPa$ and $\nu_m = 0.40$. The differences between the predictions and test data were less than 5%.

2.7 Fiber Density Function — Pan's Model

Pan [21] developed a new approach to predict the elastic constants of randomly oriented fiber composites. He started with the well-known "rule of mixtures" for an unidirectional composite to calculate composite strength, σ_c

$$\sigma_c = \sigma_f A_f + \sigma_m A_m = \sigma_f V_f + \sigma_m V_m \qquad (2.25)$$

and composite modulus, E_c

$$E_c = E_f V_f + E_m V_m \qquad (2.26)$$

Here, V_f is the fiber volume fraction and A_f is the fiber area fraction. $A_f = V_f$ for the unidirectional case, as reflected in Eq. (2.25).

The basic idea of Pan's theory was to construct a relationship between the fiber volume fraction V_f and the fiber area fraction A_f when fibers are not unidirectionally aligned.

Pan introduced a probability density function to specify the fiber orientation that was defined by a pair of angles (Θ, Φ) in the spatial curvilinear coordinate system. Then the fiber area fraction A_f is related to the fiber volume fraction V_f through another probability function

$$A_f(\Theta, \Phi) = \Omega(\Theta, \Phi) V_f \qquad (2.27)$$

where, $\Omega(\Theta, \Phi)$ is the value of the probability density function in direction (Θ, Φ).

The final result of Pan's approach is an expression for composite modulus

$$E_c(\Theta, \Phi) = E_f \Omega(\Theta, \Phi) V_f + E_m (1 - \Omega(\Theta, \Phi) V_f) \qquad (2.28)$$

For a two-dimensional random case, the equation can be simplified and the tensile

modulus can be expressed as follows

$$E_c^{2D} = E_f \frac{V_f}{\pi} + E_m(1 - \frac{V_f}{\pi}) \tag{2.29}$$

and the Poisson's ratio by the following expression

$$\nu_c^{2D} = \nu_f \frac{V_f}{\pi} + \nu_m(1 - \frac{V_f}{\pi}) \tag{2.30}$$

For the case of three-dimensional random fiber orientation, the tensile modulus is given by

$$E_c^{3D} = E_f \frac{V_f}{2\pi} + E_m(1 - \frac{V_f}{2\pi}) \tag{2.31}$$

and, Poisson's ratio by the equation

$$\nu_c^{3D} = \nu_f \frac{V_f}{2\pi} + \nu_m(1 - \frac{V_f}{2\pi}) \tag{2.32}$$

Unlike Christensen's theory, Pan's model has no restriction on the fiber volume fraction. Also, the theory can be applied to cases other than random fiber orientation as long as the fiber orientation density function is available.

Pan compared the predictions from Eq. (2.29) with those from Christensen [17] and Manera [19]. Published experimental data were used as the bases for comparison. The results indicated that at low volume fractions, the predictions by Pan's model "agree at least as well with the experimental data as those by other theories compared". He also pointed out that complete randomness of fiber orientation was more difficult to

achieve as the fiber volume fraction increased.

2.8 Modified Rule of Mixtures

The rule of mixtures does not work for random fiber composites since it does not take into account the fiber orientation and fiber-matrix interaction effects. Based on these considerations, Curtis et al. [22] modified the rule of mixtures into the following form:

$$E_c = \chi_1 \chi_2 E_f V_f + E_m V_m \tag{2.33}$$

$$\sigma_{cu} = \chi_3 \chi_4 V_f \sigma_{fu} + \sigma_{mu} V_m \tag{2.34}$$

Eq.(2.33) and Eq.(2.34) are similar to Eq.(2.18) and Eq.(2.19) and the definitions of $E_c, E_f, E_m, V_m, \sigma_{cu}$ were previously defined in Eq.(2.18) and Eq.(2.19). σ_{fu} is the fiber ultimate strength, σ_{mu} is the matrix ultimate strength, χ_1 and χ_3 represent the effect of fiber orientation. The effect of fiber length or effective length of fiber that carries load is represented by χ_2 and χ_4. χ_1 and χ_3 take the value of 3/8 for random-in-plane fiber orientation. For three-dimensional random fiber orientation, the value is taken to be 1/5.

Using Cox's shear lag analysis, Curtis et al. describe χ_2 as

$$\chi_2 = 1 - \frac{\tanh(ns)}{ns} \tag{2.35}$$

where, s is the fiber aspect ratio and n is defined as

$$n^2 = 2\frac{E_m}{E_f(1+\nu_m)\ln\frac{P_f}{V_f}} \tag{2.36}$$

where, ν_m is the Poisson's ratio of the matrix and P_f is the fiber packing factor [22].

Finally, χ_4 is obtained from

$$\chi_4 = 1 - \frac{s_c}{2s} \qquad \text{when} \quad s > s_c \tag{2.37}$$

$$\chi_4 = \frac{s}{2s_c} \qquad \text{when} \quad s < s_c \tag{2.38}$$

where, s_c is the critical fiber aspect ratio and it is determined by dividing the critical fiber length by the fiber diameter.

Eq.(2.33)-Eq.(2.38) can be used to calculate the strength and stiffness of random fiber composites if the Poisson's ratio of the matrix and the matrix yield strength in shear are known. The critical fiber length l_c can be calculated from

$$l_c = \frac{\sigma_f d}{2\tau_y} \tag{2.39}$$

where, d is the fiber diameter.

2.9 Kelly and Tyson's Model

Kelly and Tyson [23] developed a theory to predict the strength of short fiber composites. Basically, it is an extension of the "rule of mixtures" by taking into account the effects of both the fiber length and fiber orientation. The theory is expressed in the following form

$$\sigma_{uc} = \eta_0 \eta_{LS} V_f \sigma_f + \sigma_m V_m \qquad (2.40)$$

where, η_{LS} is the fiber length efficiency factor and η_O is the fiber orientation factor. η_O takes the value of 3/8 for random-in-plane fiber composites.

For the fiber length efficiency factor, Kelly and Tyson used

$$\eta_{LS} = \frac{1}{V_f}\left(\sum_i \left[\frac{L_i V_i}{2L_c}\right] + \sum_j \left[V_j\left(1 - \frac{L_c}{2L_j}\right)\right]\right) \qquad (2.41)$$

where, the first summation includes the contribution of fibers whose length is less than the critical length, and the second summation includes the strength contribution of fibers whose length is above critical length.

One problem associated with Kelly and Tyson's theory is that the estimates of strength are higher than measured [24]. To obtain better agreement with test data, Thomason et al. [25] determined a value of $\eta_O = 0.2$ by fitting η_O to strength data.

2.10 Chen's Equation

Chen [26] established equations that can be used to calculate the strength of random fiber composites from data on the corresponding unidirectional fiber composites. His theory was based on the three failure modes in a continuous fiber reinforced unidirectional composite.

In the theory, θ is defined as the angle between the applied stress and the fiber orientation. For small values of θ, the effective failure mechanism is assumed to be fiber fracture, and the failure occurs when

$$\sigma_\theta \cos^2 \theta = \xi \sigma_L \qquad (0 \le \theta \le \theta_1) \qquad (2.42)$$

where, $\theta_1 = \tan^{-1}(\frac{\tau_m}{\sigma_L})$ and τ_m is the shear strength of the matrix, σ_θ is the strength of the composite with all the fibers aligned at an angle θ to the direction of the applied stress, σ_L is the strength of the composite with fibers all aligned in the direction of the applied stress and ξ is the strength efficiency factor which relates the strength of a discontinuous fiber composite to the strength of a corresponding continuous fiber composite.

At intermediate angles, shear failure occurs at the fiber-matrix interface when

$$\sigma_\theta \sin\theta \cos\theta = \tau_m \qquad (\theta_1 \le \theta \le \theta_2) \qquad (2.43)$$

where, $\theta_2 = \tan^{-1}(\frac{\sigma_m}{\tau_m})$ and σ_m is the strength of the matrix.

At large angles, matrix failure occurs when

$$\sigma_\theta \sin^2 \theta = \sigma_m \qquad (\theta_2 \le \theta \le \frac{\pi}{2}) \qquad (2.44)$$

The strength of the random fiber composite σ is considered to be equal to the strength of corresponding unidirectional composite σ_θ integrated over all the fiber orientation angles θ (from 0^o to 90^o),

$$\sigma = \frac{\int_0^{\frac{\pi}{2}} \sigma(\theta) d\theta}{\int_0^{\frac{\pi}{2}} d\theta} \qquad (2.45)$$

and given by the following equation

$$\sigma = \frac{2\tau_m}{\pi}[2 + \ln \frac{\zeta \sigma_L \sigma_m}{\tau_m^2}] \qquad (2.46)$$

2.11 Prediction Based on Tsai-Hill Criterion

As expressed in Eq. (2.46), Chen obtained a closed form expression for the strength of random fiber composites. However, discontinuities exist at the transition angles using the three different failure modes (Eq.(2.42) to Eq.(2.44)). In order to achieve better agreement, Baxter [27] combined the three equations with the Tsai-Hill criterion for failure

$$(\frac{\sigma_x}{\sigma_L})^2 + (\frac{\sigma_y}{\sigma_T})^2 - \frac{\sigma_x \sigma_y}{\sigma_L^2} + (\frac{\sigma_{xy}}{\tau})^2 = 1 \qquad (2.47)$$

where, σ_x is the stress components parallel to the fiber, σ_y is the stress components perpendicular to the fiber and σ_{xy} is the shear stress component in a two-dimensional problem. The subscript "L" represents "longitudinal" and "T" represents "transverse".

The strength of composite can be obtained by replacing σ_x, σ_y and σ_{xy} in Eq. (2.47) with the expressions in Eq. (2.42) to Eq. (2.44) as follows

$$\sigma(\theta) = [\frac{\cos^4\theta}{\sigma_L^2} + (\frac{1}{\tau^2} - \frac{1}{\sigma_L^2})\sin^2\theta\cos^2\theta + \frac{\sin^4\theta}{\sigma_T^2}]^{\frac{-1}{2}} \qquad (2.48)$$

Then an averaging idea is used by considering the random fiber composite as an infinite numbers of oriented laminate sheets stacked together. The sheets are oriented from 0^o to 180^o with respect to the direction of applied load. The strength σ_c of a composite with randomly oriented fibers can be expressed by the following equation

$$\sigma_c = \frac{1}{\pi}\int_0^{\pi} \sigma(\theta) d\theta \qquad (2.49)$$

where, $\sigma(\theta)$ is expressed by Eq. (2.48).

2.12 Hahn's Model for Progressive Ductile Failure

A rule of mixture equation for strength [28] can be expressed as

$$\overline{X} = \int_0^{\frac{\pi}{2}} h(\theta) X(\theta) d\theta \qquad (2.50)$$

where, $X(\theta)$ represents the failure stress function in terms of θ (the angle between fiber orientation and applied stress) and $h(\theta)$ is the fiber orientation density function.

For the random fiber composite, the fiber orientations are uniformly distributed, therefore the thickness ratios of the unidirectional plies are the same

$$h(\theta) = 2/\pi \qquad (2.51)$$

which results in the following equation for $\overline{X}$, the strength of the random fiber composite

$$\overline{X} = \frac{2}{\pi} \int_0^{\frac{\pi}{2}} X(\theta) d\theta \qquad (2.52)$$

Using the maximum stress failure criteria, Hahn developed the expression

$$\overline{X} = \frac{2}{\pi} [X \int_0^{\frac{\pi}{2}} \frac{d\theta}{\cos^2 \theta} d\theta + S \int_{\theta_1}^{\theta_2} \frac{d\theta}{\sin\theta \cos\theta} + Y \int_{\theta_2}^{\frac{\pi}{2}} \frac{d\theta}{\sin^2 \theta}] \qquad (2.53)$$

where, θ_1 and θ_2 are the intersection angles between various failure mechanisms,

$$\theta_1 = \tan^{-1}(S/X), \quad \theta_2 = \tan^{-1}(Y/S) \qquad (2.54)$$

and X is the on-axis longitudinal strength, Y is the on-axis transverse strength, and S is the on-axis shear strength.

Furthermore, if we define $\alpha = S/Y$, which is the ratio of the shear strength to transverse strength, a close form solution of the integral in Eq.(2.53) can be obtained.

$$\frac{\overline{X}}{Y_t} = \begin{cases} \frac{4}{\pi}\alpha[1+\frac{1}{2}\ln(X/\alpha^2 Y)], \alpha \le (X/Y)^{\frac{1}{2}} \\ \frac{4}{\pi}(X/Y)^{\frac{1}{2}}, \alpha > (X/Y)^{\frac{1}{2}} \end{cases} \tag{2.55}$$

Again, unless relevant experimental data on the unidirectional composite materials are available, it is practically impossible to use Eq.(2.55) to predict the strength of the corresponding random fiber composite.

2.13 Partially Aligned Discontinuous Composites

Kuriger and Alam [29] developed an experimental and theoretical approach for the determination of the strength of partially aligned discontinuous fiber-reinforced composites.

Following the approach of Hahn [28], an expression for the strength of a composite as a function of the angle between the fiber direction and the applied stress was developed

$$\sigma(\theta) = [\frac{\cos^4\theta}{\sigma_L^2} + (\frac{1}{\tau_{LT}^2} + \frac{1}{\sigma_L^2})\sin^2\theta\cos^2\theta + \frac{\sin^4\theta}{\sigma_T^2}]^{-\frac{1}{2}} \tag{2.56}$$

where, σ_L represents the longitudinal tensile strength, σ_T the transverse tensile strength and τ_{LT} the shear strength of the composite material.

An x-ray-diffraction technique was used to obtain the fiber alignment data which was described by a Gaussian distribution. This Gaussian distribution $F(\theta)$ accounting for the fiber orientation is added as a weighting factor into Eq. (2.52), resulting in the following equation for composite strength

$$\sigma_c = 2\int_0^{\frac{\pi}{2}} F(\theta)\sigma(\theta)d\theta \qquad (2.57)$$

From experiments, it was found that

$$F(\theta) = \frac{2.35}{Z\sqrt{2\pi}} e^{-1/2(2.35\theta/Z)^2} \qquad (2.58)$$

where, Z represents the fiber orientation along the preferred axis of the composite samples at various fiber volume fractions. It is determined by applying the above-mentioned x-ray-diffraction method.

The theoretical results were compared with test data of a partially aligned composite made of vapor-grown carbon fiber (VGCF) and polypropylene. Reasonably good agreement between the theoretical prediction and test results was achieved. It was determined that the strength increases with fiber volume fraction up to 17% before descending, probably the results from the incomplete fiber wetting and infiltration of the VGCF.

2.14 Summary of Some Experimental Work on Random Fiber Composites

A study was done on random flax fiber reinforced polypropylene composites made by two different techniques, namely, film-stacking and suspension impregnation [24]. Tensile tests were conducted on the specimens following the ASTM-D 638 standard. The fiber volume fraction of the composite had a range of 0.10 to 0.44. The results showed that the tensile modulus had a maximum at about 0.28 fiber volume fraction. Above that volume fraction, the tensile modulus started to descend and then rose again at 0.44 fiber volume fraction. For the tensile strength, an irregular trend was observed. There seemed to be a lot of fluctuations in the results. The values went up and down before reaching a maximum at 0.44 fiber volume fraction.

Thomason et al. [25, 32] examined the properties of glass fiber-reinforced polypropylene laminates. The fiber weight fraction ranged from 0.03 to 0.40, which corresponded to 0.01 to 0.19 in terms of volume fraction. Also, different fiber lengths from 0.1 mm to 50 mm were tried. Within the range of volume fractions studied, predictions from the Kelly-Tyson model (Section 2.9) correlated well with the experimental data. The modulus/strength of the laminates increased linearly with the fiber weight content up to 0.40. After that the modulus improvement was considerably less due to fiber packing problems that resulted in increasing void content and out of plane fiber orientation.

Baxter [27] studied the strength of metal matrix reinforced with randomly oriented discontinuous graphite fibers. He found that there was a significant strength reduction as the fiber volume fraction become higher. It was also found that if the interfacial

bond is weaker than the matrix, then the strength of the randomly oriented composites could increase only modestly or not at all with the fiber volume fraction. He concluded that for fiber volume fractions higher than 0.3, imperfections in the composite such as clustering of the graphite fibers or spaces between fibers that were not infiltrated by the aluminum matrix and served as debilitating micro-cracks.

Li and Mai [30] obtained experimental data on sisal/polystyrene randomly oriented composites. At fiber weight contents of 0 (pure resin), 0.10, 0.20 and 0.30, the corresponding ultimate tensile strengths were 34.9 MPa, 24.72 MPa, 31.14 MPa and 30.09 MPa, respectively. For the Young's modulus, the values were 390 MPa, 457.4 MPa, 543.3 MPa and 710.7 MPa. It can be seen that the strength of the composite was less than that of the resin. A decrease in strength was observed as the fiber weight fraction increased from 0.20 to 0.30. On the other hand, there was only a modest increase in modulus as the fiber content increased. One of the reasons was believed to be the fiber-fiber interaction at high volume fraction that led to poor dispersion of fibers.

Similar phenomena were observed on the examination of mechanical properties of wood flake/polyethylene composites by Balasuriya et al. [31]. The deduction in strength was concluded to be due to the increase in interactions between flakes fibers that resisted the uniform dispersion of the flakes. SEM micrographs of the high wood flake content composites supported this suggestion.

Although different combinations of fiber/resin were used in the above studies, some common patterns can be seen.

The fiber volume fraction of the random fiber composites was usually less than 0.40. This is the limit that ordinary manufacturing methods can achieve if a good randomness is expected. It is difficult to maintain a random dispersion at high fiber volume fraction.

On the other hand, it has been found by different researchers [24-25, 27, 30-32] that the tensile modulus/strength tends to show only small increase or even decrease at high fiber volume fractions.

Chapter 3. Experimental

3.1 Wetlay Processing

The wetlay process uses the paper making technique. The technique provides a method for achieving a uniform, homogeneous dispersion of reinforcing fibers and thermoplastic resin fibers. The polymer fibers are uniformly distributed within the reinforcing fibers, resulting in products with uniform properties. The wetlay machine is located in the VT-DuPont Random Wetlay Laboratory [33]. A schematic diagram of the wetlay process is shown in Figure 3.1.

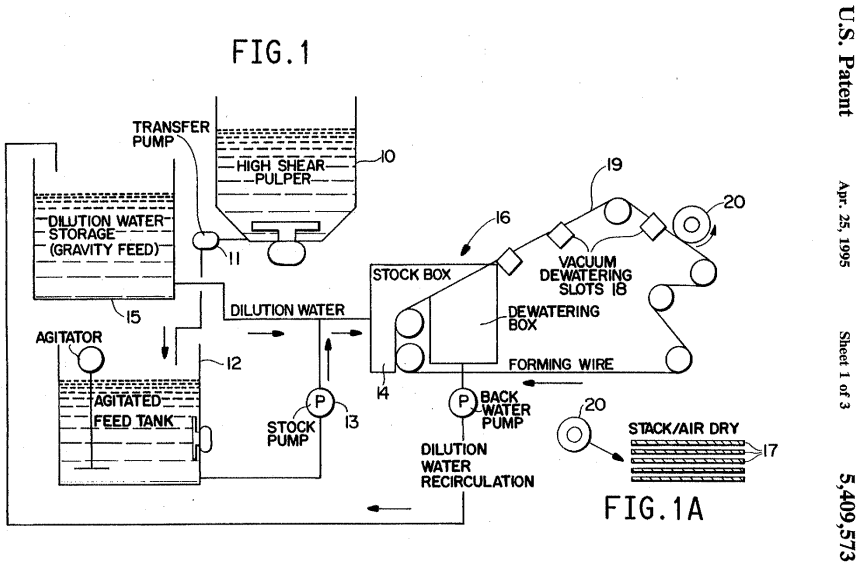

U.S. Patent Apr. 25, 1995 Sheet 1 of 3 5,409,573

Figure 3.1 Schematic diagram of the wetlay process [34]

Referring to Figure 3.1, the main body of the lab equipment consists of a pulper 10, a transfer pump 11, an agitated feed tank 12, the head box 14 of an inclined wire wetlay apparatus 16, a dewatering section 18, a windup spool 20, an 800-liter whitewater tank 15 and two 400-liter stock tanks 12. A 10 feet dryer oven (Figure 3.6) is located next to the wetlay apparatus.

Figure 3.2 Picture of the pulper

In the pulper (Figure 3.2), the reinforcing fibers and the thermoplastic polymer fibers are added to an aqueous solution to create a slurry. Viscosity modifier, surfactant and antifoam are used to get the fiber well dispersed in the slurry.

Figure 3.3 Picture of the stock tank

The slurry is pumped from the pulper via pump 11 into the stock tanks (Figure 3.3).

Each stock tank is equipped with a three-blade variable-speed agitator to maintain the aqueous fiber slurry in suspension until it is ready to be used.

Next, the slurry in the stock tank is pumped to the headbox (Figure 3.4) and further diluted with white water from the white water tank. The 800-liter whitewater tank is used to provide a closed-loop dilution feed into the headbox.

The formation of the random wetlay mat takes place in the headbox of the inclined wire wetlay machine. The slurry is drained through the forming wire and rapidly de-watered by passing over suction slots in the dewatering section. Figure 3.5 shows a close-up view of the preform sheet.

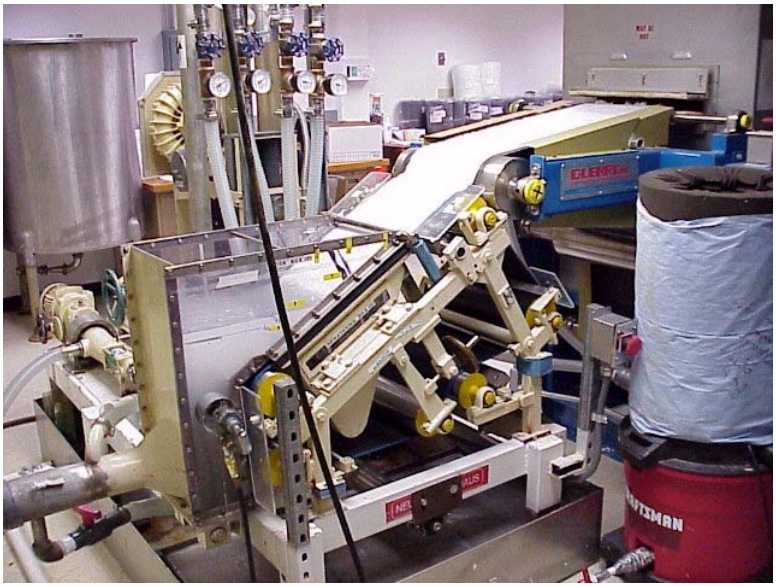

Figure 3.4 Picture of the headbox

Figure 3.5 A close-up view of the preform sheet

Finally, the dewatered mat passes through the Glenro 10-foot convection dryer oven (Figure 3.6) in which the remaining water vaporizes and the resin melts to hold the fibers. Figure 3.7 shows a typical roll of the thermoplastic composite sheet (Glass/PET) made by the wetlay process.

Figure 3.6 Picture of the 10-feet convection dryer oven

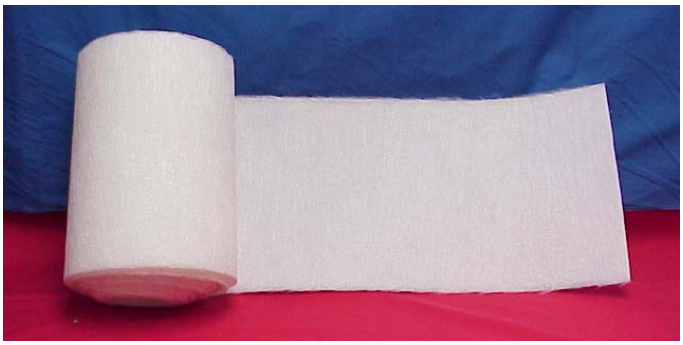

Figure 3.7 A roll of the thermoplastic composite sheet (Glass/PET)

These preform sheets (Figure 3.7) made from the above process will then be stacked and placed into a heated platen press where they are molded into the desired shape. During this process the resin is re-melted. Details of the molding process are talked about in Section 3.4.

3.2 Constituent Materials

The typical properties of the fibers used in the process are listed below:

(1) The one inch and half-inch wet-chop E-glass fibers from PPG (Figure 3.8) have a diameter of about 13.5 μm and a density of 2.59g/cm^3. The tensile modulus is 72.4 GPa.

(2) The one inch wet-chop carbon fiber from Zoltek (Figure 3.9) has a diameter of about 7.2 μm and a density of 1.11g/cm^3. The tensile modulus is 228 GPa.

The typical polymers used are:

(1) Half-inch polypropylene (Figure 3.10) with a density of 0.91g/cm^3 from Montell

(2) Half-inch PET (Polyethylene Terephthalate, Figure 3.11) with a density of 1.35g/cm^3 from Dupont

Figure 3.8 Half-inch glass fiber

Figure 3.9 One-inch carbon fiber

Figure 3.10 Polypropylene resin

Figure 3.11 PET resin

Polypropylene is an economical material. It is light in weight, resistant to stain, and has a low moisture absorption rate. The typical properties of commercial polypropylene can be found in sources [35,36].

PET has a much higher melting point (249 °C, [36]) than polypropylene (174 °C, [35]). It also has a higher glass transition temperature, T_g of 74 °C compared to -17 °C of polypropylene. Both tensile and flexural tests were conducted on the PET resin used in the wetlay process. The test results are shown in Chapter 4.

3.3 Procedures to Make Wetlay Materials

3.3.1 Conversions between Fiber Volume Fraction & Weight Fraction

While it is more convenient to use weight fraction measurements during the wetlay process to make the thermoplastic composite sheet, fiber volume fraction is more widely used in the literature to analyze the mechanical properties of the fiber reinforced composites. Fiber volume fraction is also used in the data analysis in Chapter 4. Therefore, it is necessary to convert the fiber weight fraction to fiber volume fraction, or, vice versa using the following equations

$$WF = \frac{VF \cdot \rho_f}{VF \cdot \rho_f + (1 - VF) \cdot \rho_r} \qquad (3.1)$$

$$VF = \frac{WF \cdot \rho_r}{WF \cdot \rho_r + (1 - WF) \cdot \rho_f} \qquad (3.2)$$

where, WF represents the fiber weight fraction, VF the fiber volume fraction, ρ_f is the density of the fiber and ρ_r is the density of the resin.

As an example, Figure 3.12 shows the relationship between fiber volume fractions and fiber weight fractions for Glass/PP composites.

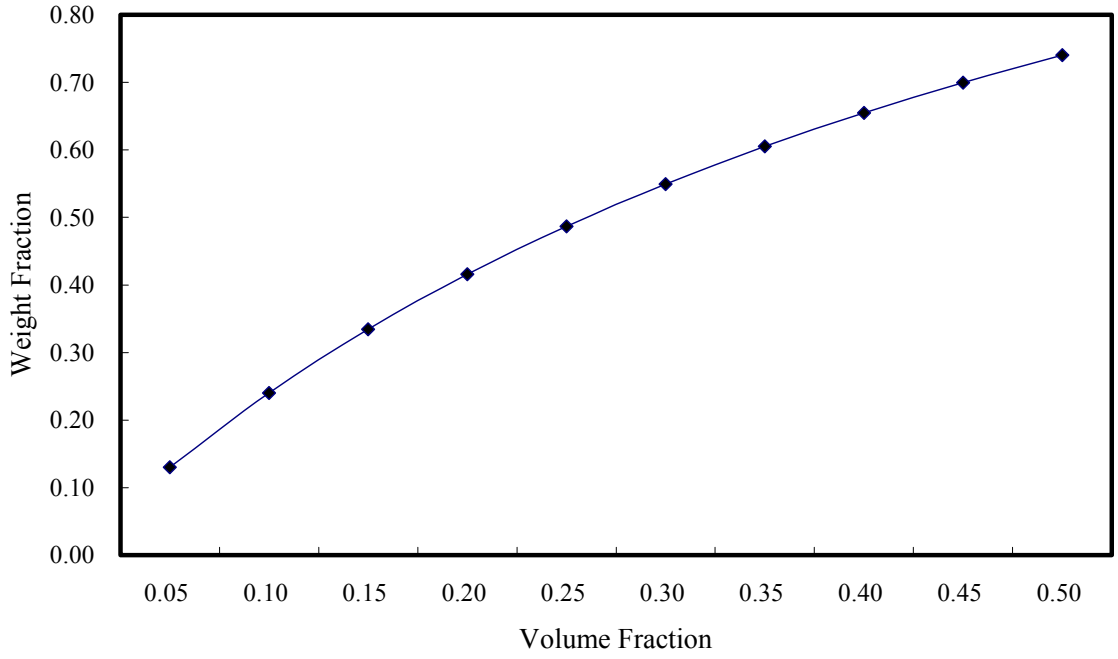

Figure 3.12 Conversion between weight fraction and volume fraction for Glass/PP

3.3.2 Glass/PP Composite Sheet

The detailed procedure of wetlay processing has been introduced in Section 3.1. As an example, we want to make 10 batches of Glass/PP composite sheets with the fiber volume fraction ranging from 0.05 to 0.50 at an increment of 0.05. The ultimate goal is to find out how the change of fiber volume fraction affects the mechanical properties of these materials.

One thousand grams of raw materials (Glass+PP) are used during one process cycle (corresponding to one fiber volume fraction). Since it takes about 100 grams of preform composite sheet to make a plaque, 1000 grams of raw material will guarantee that enough plaques can be made for testing. Figure 3.12 or Eq.(3.1) is used to get the weight fraction of the glass fiber and polypropylene at each fiber volume fraction. Moisture content of the raw material must also be taken into consideration. In this

case, the moisture content for the glass fiber is 11.49% and polypropylene 0.78%. Based on these values, the amount of raw materials needed at each fiber volume fraction is listed in Table 3.1.

Table 3.1 Weight of glass and PP used during one process

Volume Fraction	Weight of Fiber, g	Weight of PP, g
0.05	147.10	876.64
0.10	271.38	765.77
0.15	377.70	670.93
0.20	469.66	588.89
0.25	550.11	517.13
0.30	620.83	454.04
0.35	683.65	398.00
0.40	739.92	347.81
0.45	790.42	302.76
0.50	836.06	262.04

The remaining steps will follow what is described in Section 3.1. One thing to mention is that the PP does not require pre-pulping since it disperses easily into the chemically treated pulper solution. The oven temperature is set at 87 ºC.

To make Glass/PET, Carbon/PP, or Carbon/PET composite sheet, the procedures are similar to what is described above. When PET is used as the resin, it is mixed for 5 minutes in the pulper before the glass (or Carbon) is added so that the PET can completely disperse into the chemically treated pulper solution. The oven temperature is set to 207ºC.

To make Carbon/PP sheets, five hundred grams of the raw materials (Carbon+PP) are used per process cycle. This is because carbon fibers tend to form bundles and tangle under the condition of higher basis weight. Hence, only five hundred grams rather than one thousand grams raw materials are used. The oven temperature is set at 87ºC. However, carbon is added directly to stock tank rather than into the pulper. It is agitated until thoroughly mixed to prevent the formation of fiber bundles.

3.4 Molding Process

3.4.1 Molding Cycle

The fiber reinforced thermoplastic sheets produced from the wetlay process are used to make plaques to evaluate the mechanical properties of the composite. Several layers of the sheets are cut to the dimensions of the mold, stacked to get the required thickness and placed in the mold. The mold is then placed in a heated platen press (Figure 3.13).

Figure 3.13 Heated platen press

The molding process takes between 60 minutes and 100 minutes. The plaques made

from this process are 151.8 mm in length and 151.8 mm in width with a thickness between 2.5 mm to 3.8 mm. Each plaque will be cut into specimens for tensile and flexural testing.

Figure 3.14 shows the change of molding temperatures versus time during the consolidation of a Glass/PET (Dupont SC125 material—25% weight glass fiber + 75% weight PET) plaque. Figure 3.15 shows the change of molding pressure versus time during the consolidation of the plaque.

A typical molding process for a Dupont SC125 Glass/PET plaque consists of the following procedures:

(1) Increase the consolidation pressure to 82.74 kPa (12 psi).
(2) Heat the top and bottom platens until the mold temperature reaches 250°C (the set point mold temperature). During this process, the hydraulic pressure is held constant.
(3) Increase the consolidation pressure to 5.06 MPa.
(4) Hold the consolidation pressure constant and stop heating the platens. Turn on the cooling air to cool down the mold.
(5) When the mold temperature drops to 100°°C, the cooling water is turned on.
(6) When the mold temperature drops even more to a certain value, say, 30°C or room temperature, the cooling water is turned off.

Because different types of resin have different melting points, the set-point molding temperatures and the molding pressures have to be adjusted accordingly. Table 3.2 shows the set point mold temperature for four types of material combination. Shown in Figure 3.16 are some plaques made from the hot-press molding.

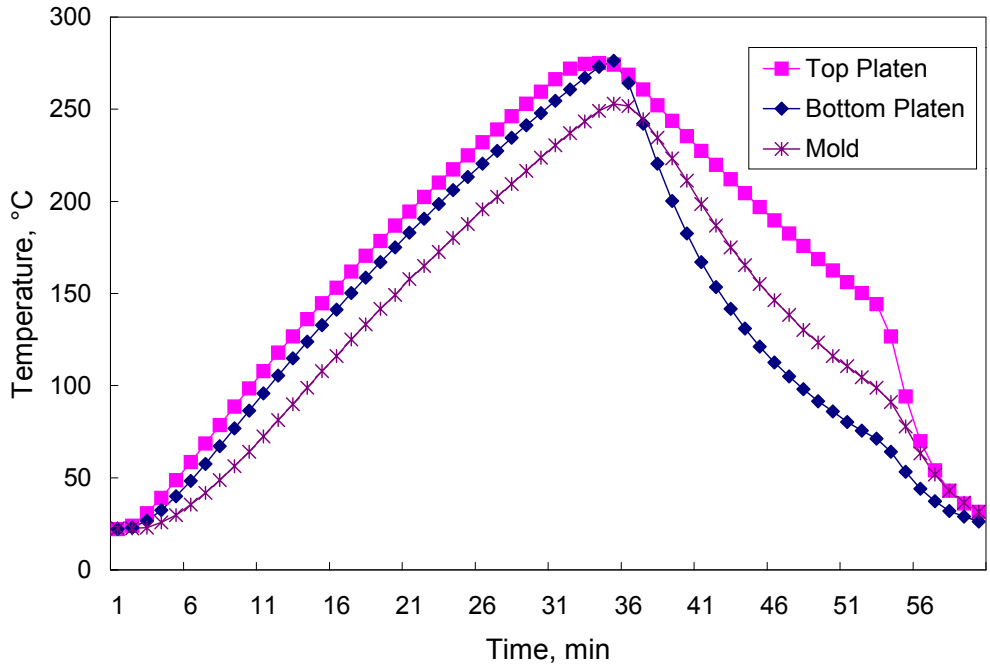

Figure 3.14 Molding temperature vs. time for a Glass/PET (SC125) plaque

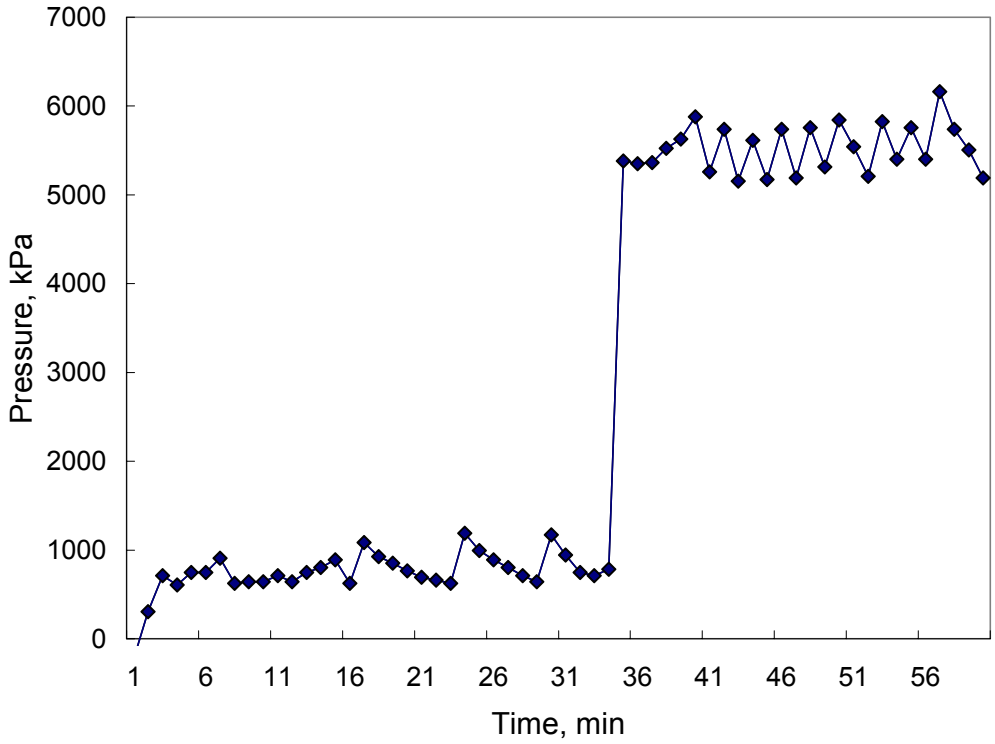

Figure 3.15 Molding pressure vs. time for a Glass/PET (SC125) plaque

Table 3.2 Set-point molding temperatures

Material type	Set point molding temperature, °C
Glass/PP	185 °C
Glass/PET	250 °C
Carbon/PET	270 °C
Dupont SC125	250 °C

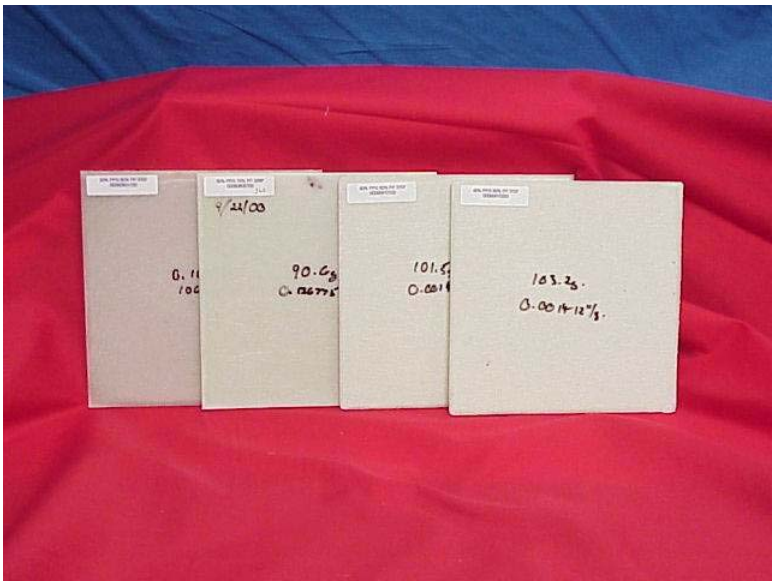

Figure 3.16 Glass/PP plaques made from the hot-press molding

3.4.2 C-Scan

The ultrasonic C-scan technique is used to inspect the internal structure of the consolidated composite plaques. From the C-scan image, defects within the microstructure such as uneven resin flow, porosity and formation of fiber bundles can be seen and modifications of the manufacturing process can then be made to prevent defects in future plaques.

Figure 3.17 shows an example of a C-scan image of a Glass/PET plaque. In the figure, the fiber bundles can clearly be seen, indicating that the fibers in the

bundle do not separate from each other in the slurry during wetlay processing. Increasing the stirring time or the speed of the agitator may be one way to solve this problem. The small white dots in Figure 3.17 are reflections of the air bubbles in the water during the C-scan and are not defects in the plaques. However, the large circular whitish region indicates that the consolidation at the center of the plaque is poor. Therefore the molding process needs to be improved, which can be achieved by changing the set-point molding pressure or molding temperature.

Figure 3.18 shows a C-scan image of a well-consolidated Glass/PP plaque. Some of the glass fibers can still be seen, but they do not form bundles. The fibers are randomly distributed in the plaque.

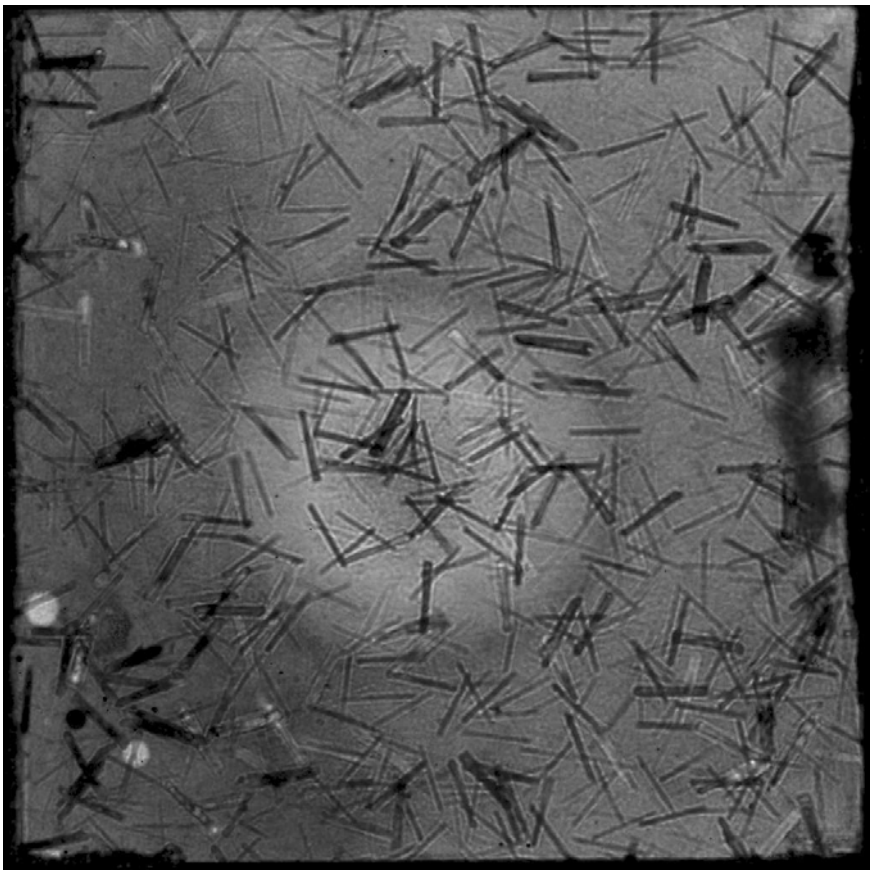

Figure 3.17 A C-scan image of Glass/PET plaque

Figure 3.18 A C-scan image of Glass/PP plaque

3.5. Experimental Methods

3.5.1 Specimen Cutting

The specimens are cut from the molded plaques. Typical directions of cutting involve machine direction and transverse direction. Figure 3.19 illustrates how a plaque is cut in the machine direction. Out of one plaque, six tensile specimens and eight flexural specimens can be obtained. Figure 3.20 shows how a plaque is cut in the transverse direction.

The tensile specimens are 152.4 mm in length and 25.4 mm in width, which fulfills the requirement of ASTM D 3039/D 3039M [5]. The flexural test specimens are 76.2 mm in length and 25.4 mm in width. However, in the 3-point flexural test, the span is usually set at around 50 mm, so a small end portion of the specimen is cut off to better fit into the test fixture.

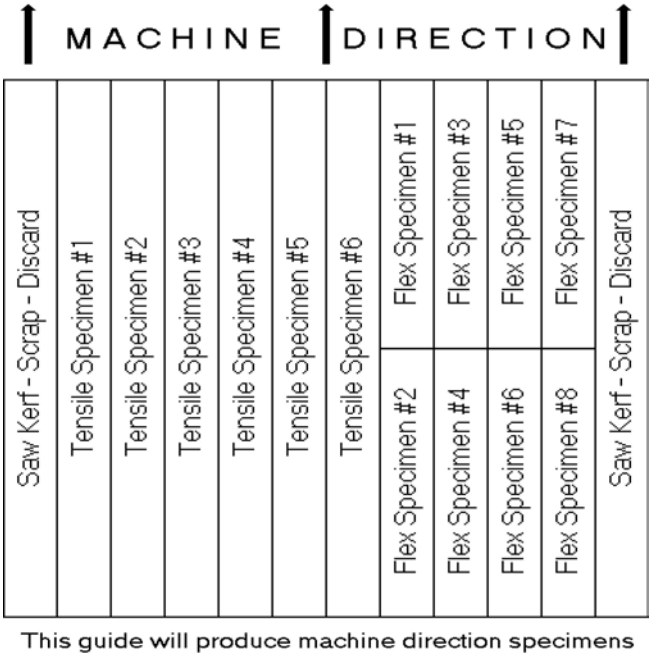

Figure 3.19 Test specimens cut in machine direction

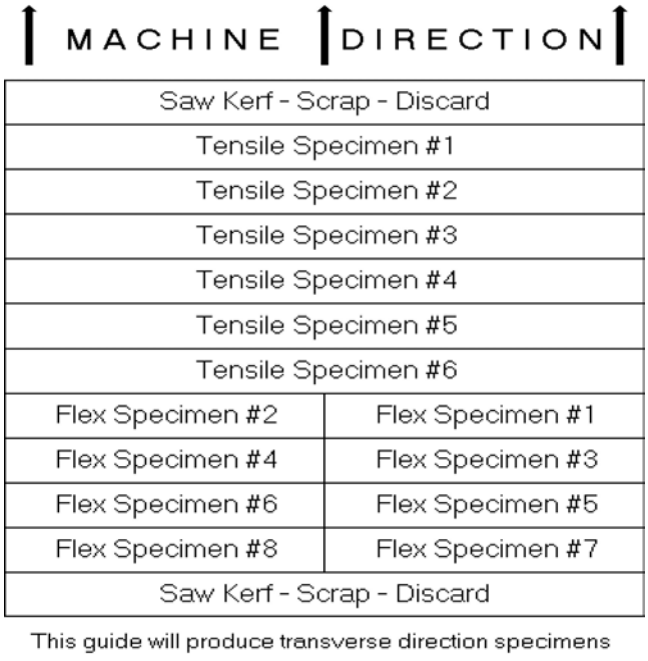

Figure 3.20 Test specimens cut in transverse direction

3.5.2 Tensile Test

The tensile tests were performed in accordance with ASTM D 3039/D 3039M [5]. Tests were conducted on an Instron-4468 testing machine with a 1 kN load cell and a cross head speed of 1mm/min. Figure 3.21 shows a specimen in the tensile test.

Figure 3.21 Tensile test

Eq. (3.3) to Eq. (3.5) are used to calculate the modulus of elasticity, the ultimate strain and the ultimate strength.

Modulus of Elasticity: $E = \Delta\delta / \Delta\varepsilon$ (3.3)

where: E = elastic modulus (MPa)

$\Delta\delta$ = change in stress

$\Delta\varepsilon$ = change in strain

Ultimate Strain: $\varepsilon_f = \Delta_f / L_g$ (3.4)

where: ε_f = final strain (mm/mm)

Δ_f = extensometer displacement (mm)

L_g = extensometer gage length (mm)

Ultimate Strength: $\sigma_f = P_f / A$ (3.5)

where: σ_f = final stress (MPa)

P_f = final load (N)

A = cross sectional area (mm^2)

Figure 3.22 shows a typical load-strain curve of a Glass/PP composite from the tensile test. Figure 3.23 shows a typical load-strain curve of a Glass/PET composite from the tensile test.

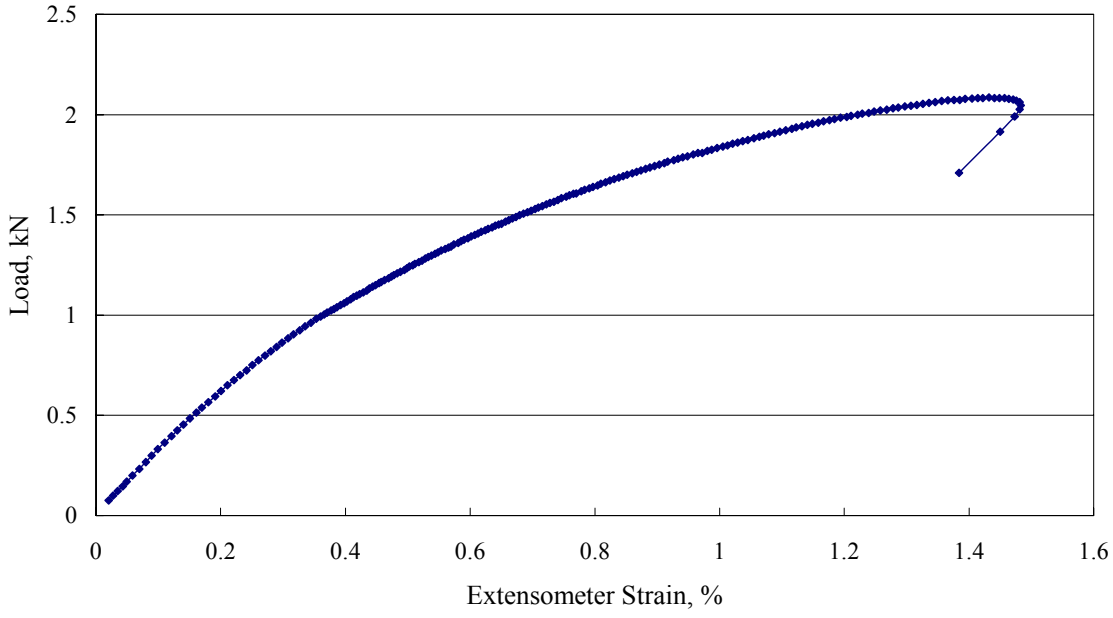

Figure 3.22 A typical load-strain curve of Glass/PP in tensile test

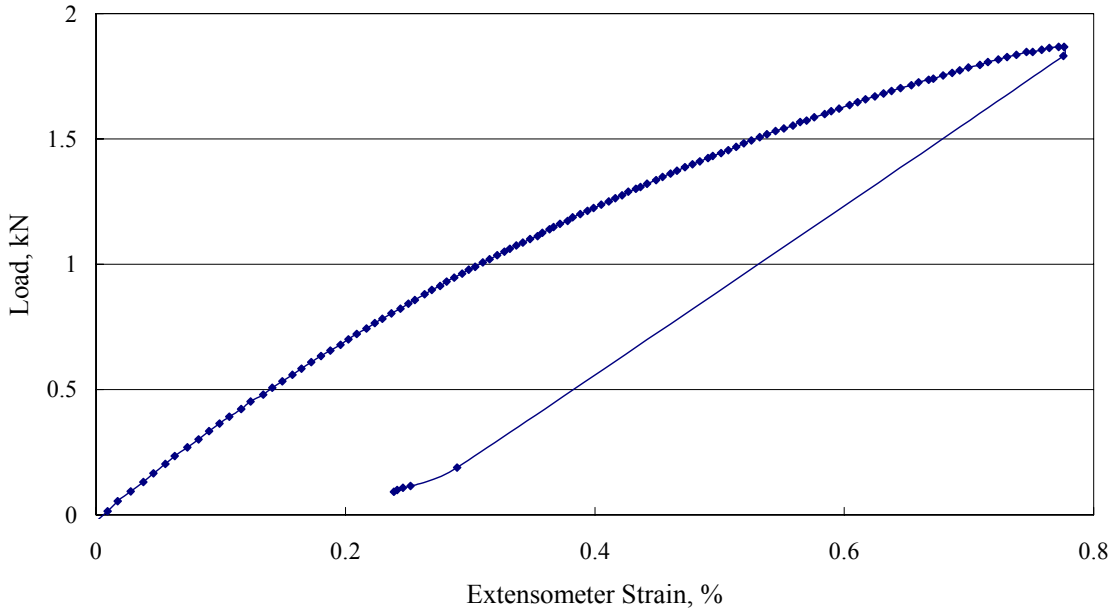

Figure 3.23 A typical load-strain curve of Glass/PET in tensile test

3.5.3 Flexural Tests

The flexural tests were performed in accordance with ASTM D790-98 [6]. Tests are conducted on an Instron-4204 testing machine with the cross head speed set at 1.4 mm/min. Figure 3.24 shows a specimen in a 3-point bending test.

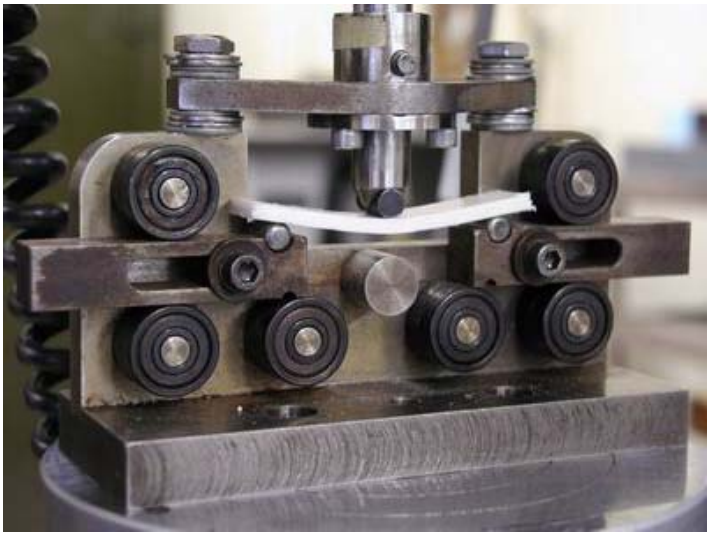

Figure 3.24 Three-point bending test

As described in the ASTM standard [6], the span has to be at least 16 times the depth of the beam. For specimens 3.175 mm (0.125 in.) thick, it is necessary to have a 50.8 mm (2 in.) span length.

Eq.(3.6) to Eq. (3.8) are used to calculate the strength, the ultimate strain and the modulus of elasticity.

Flexural Strength: $$\sigma_f = \frac{3PL}{2bd^2} \quad (3.6)$$

Where:

σ_f = final stress in the outer fibers at midpoint, MPa (psi),

P = load at a given point on the load-deflection curve, N (lbf),

L = support span, mm (in.),

b = width of specimen tested, mm (in.), and

d = depth of specimen tested, mm (in.).

Flexural Strain: $$\varepsilon_f = \frac{6Dd}{L^2} \quad (3.7)$$

Where ε_f =strain in the outer surface

D=maximum deflection of the center of the beam, mm (in.),

L=support span, and

d=depth of the specimen tested.

Tangent Modulus of Elasticity: $$E_B = \frac{L^3 m}{4bd^3} \quad (3.8)$$

Where E_B =modulus of elasticity in bending

L=support span,

b=width of specimen tested,

d=depth of the specimen tested, and

m=slope of the tangent to the initial straight-line portion of the load-deflection curve

Figure 3.25 shows a typical load-displacement curve of a Glass/PP composite from the flexural test and Figure 3.26 shows a typical load-displacement curve of a Glass/PET composite from the flexural test.

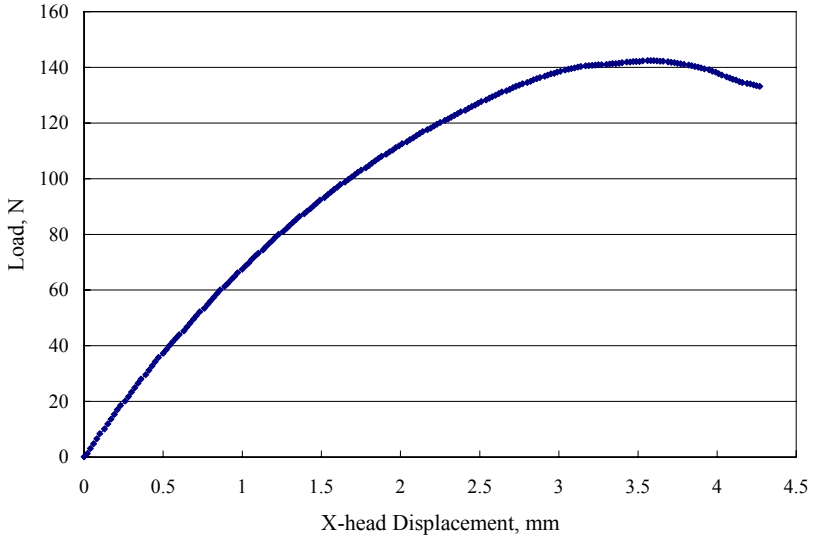

Figure 3.25 A typical displacement-load curve of Glass/PP in flexural test

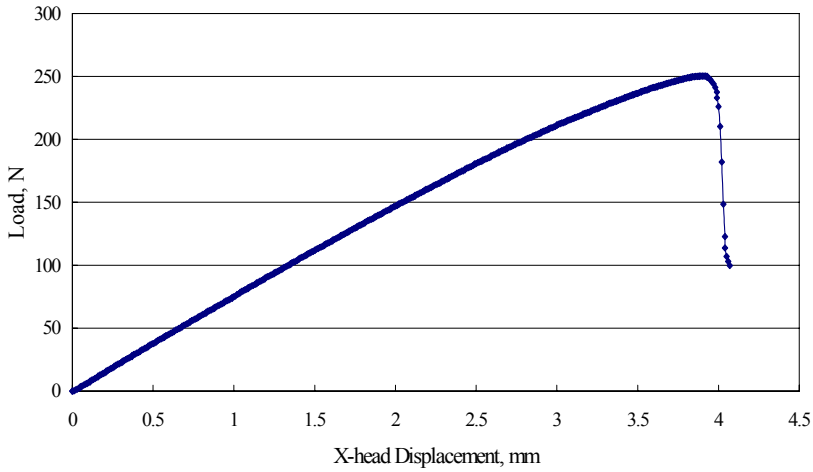

Figure 3.26 A typical displacement-load curve of Glass/PET in flexural test

3.5.4 Fiber Content Measurement

After the tensile and flexural tests, burn-out tests are carried out in order to determine the actual fiber volume fraction (weight fraction) of the specimen.

The actual fiber weight fraction is determined by:

$$WF = \frac{W_f}{W_i} \qquad (3.9)$$

where, W_i is the initial weight of the composite and W_f is the final weight of the fibers after the burn-out test. After the actual fiber weight fraction of the fiber is determined, Eq.(3.2) is used to obtain the corresponding actual fiber volume fraction.

Chapter 4. Test Results and Analysis

Mechanical tests were conducted on Glass/PP and Glass/PET composites following the procedures described in Chapter 3. All the tensile test in this chapter followed the ASTM D 3069/D 3039M-95a standard. All the flexural test in this chapter followed the ASTM D790-98 standard.

The detailed test results can be found in Appendix A-D. A summary of the test results is given in this section. Carbon/PET composites were made and test results were compared with those of Glass/PET composites. Micrographs of selected Glass/PP and Glass/PET composites were taken and analyzed.

4.1 Test Results

4.1.1 Glass/PP Composites

Glass fiber and polypropylene composites were fabricated with fiber volume fractions ranging from 0.05 to 0.50. Figure 4.1 and Figure 4.2 show the tensile test results. The flexural test results are shown in Figure 4.3 and Figure 4.4.

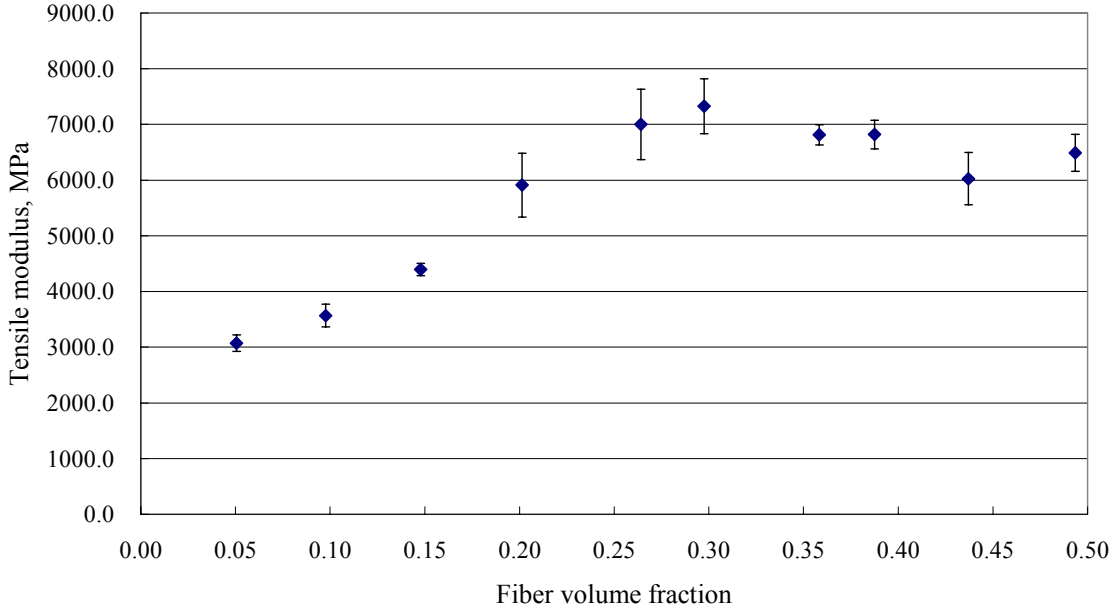

Figure 4.1 Tensile modulus vs. fiber volume fraction for Glass/PP composites

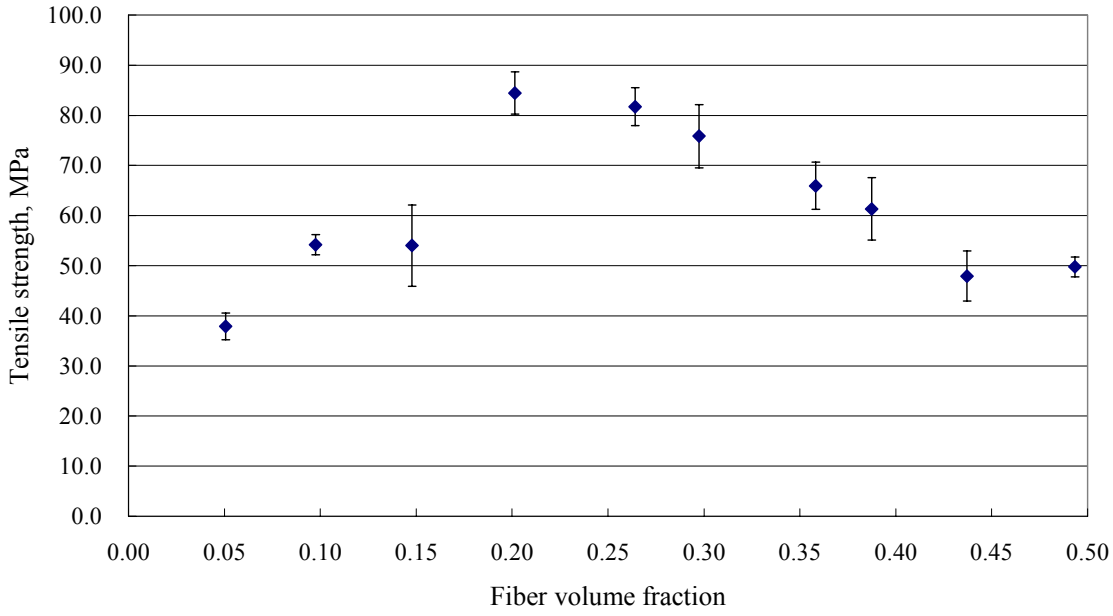

Figure 4.2 Tensile strength vs. fiber volume fraction for Glass/PP composites

In Figure 4.1 and Figure 4.2, six specimens were tested at each fiber volume fraction, which is in accordance with the requirement of the ASTM standard D3039/D3039M. Each data point shown in Figure 4.1 and Figure 4.2 is the average of six tests. All

together, 120 specimens were tested to get the results in Figure 4.1 and Figure 4.2. In Figure 4.3 and Figure 4.4, eight specimens were tested at each fiber volume fraction and altogether 160 specimens were tested to get the results in these two figures.

Unlike unidirectional fiber-reinforced composites whose tensile modulus and strength show a continuous increase with an increase in fiber volume fraction, the tensile modulus and strength of the random fiber composites increase with fiber volume fraction up to a certain maximum value and then start to decrease.

For Glass/PP composites, the tensile modulus reaches its maximum at a fiber volume fraction of about 0.30, while the tensile strength reaches its maximum at a fiber volume fraction of about 0.20.

One reason for the decrease in strength and modulus at high fiber volume fraction shown in Figure 4.1 and Figure 4.2 is the interactions between the fibers. Since the fibers in the wetlay-made composites have a random-in-plane distribution, interactions between the fibers are inevitable. When the fiber volume fraction is low, the fibers play the role of reinforcement. This is why below a certain fiber volume fraction, the tensile modulus and strength of the composite increase with increasing V_f. As the fiber volume fractions becomes higher, there will be more interaction between the fibers during the molding process, which may lead to voids and poor bonding between the fibers and the resin. Hence, the tensile modulus and strength start to decrease as fiber volume fraction increases above a critical value.

The data in Figure 4.3 show that the flexural modulus reaches its maximum value at a fiber volume fraction of 0.35, compared with the maximum tensile modulus at a fiber volume fraction of about 0.30. In Figure 4.4, the flexural strength reaches its maximum at a fiber volume fraction of 0.20, the same fiber volume fraction at which tensile strength reaches its maximum.

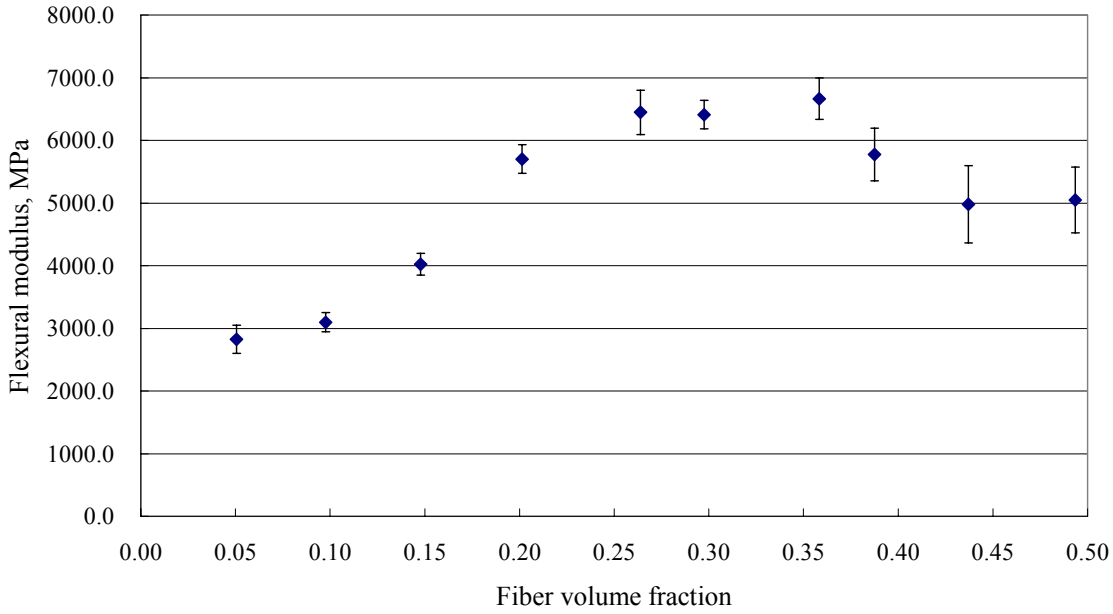

Figure 4.3 Flexural modulus vs. fiber volume fraction for Glass/PP composites

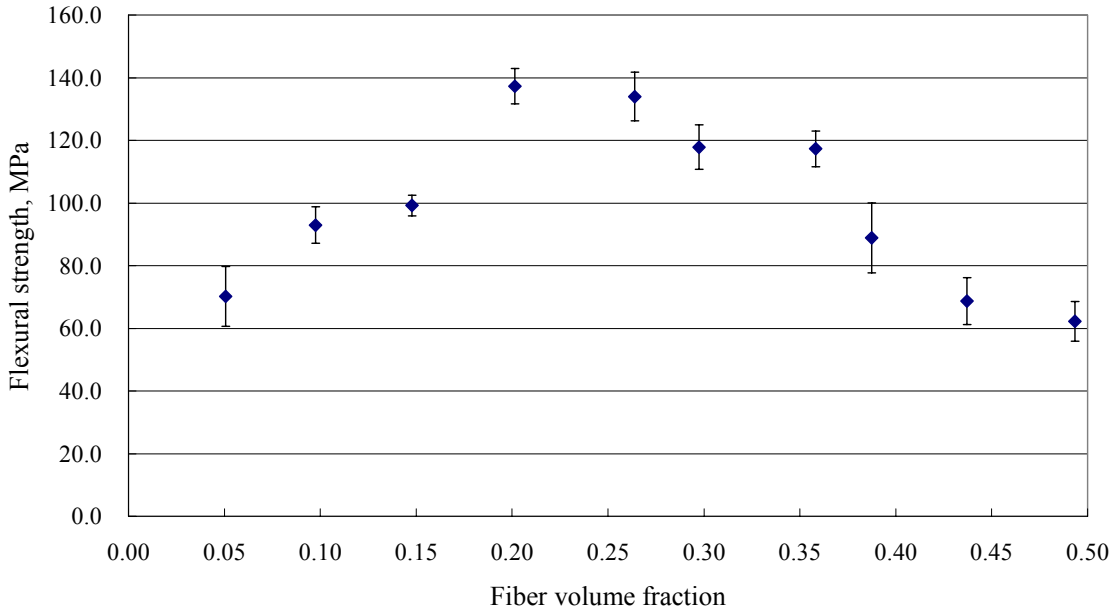

Figure 4.4 Flexural strength vs. fiber volume fraction for Glass/PP composites

4.1.2 Glass/PET Composites

Glass fiber and PET composites were fabricated with fiber volume fractions ranging from 0.05 to 0.50. Figure 4.5 and Figure 4.6 show the tensile test results. The flexural test results are shown in Figure 4.7 and Figure 4.8. The actual fiber volume fractions vary a little bit from the object fiber volume fractions.

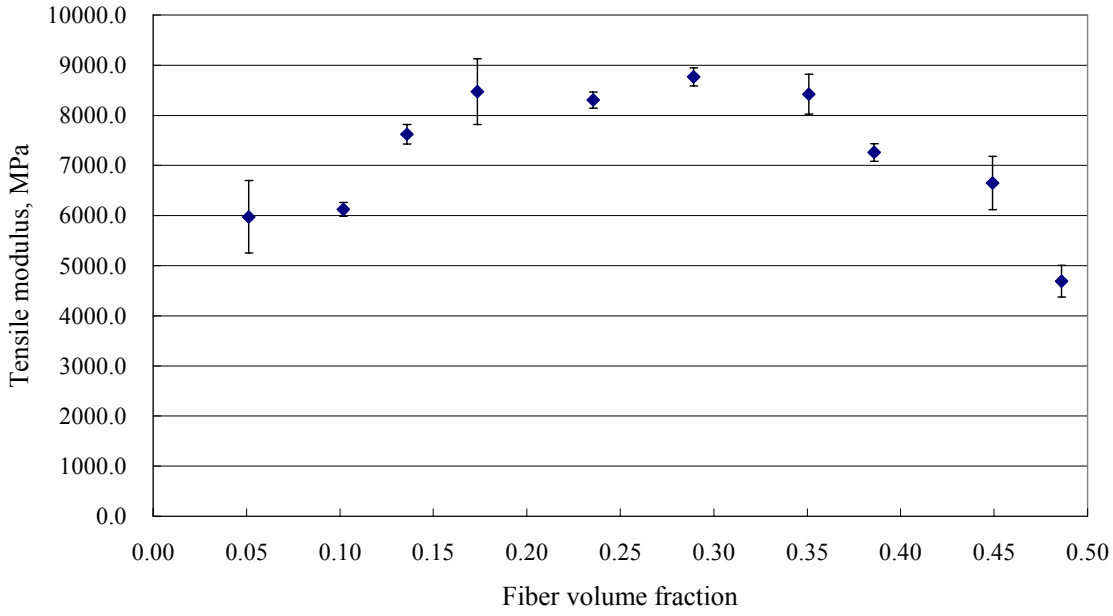

Figure 4.5 Tensile modulus vs. fiber volume fraction for Glass/PET composites

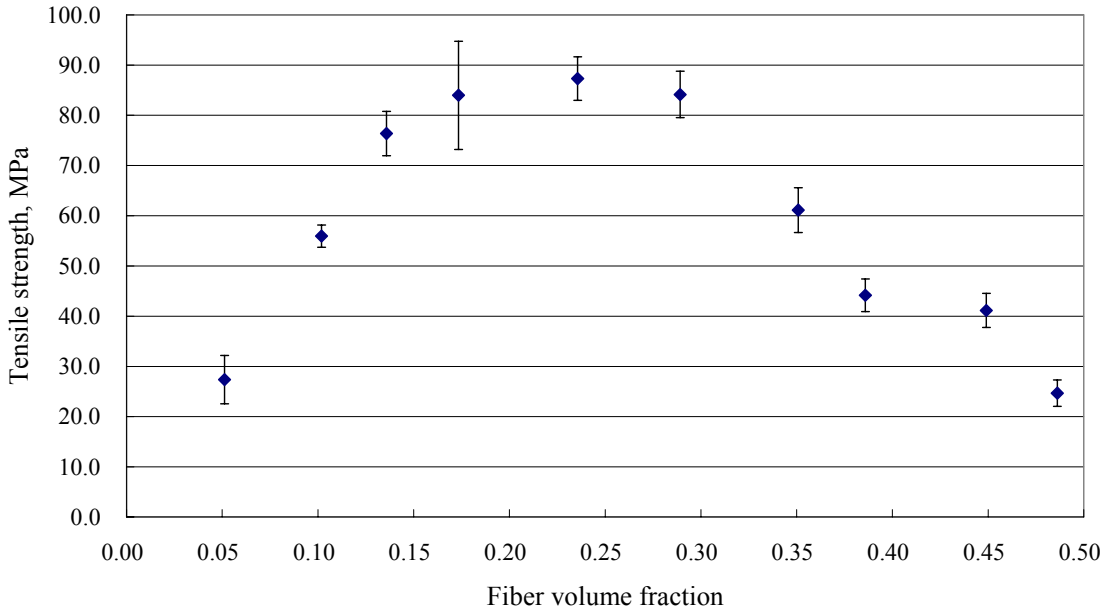

Figure 4.6 Tensile strength vs. fiber volume fraction for Glass/PET composites

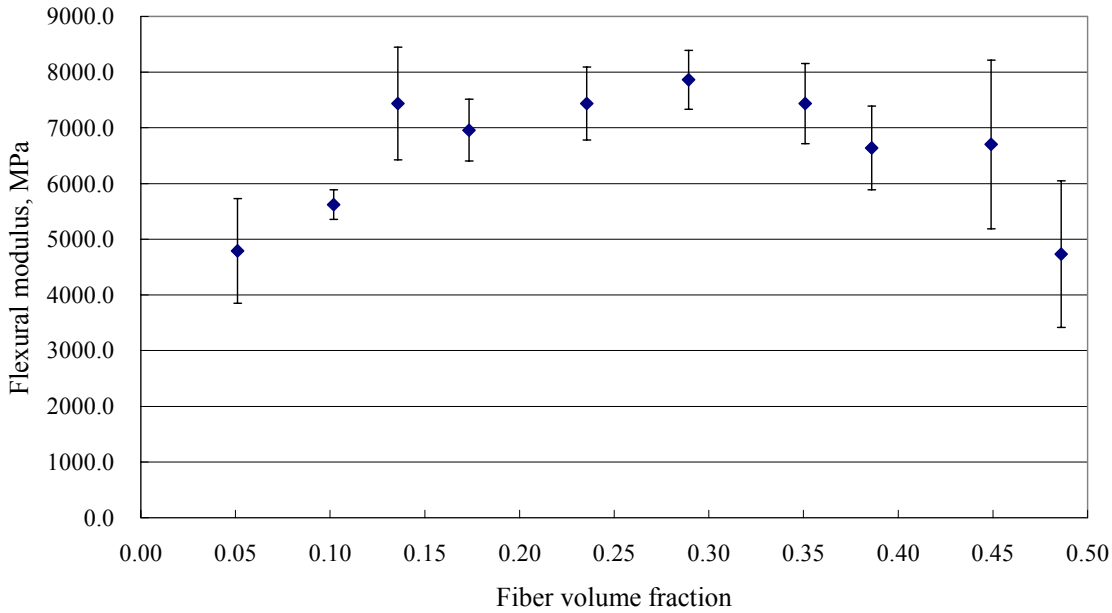

Figure 4.7 Flexural modulus vs. fiber volume fraction for Glass/PET composites

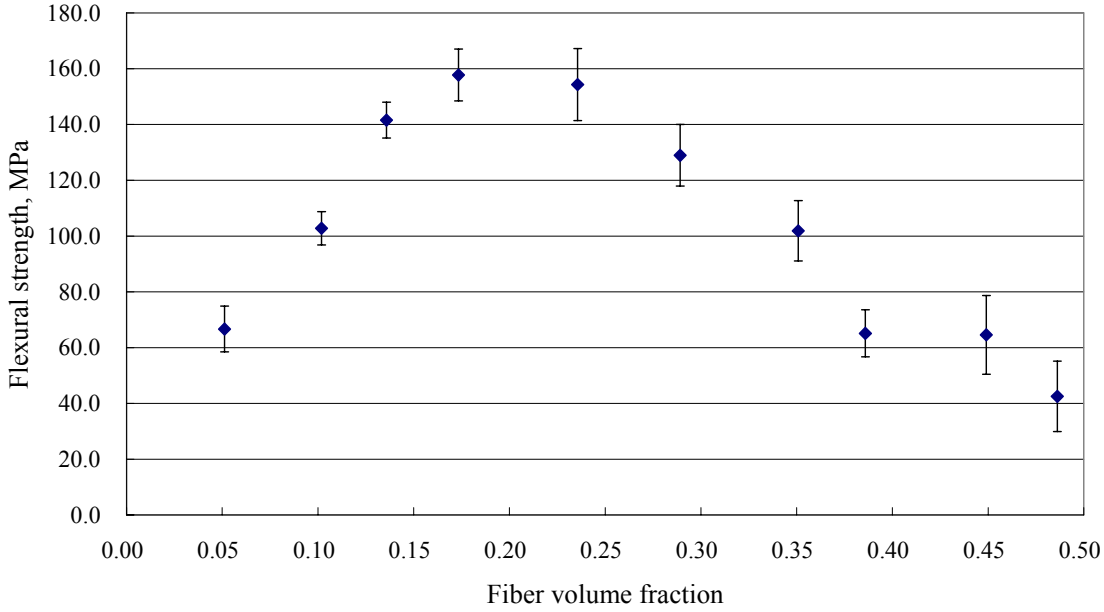

Figure 4.8 Flexural strength vs. fiber volume fraction for Glass/PET composites

Figure 4.5 and Figure 4.6 show a similar trend as Figure 4.1 and Figure 4.2. For the Glass/PET composites, 0.3 seems to be an optimal fiber volume fraction for tensile modulus. But a maximum in tensile strength is achieved at a fiber volume fraction of about 0.25.

Consider the flexural test results in Figure 4.7 and Figure 4.8. In Figure 4.7, the flexural modulus reaches its maximum at a fiber volume fraction of about 0.30. In Figure 4.8, the flexural strength reaches its maximum at a fiber volume fraction of about 0.20.

4.1.3 PET Resin

The test results of Glass/PET composites were much lower than expected. In order to determine if the problem is due to low properties of the PET resin used in the wetlay

process, tensile and flexural tests were conducted on specimens of PET. Table 4.1 shows the tensile test results. The flexural tests results are shown in Table 4.2. The detailed test results can be found in Appendix E.

Table 4.1 Tensile test results of PET resin

Strength, MPa		Modulus, MPa	
Average	Standard Deviation	Average	Standard Deviation
13.27	5.98	3936.63	183.68

Table 4.2 Flexural test results of PET resin

Strength, MPa		Modulus, MPa	
Average	Standard Deviation	Average	Standard Deviation
43.37	7.02	3716.75	247.97

The tensile and flexural strengths of the PET resin in the tests are much lower than the reported value in the literature. For example, the tensile strength ranges 45.5-72.4 MPa and flexural strength 82.7-124.1 MPa [36,37]. On the other hand, the tensile and flexural modulus are close to the values generally reported in the references. For example, the tensile modulus is 2758-4137 MPa in [37] while the flexural modulus is 2400-3100 MPa in [36,37]. Therefore it is concluded that the poor bonding of glass fiber and PET results in the low properties of the Glass/PET composite.

4.2 Effects of Fibers

The mechanical properties of reinforcing fibers differ greatly from each other. Therefore, composites made from the same resin but different types of fiber will have significant differences in the mechanical properties. In order to study the effects of different fibers on the composites properties, plaques made of carbon fibers and PET resin were tested. The specimens in the tests had carbon fiber volume fraction ranging

from 0.32 to 0.41, which corresponded to 0.39 to 0.48 in terms of weight fraction of carbon fiber. Results of these tests are compared with those of glass fiber composites.

Figures 4.9 and 4.10 show the results of tensile tests of carbon/PET composites. Results of flexural tests are shown in Figures 4.11 and 4.12.

By comparing the values in Figures 4.5-4.8 to those in Figures 4.9-4.12, it can be seen that carbon fiber reinforced composites have much higher tensile and flexural moduli and strengths than glass fiber reinforced composites.

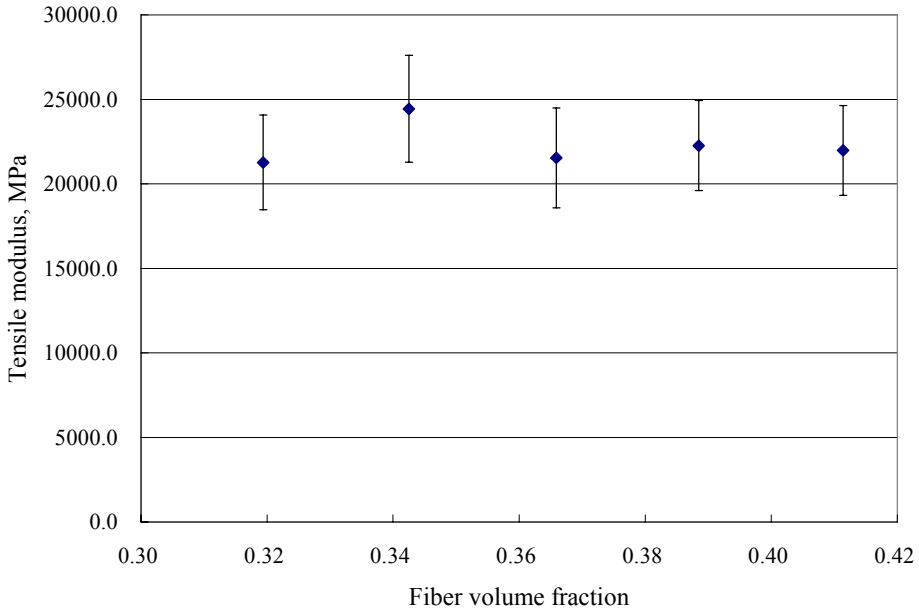

Figure 4.9 Tensile modulus vs. fiber volume fraction for Carbon/PET composites

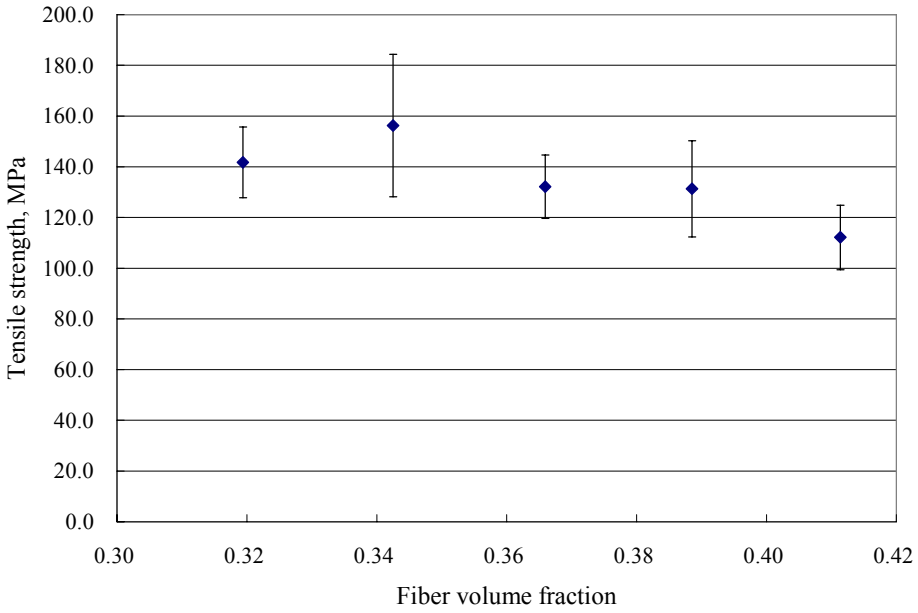

Figure 4.10 Tensile strength vs. fiber volume fraction for Carbon/PET composites

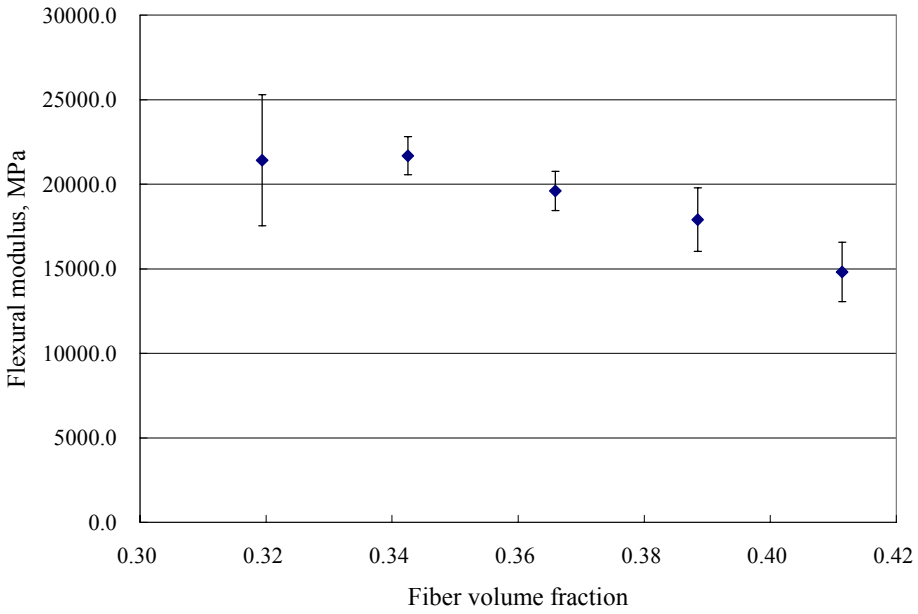

Figure 4.11 Flexural modulus vs. fiber volume fraction for Carbon/PET composites

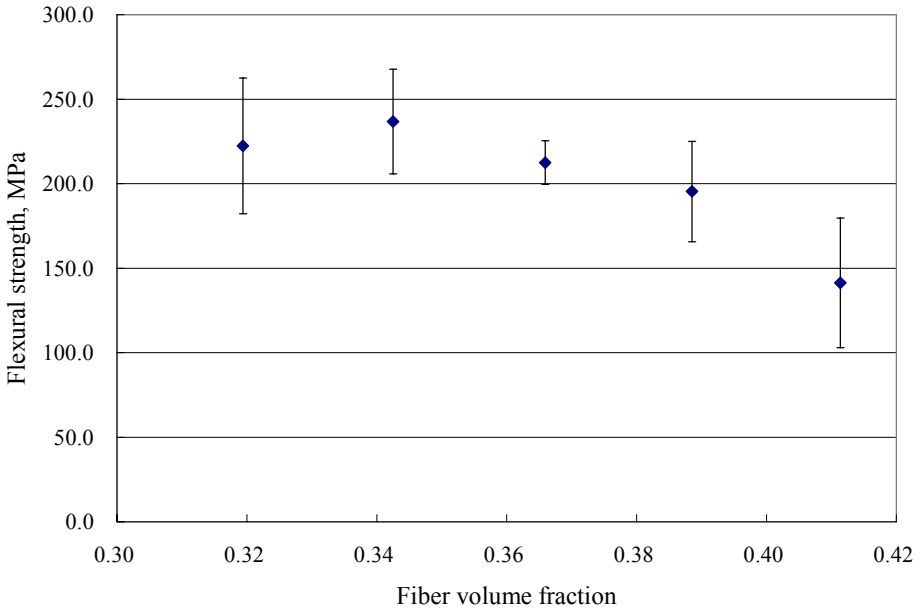

Figure 4.12 Flexural strength vs. fiber volume fraction for Carbon/PET composites

Figure 4.9 and Figure 4.10 indicate that both the highest tensile modulus and tensile strength are achieved at a fiber volume fraction of 0.34. The tensile modulus does not change significantly within the range of fiber volume fractions studied.

In Figure 4.11 and Figure 4.12, the highest flexural modulus and flexural strength are also obtained at a fiber volume fraction of 0.34. The flexural modulus decreases with increasing fiber volume fraction. Judging from the test results, 0.34 is an optimal value of fiber volume fraction within 0.32 to 0.41 to yield the best modulus/strength of carbon/PET composites.

4.3 Micrographs of Glass/PP and Glass/PET Composites

Micrographs were taken of selected specimens after mechanical testing to examine the internal structure of the composites. Microstructural defects such as non-uniform fiber distribution, fiber-resin separation and voids can be found. Figure 4.13 shows four micrographs of Glass/PET at 0.35 fiber volume fraction. Figure 4.14 shows four micrographs of Glass/PET at 0.40 fiber volume fraction. Four micrographs of Glass/PP at 0.30 fiber volume fraction are shown in Figure 4.15.

Some common features can be observed in the micrographs. First, voids exist in the microstructure and appear as the dark areas around the fibers in Figure 4.13-Figure 4.14. It was suspected at first that the dark areas were dust that filled the holes that were created when the fibers were pulled away during the polishing process. However, the dark areas remained after ultra-sonic cleaning of the polished surfaces. Therefore, it was concluded that the dark areas are the voids in the composites.

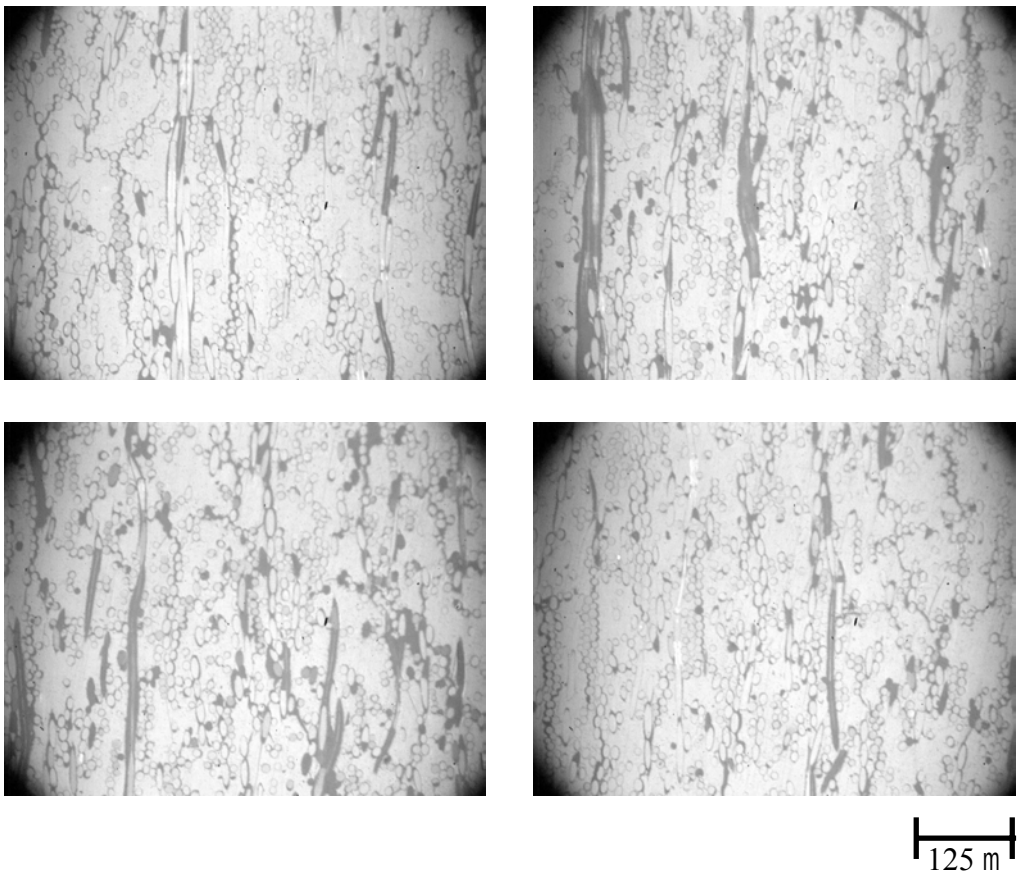

Figure 4.13 Micrographs of Glass35/PET65 (volume fraction)

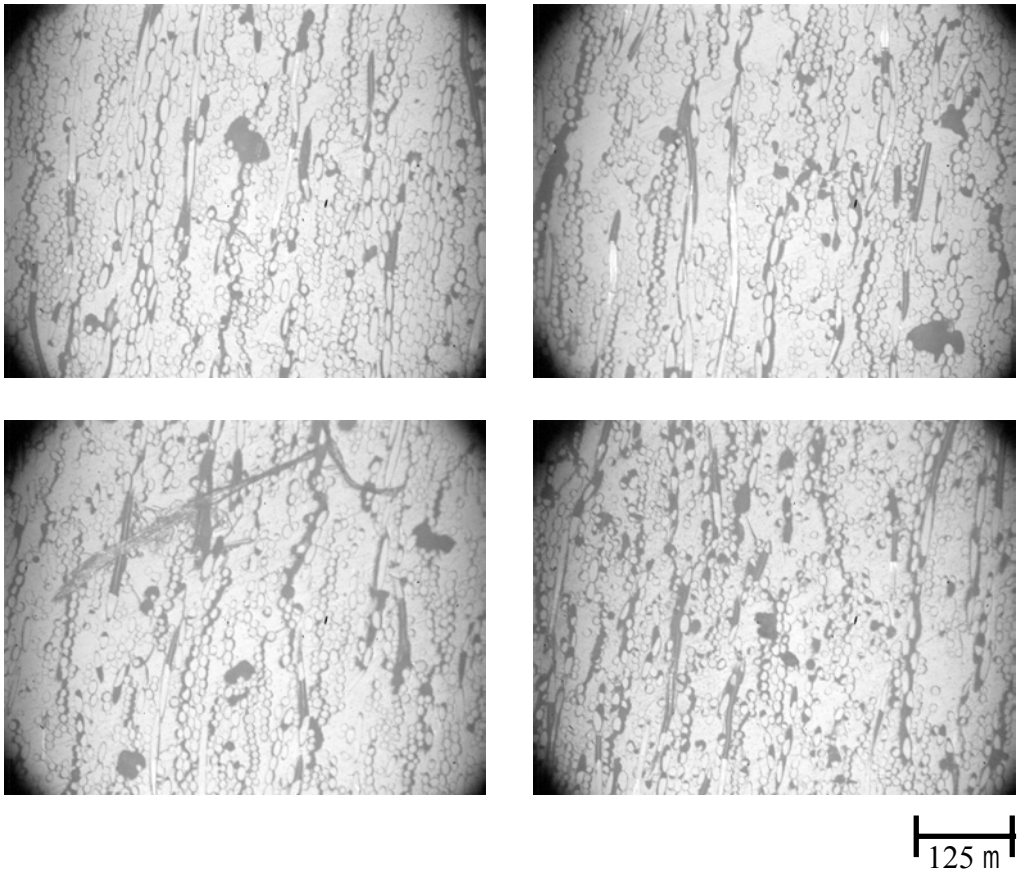

Figure 4.14 Micrographs of Glass40/PET60 (volume fraction)

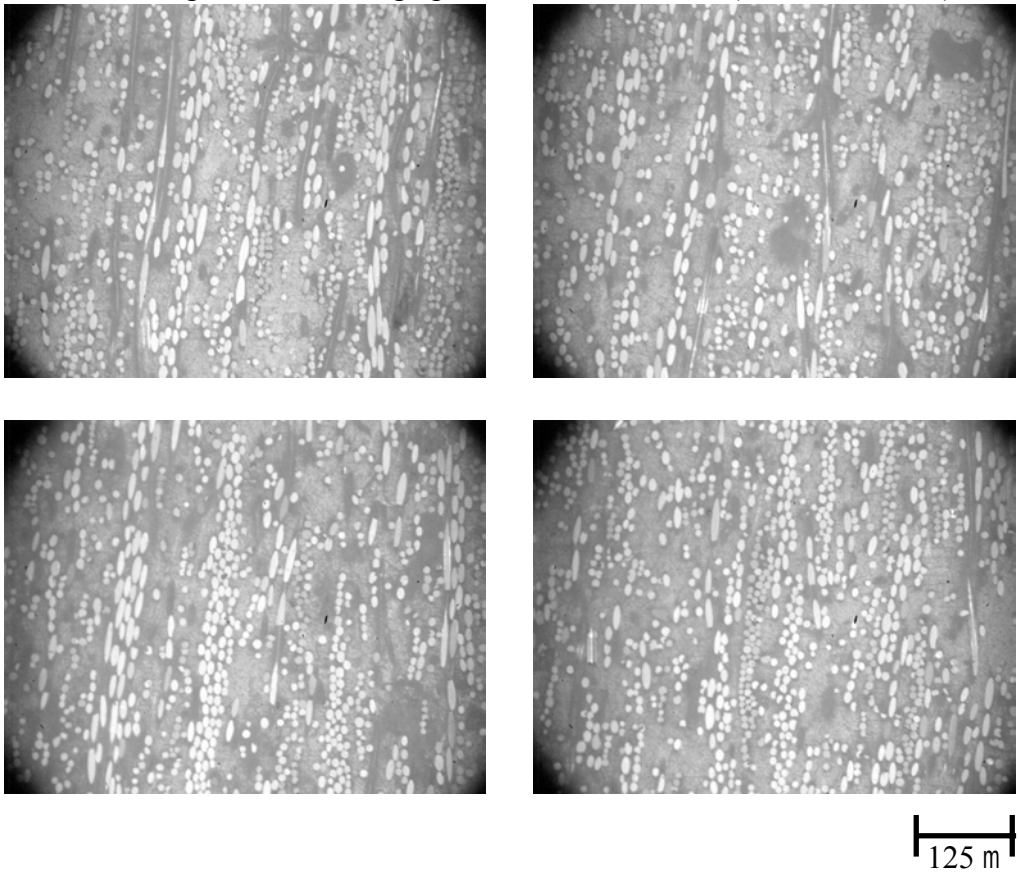

Figure 4.15 Micrographs of Glass30/PP70 (volume fraction)

The void content tends to increase as the fiber volume increases for Glass/PET composites. This can be seen by comparing the images in Figure 4.13 to those in Figure 4.14. The voids get bigger in size and larger in number as the fiber volume fraction increases from 0.35 to 0.40. This may be one reason that the strength and stiffness of Glass/PET decrease at higher fiber volume fractions.

After comparing the images in Figure 4.13-Figure 4.14 to those in Figure 4.15, it can be seen that glass fiber has a better distribution in PP than in PET. The images in Figure 4.15 look darker because an old epoxide resin was used to make the micrograph specimens. Also, a lower void content was observed in the Glass/PP composite.

4.4 Summary

The tensile and flexural test results of both Glass/PP and Glass/PET composites are summarized in this chapter. For both types of material, the results display a similar pattern, i.e., the strength or modulus increases with fiber volume fraction to a maximum value and then decreases with increasing fiber volume fraction. This is one of the significant differences between random, discontinuous fiber composites and unidirectional fiber reinforced composites.

One of the objectives of this study was to find the fiber volume fraction at which the Glass/PP or Glass/PET composites have the highest strength or stiffness. For Glass/PP composites, this value is 0.2 for both tensile and flexural strength, 0.3 for tensile modulus and 0.35 for flexural modulus. For Glass/PET composites, this value is about 0.3 for both tensile and flexural modulus, about 0.25 for tensile strength and

about 0.2 for flexural strength.

Carbon/PET composites with fiber volume fractions ranging from 0.32 to 0.41 were tested. The highest modulus and strength in both tensile and flexural tests were achieved at a fiber volume fraction of 0.34.

The mechanical properties of Glass/PET were lower than expected. Measurements of the tensile and flexural properties of neat resin PET showed that the strength of the PET was lower than the data reported in the literature. Hence, the PET resin may have degraded. On the other hand, micrographs of the Glass/PET specimens show that voids exist. A possible explanation for this is that the surface treatment of the glass fibers used in this study does not promote good bonding with the PET resin.

Chapter 5. Evaluation of Micromechanics Models

In chapter 2, micromechanics models were presented which can predict the strength and modulus of the random discontinuous fiber composites. The models are applied in this chapter by substituting the corresponding properties of the constituent materials to theoretically calculate the modulus and strength of the wetlay composites. The tensile modulus of the E-glass fiber used in the calculations in this chapter is 72.395 GPa and the strength is 2400 MPa (manufacturer's data). Polypropylene has a tensile modulus of 1344.5 MPa and a strength of 33.1 MPa (manufacturer's data). According to the test results in Section 4.1.3, the tensile modulus of the polyethene terephthalate (PET) is 3936.6 MPa and the strength is 13.3 MPa.

5.1 Fiber Efficiency Factor Approach

To use this approach, the average ultimate strains (fracture strains) must be known in order to calculate the $\sigma_m^{'}$, the matrix stress at the fracture strain of the composite, in Eq. (2.18). The average ultimate strains measured during the tensile tests are shown in Table 5.1 and Table 5.2.

Table 5.1 Average ultimate strain for Glass/PP composites

Volume fraction	Average ultimate strain of composite, %
0.05	**2.194**
0.10	**2.712**
0.15	**1.828**
0.20	**2.133**
0.26	**1.827**
0.30	**1.682**
0.36	**1.848**
0.39	**1.672**
0.44	**1.562**
0.49	**1.212**

Table 5.2 Average ultimate strain for Glass/PET composites

Volume fraction	Average ultimate strain of composite, %
0.05	**0.543**
0.10	**2.530**
0.14	**2.247**
0.17	**1.601**
0.24	**1.554**
0.29	**1.298**
0.35	**0.978**
0.39	**0.784**
0.45	**0.799**
0.49	**0.574**

Using Eq. (2.18) and Eq. (2.19), the following fiber efficiency factors for the wetlay-made random fiber composites are obtained and shown in Table 5.3 and Table 5.4.

The results in Table 5.3 and Table 5.4 have similar range as reported by Blumentritt and Cooper [15]. For the Glass/PP composites, the fiber efficiency factor K_E ranges from 0.48 to 0.16 and K_σ from 0.13 to 0.03. For the Glass/PET composites, the fiber efficiency factor K_E ranges from 0.61 to 0.08 and K_σ from 0.08 to 0.01. At

fiber volume fractions of 0.1 and 0.14, the fiber efficiency factor is zero and negative, respectively. Hence, the fibers do not improve the properties of the composites.

Table 5.3 Fiber efficiency factors for Glass/PP composites

	Efficiency factor	
Volume fraction	K_E	K_σ
0.05	**0.472**	**0.085**
0.10	**0.333**	**0.091**
0.15	**0.304**	**0.093**
0.20	**0.332**	**0.127**
0.26	**0.314**	**0.100**
0.30	**0.296**	**0.084**
0.36	**0.229**	**0.058**
0.39	**0.214**	**0.051**
0.44	**0.167**	**0.034**
0.49	**0.163**	**0.035**
Average	**0.282**	**0.076**

Table 5.4 Fiber efficiency factors for Glass/PET composites

	Efficiency factor	
Volume fraction	K_E	K_σ
0.05	**0.605**	**0.058**
0.10	**0.351**	**-0.137**
0.14	**0.429**	**0.000**
0.17	**0.416**	**0.077**
0.24	**0.311**	**0.072**
0.29	**0.285**	**0.069**
0.35	**0.231**	**0.043**
0.39	**0.173**	**0.027**
0.45	**0.138**	**0.022**
0.49	**0.076**	**0.011**
Average	**0.302**	**0.024**

It can be seen that this is a simple but effective approach to predict the strength or modulus of random fiber composites. For the same type of composite, if the fiber volume fraction is not listed in Table 5.3 or Table 5.4, interpolation method can be used to get the values of the corresponding K_E and K_σ. Then from Eq. (2.18) and

Eq. (2.19) the tensile strength and modulus can be estimated. The disadvantage of this method is that experiments must be done to determine the fiber efficiency factors.

5.2 Christensen and Waals's Model

This model was given by Eq. (2.21). It should be noted that while deriving their model, Christensen and Waals set the fiber volume fraction to be less than 0.2. Substituting the values of the constituent material properties into Eq. (2.21) gives predictions for the wetlay-made random fiber composites. The comparison between the predictions and test data for Glass/PP composites is shown in Figure 5.1 for fiber volume fractions less than 0.30. Figure 5.2 shows the comparison for Glass/PET composites for fiber volume fractions less than 0.25. At fiber volume fractions higher than 0.25, the model over-estimates the tensile modulus.

From Figure 5.1 and Figure 5.2, it can be seen that Eq. (2.21) works well for low fiber volume fractions. However, at high fiber volume fractions it fails to give good predictions of the modulus.

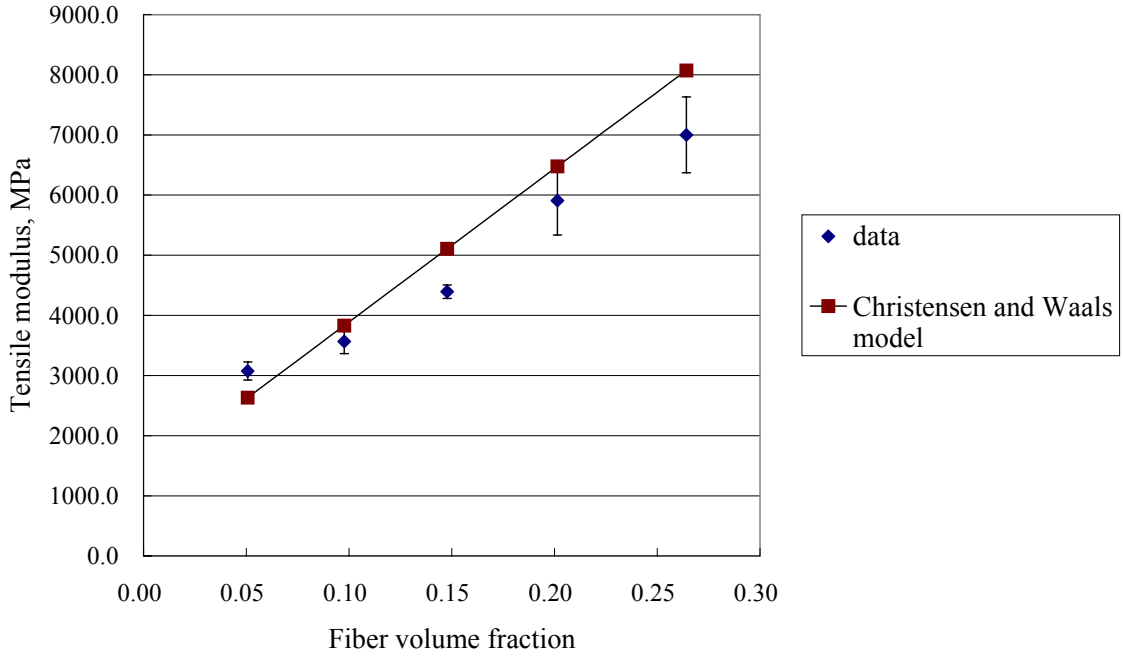

Figure 5.1 Tensile modulus vs. fiber volume fraction for Glass/PP composites

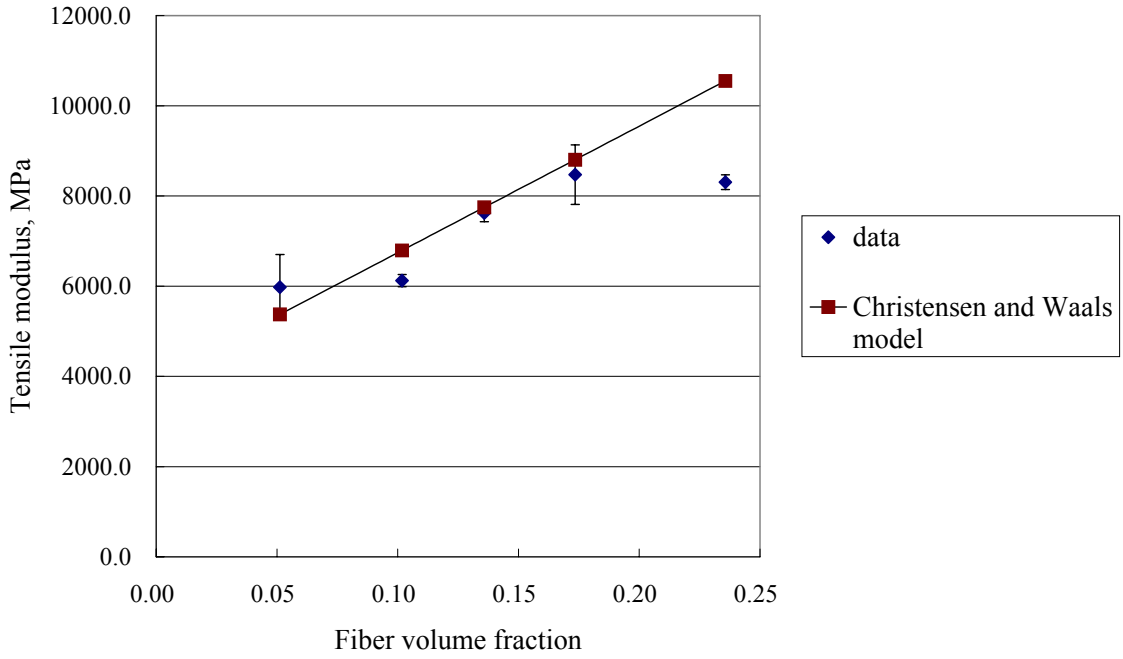

Figure 5.2 Tensile modulus vs. fiber volume fraction for Glass/PET composites

5.3 Modified Rule of Mixtures (MROM)

The predictions of tensile modulus and strength based on the MROM model given in Eq.(2.33) and Eq.(2.34) for Glass/PP composites are shown in Figure 5.3 and Figure 5.4.

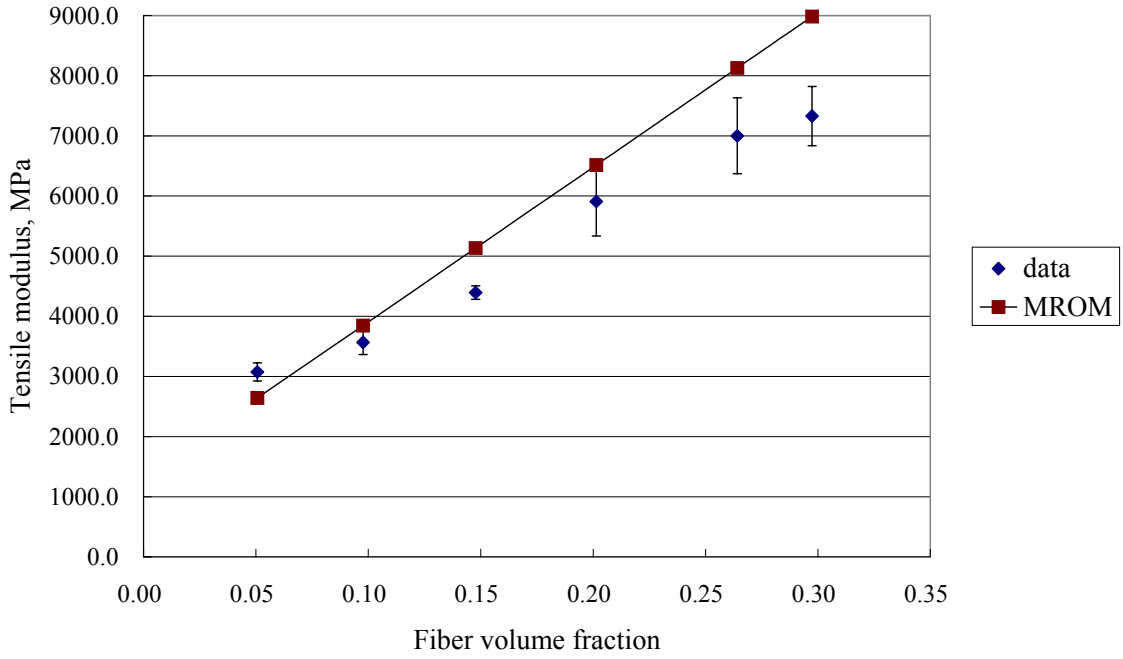

Figure 5.3 Tensile modulus vs. fiber volume fraction for Glass/PP composites

The MROM model predictions are close to the test data for fiber volume fractions less than 0.15. The modulus is predicted to increase linearly with the fiber volume fraction, which is not true for the random fiber composites.

The tensile strength calculated from the MROM model is significantly higher than the test data even at low fiber volume fractions.

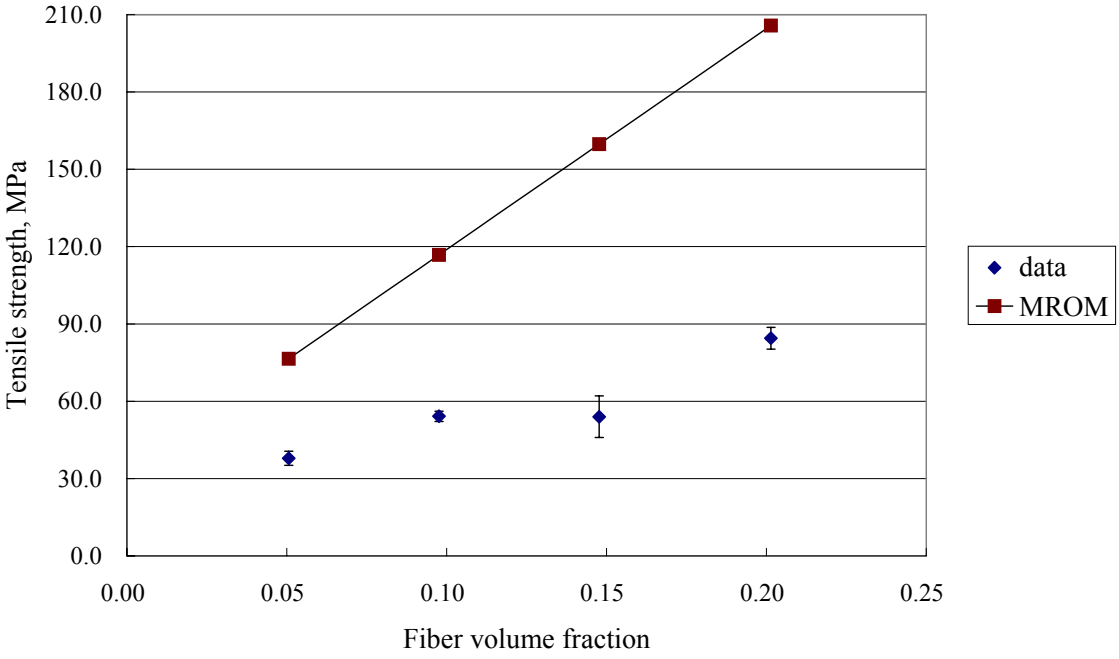

Figure 5.4 Tensile strength vs. fiber volume fraction for Glass/PP composites

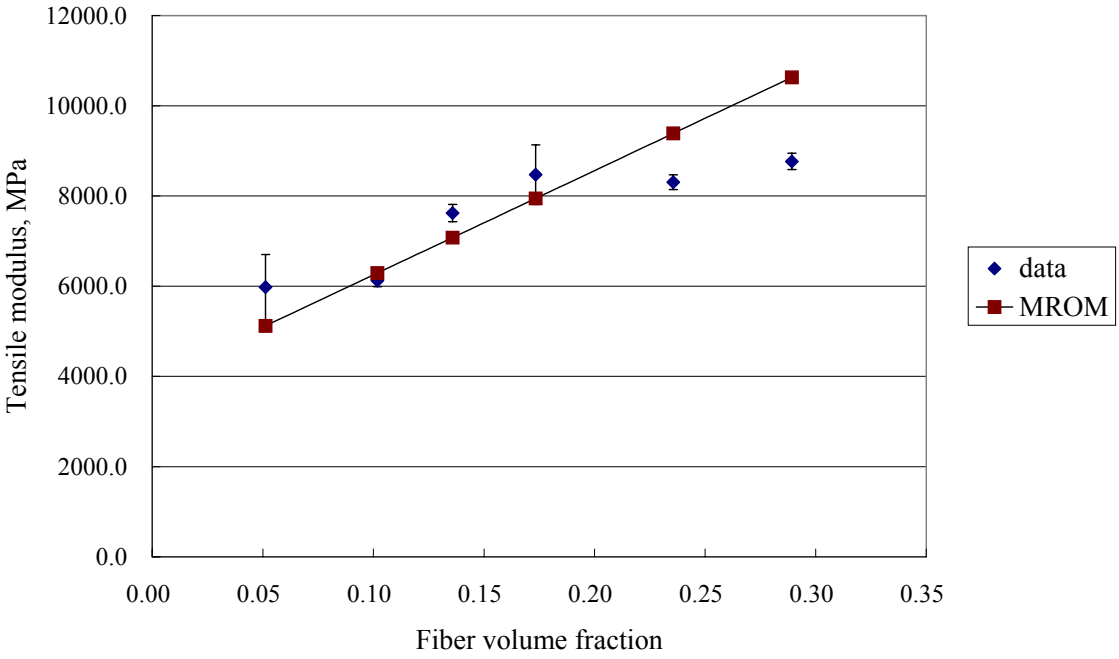

Figure 5.5 Tensile modulus vs. fiber volume fraction for Glass/PET composites

The modulus predictions of the Glass/PET composites are shown in Figure 5.5. The model gives reasonable good predictions up to fiber volume fraction of about 0.20.

5.4 Manera Model

This model is expressed by Eq. (2.22). The comparisons between the test data and the model predictions are shown in Figure 5.6 and 5.7.

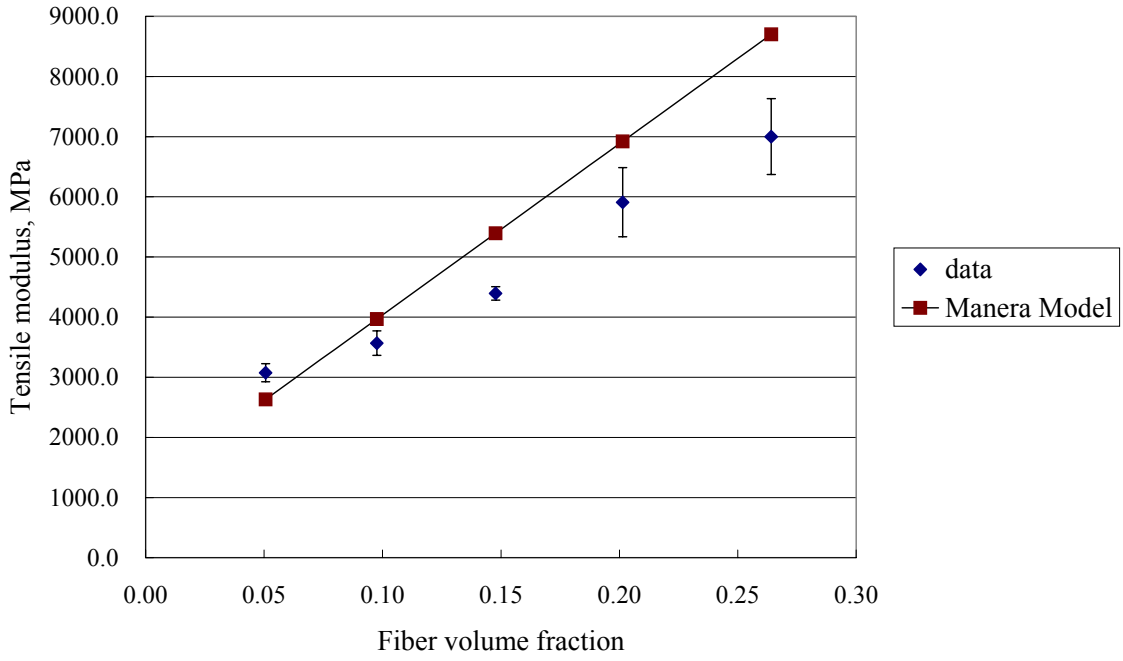

Figure 5.6 Tensile modulus vs. fiber volume fraction for Glass/PP composites

Recall that in his original work, Manera proposed this model for random fiber composites with fiber volume fractions between 0.1 and 0.4. However, the results indicate that Manera's model does not predict the modulus very well within this range of fiber volume fractions for the Glass/PP and Glass/PET composites. The difference between the predicted and measured moduli increases as the fiber volume fraction increases above 0.2.

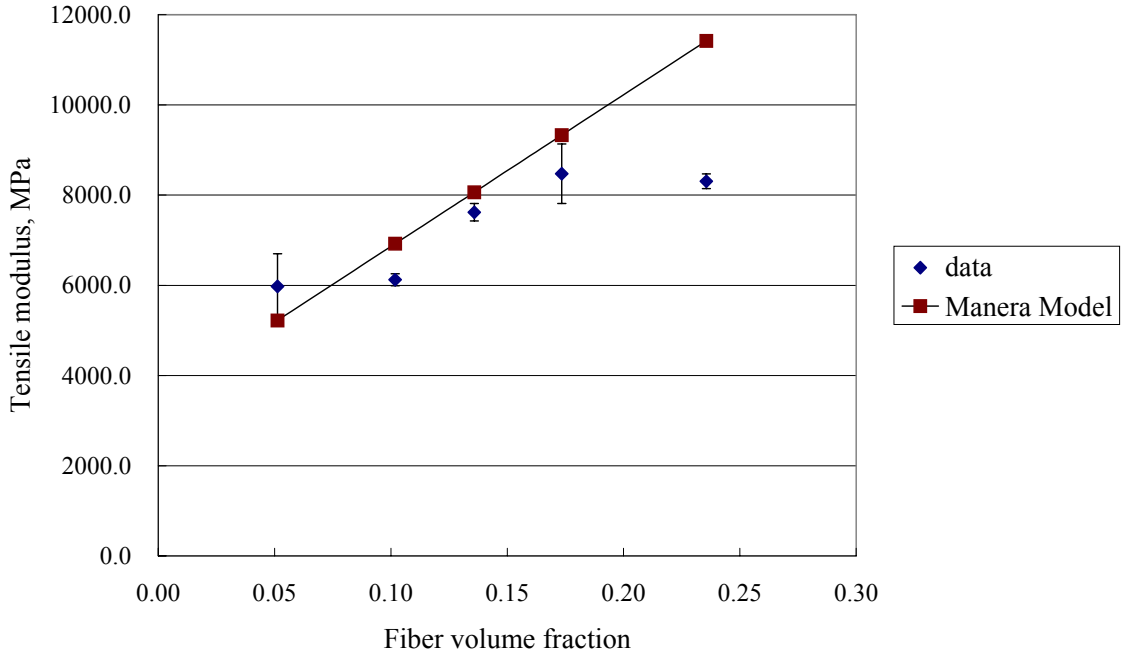

Figure 5.7 Tensile modulus vs. fiber volume fraction for Glass/PET composites

5.5 Pan's Model

Pan's theory is represented by Eq.(2.29) for two-dimensional case. Figure 5.8 and Figure 5.9 show the comparisons between the model estimates and data for Glass/PP and Glass/PET composites, respectively.

It can be concluded from Figure 5.8 that Pan's model gives the best prediction of modulus for Glass/PP composites at fiber volume fractions less than 0.30. For fiber volume fractions greater than 0.30, the model over-predicts the modulus. For Glass/PET composites, the modulus predictions are close to the data for fiber volume fractions lower than 0.25.

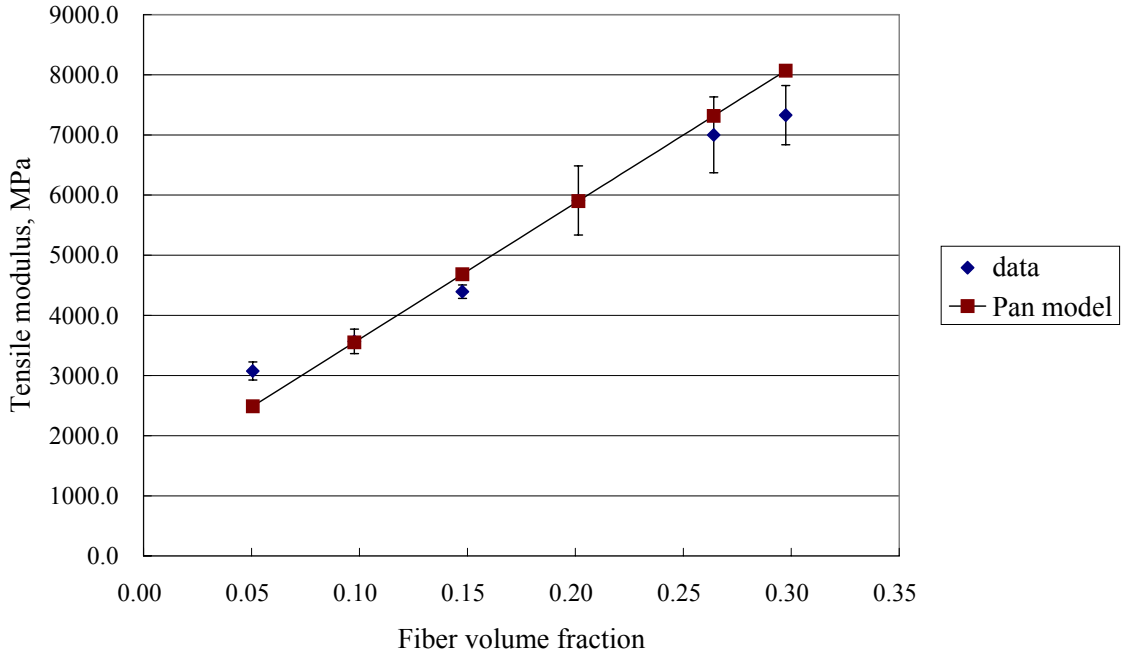

Figure 5.8 Tensile modulus vs. fiber volume fraction for Glass/PP composites

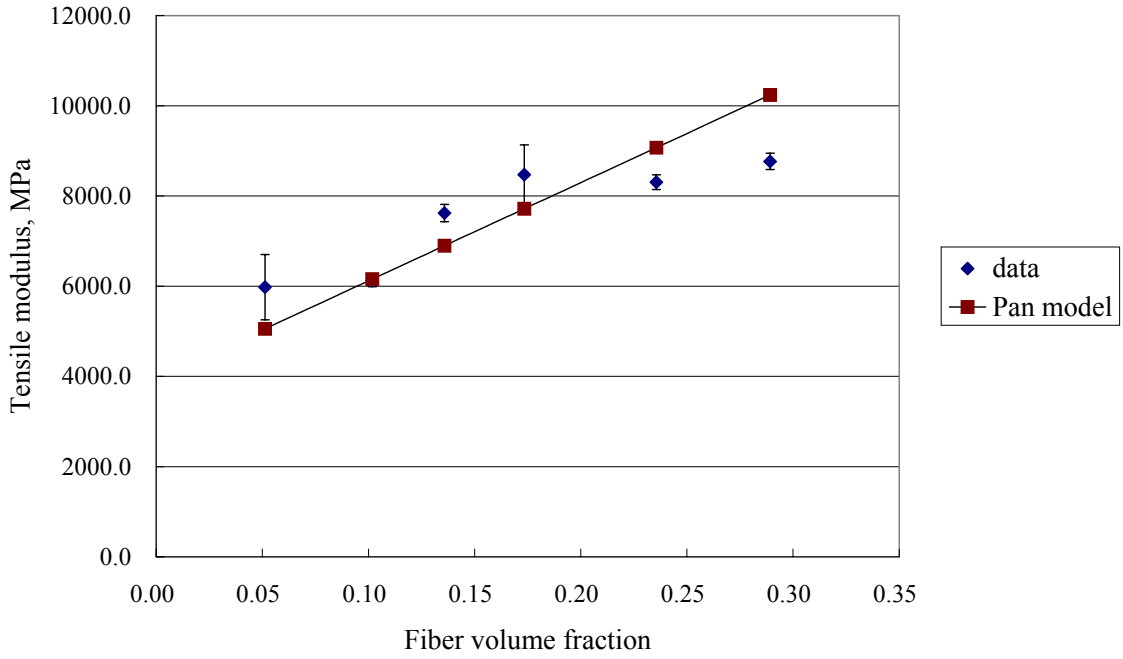

Figure 5.9 Tensile modulus vs. fiber volume fraction for Glass/PET composites

5.6 Some Remarks On the Models Predicting the Strength of Random Fiber Composites

Models that predict the tensile modulus of random discontinuous fiber reinforced composites have been examined. Only a few models that estimate the strength of random fiber composites have been examined. This is because the models that predict the strength of random fiber composites are difficult to apply. Usually data in addition to the basic properties of the fiber/resin and fiber volume fraction are required. For example, Chen's equation (Eq.(2.46)) requires that the longitudinal strength of the corresponding unidirectional composite and the shear and tensile strengths of the resin be measured. Also, the strength efficiency factor must be known. Hahn's ductile failure model (Eq.(2.53) to Eq.(2.55)) requires data on the on-axis longitudinal strength, on-axis transverse strength and on-axis shear strength of the corresponding unidirectional composite material. These data are not readily available, which was the case of the random fiber composites used in the present study. These drawbacks greatly reduce the practicality of the models.

5.7 Summary

Not all of the models reviewed in Chapter 2 were discussed in this section because they gave poor predictions of the properties of random fiber composites. The theories based on unidirectional composite properties in Section 2.3 give extremely high

predictions for the tensile modulus of random fiber composites. For Glass/PP, the calculated modulus is about 24 times higher than measured at 0.05 fiber volume fraction and about 200 times higher at 0.50 fiber volume fraction. This is understandable since the models do not take into account any effects such as fiber/resin interaction, fiber length and fiber orientation. A model that can predict the properties of random fiber composites must consider these effects.

The models discussed in Chapter 2 predict that the moduli of random fiber composites increase linearly with the fiber volume fraction. Test results for both Glass/PP and Glass/PET composites show that this is not true for wetlay random fiber composites. The models also tend to predict moduli that are much higher than measured at fiber volume fractions above 0.25.

The model of Pan gave the best predictions of modulus for fiber volume fractions up to 0.30 for Glass/PP composites and 0.25 for Glass/PET composites. However, none of the models gave even close predictions of modulus for the wetlay random fiber composite at higher fiber volume fractions. The models do not explain why the modulus or strength of the random fiber composites reaches a maximum at a certain fiber volume fraction and then starts to decrease. The underlying reason for this phenomenon may be due to the interactions between fibers that outweigh the reinforcement effects of the fibers at high fiber volume fractions.

The models did not predict the properties of Glass/PET very well, even at low fiber volume fractions. Test results summarized in the Appendix A-D and Chapter 4 showed that the modulus and strength data for Glass/PET are lower than expected, possibly due to degradation of PET resin and poor bonding between the glass fiber and PET resin.

Chapter 6. Molding Parameters

In order to determine the effects that the molding parameters have on the mechanical properties of the composites, plaques molded under different processing conditions were tested. All the tensile test in this chapter followed the ASTM D 3069/D 3039M-95a standard. All the flexural test in this chapter followed the ASTM D790-98 standard. The parameters that were examined included set-point mold pressure, set-point mold temperature and cooling methods. The test procedures described in Chapter 3 were followed in the study discussed in this chapter. The raw material used in the investigation was Dupont SC125 Glass/PET (25% glass and 75% PET in weight fraction) thermoplastic sheet.

6.1 Effects of Mold Pressure

There are many molding parameters that will affect the final mechanical properties of the plaques molded from hot press. One of them is the set-point mold pressure. The pressure applied will determine how well the plaque is consolidated. If the pressure is too high, it will cause excessive resin flow and leakage from the mold. In order to determine the optimal pressure for the molding process, 7.62 cm by 7.62 cm (3 inch by 3 inch) composite plaques were consolidated at set-point mold pressures of 5.06 MPa, 6.75 MPa, 8.43 MPa and 10.12 MPa, respectively. Each of these plaques was cut into ten specimens 7.62 cm long by 1.27 cm wide for flexural testing. The 11.81

MPa pressure was tried once but caused excessive resin leakage. Hence, pressures of 11.81 MPa or higher are too high for the SC125 Glass/PET thermoplastic sheet.

A typical curve of molding pressure versus time for the 10.12 MPa set-point mold pressure is shown in Figure 6.1. Figure 6.2 shows the temperature process cycle for the 10.12 MPa set-point mold pressure. “Platen-T” refers to the temperature of the top platen of the hot-press, “Platen-B” refers to the temperature of the bottom platen and “MoldTemp” represents the mold temperature.

The tests results are plotted in Figure 6.3 and Figure 6.4. Figure 6.3 shows the flexural moduli of plaques molded with different set-point molding pressures. Figure 6.4 shows the flexural strengths of plaques molded with different set-point molding pressures.

The results show that the set-point mold pressure does not significantly affect the flexural modulus or strength. For example, there was about a 6.8% increase in the flexural modulus when the pressure is doubled from 5.06 MPa to 10.12 MPa. Therefore, it is reasonable to assume that a set-point mold pressure between 5.06 MPa and 10.12 MPa will result in fully consolidated plaques and acceptable mechanical properties.

On the other hand, a set-point mold pressure of 11.81 MPa was too high for the SC125 material. The maximum consolidation pressure will be between 10.12 MPa and 11.81 MPa. A value of 5.06 MPa was selected as the consolidation pressure for the investigation in this study.

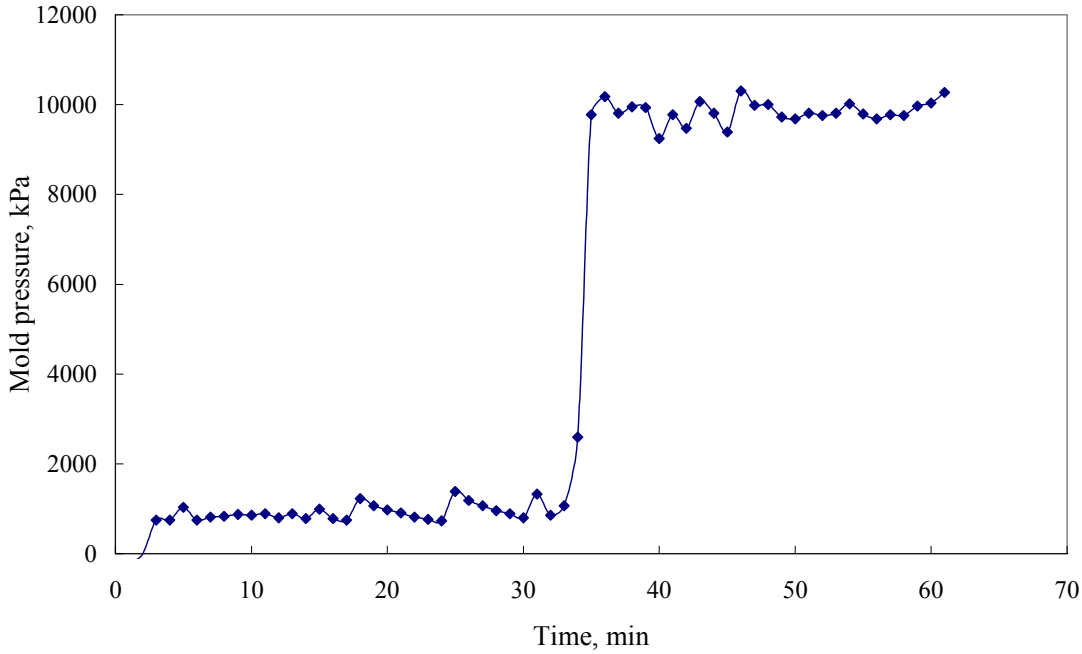

Figure 6.1 Molding pressure vs. time during a process under 10.12 MPa set-point mold pressure

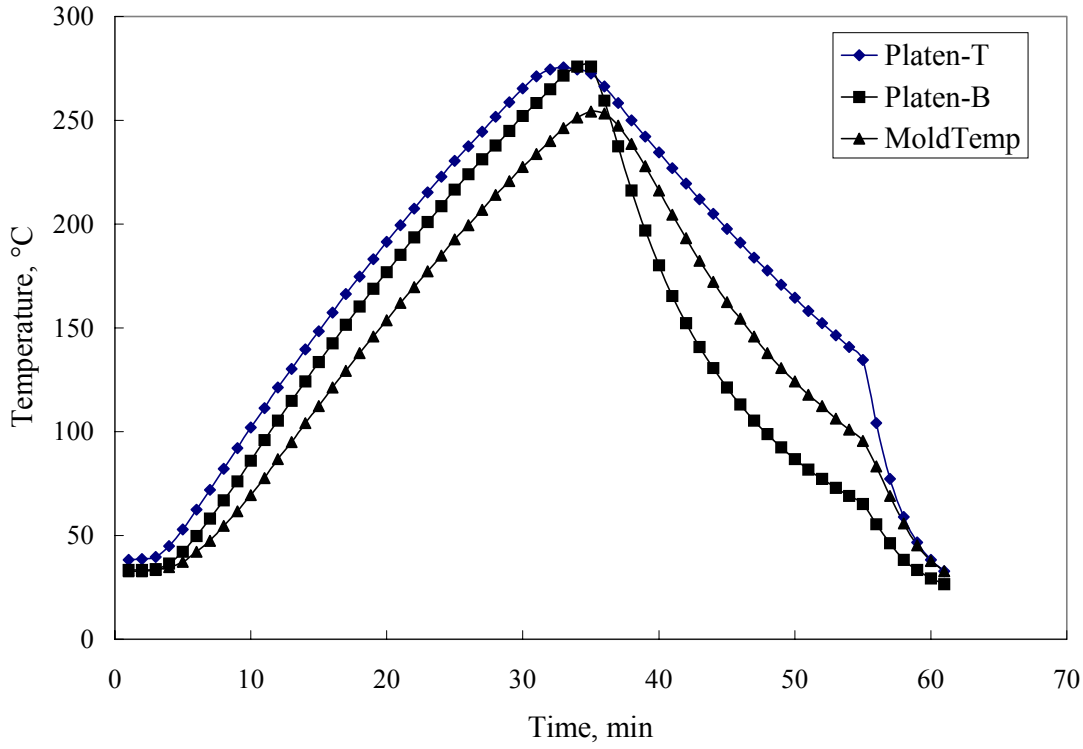

Figure 6.2 Temperatures vs. time during a process under 10.12 MPa set-point mold pressure

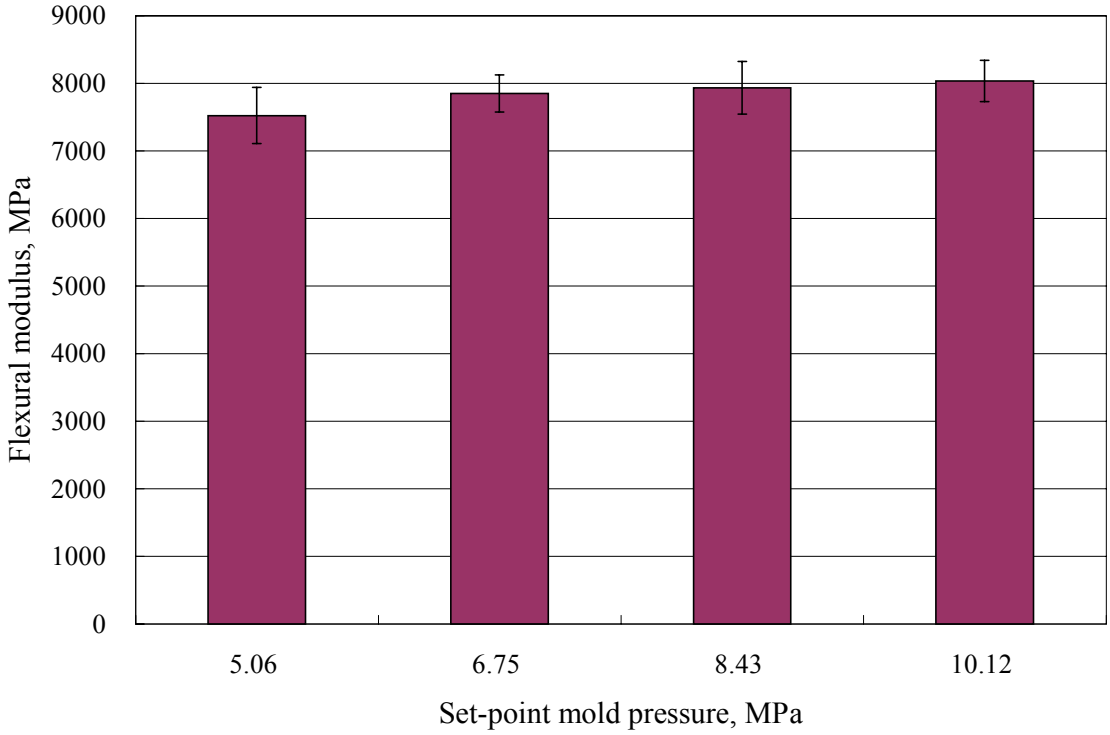

Figure 6.3 Flexural modulus vs. set-point mold pressure

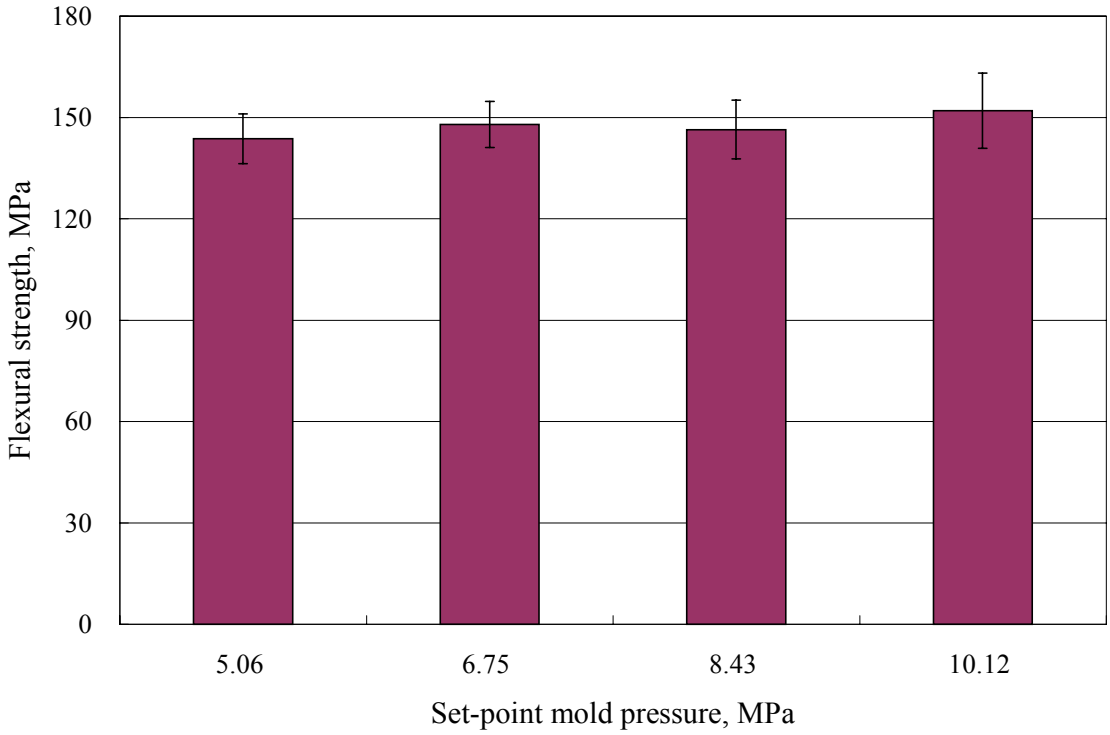

Figure 6.4 Flexural strength vs. set-point mold pressure

6.2 Effects of Mold Temperature

Plaques were molded with different set-point mold temperatures and a set-point molding pressure of 5.06 MPa. This was done to see how the variation of the set-point mold temperatures would affect the flexural modulus or strength of the composite. Figure 6.5 shows the change of mold pressure during a consolidation process with 250°C set-point mold temperature. For each set-point mold temperature, six specimens were tested in tensile and six in flexure. The tensile test results are shown in Figure 6.6 and Figure 6.7. The flexural tests results are shown in Figure 6.8 and Figure 6.9.

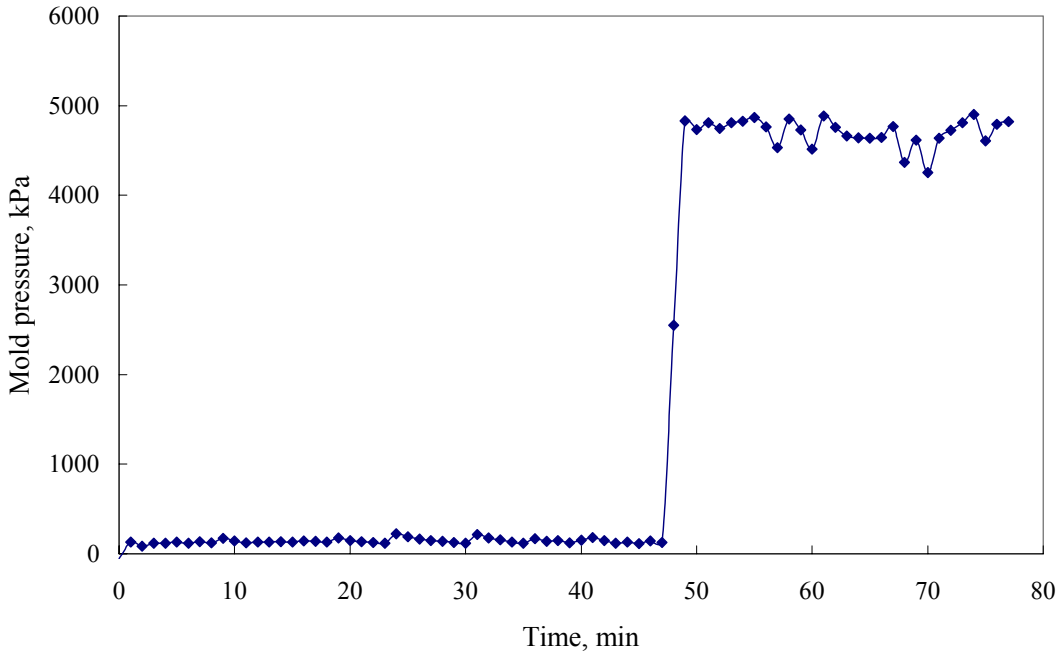

Figure 6.5 Mold pressure vs. time during a process with 250°C set-point mold temperature

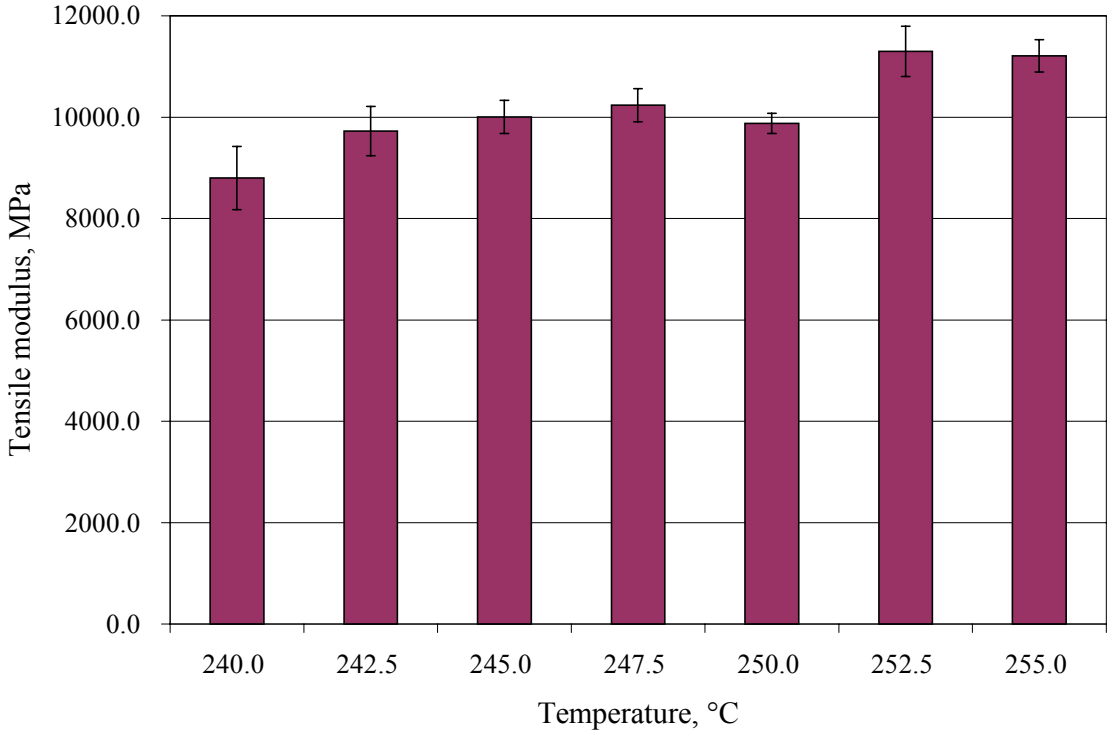

Figure 6.6 Tensile modulus vs. set-point mold temperature

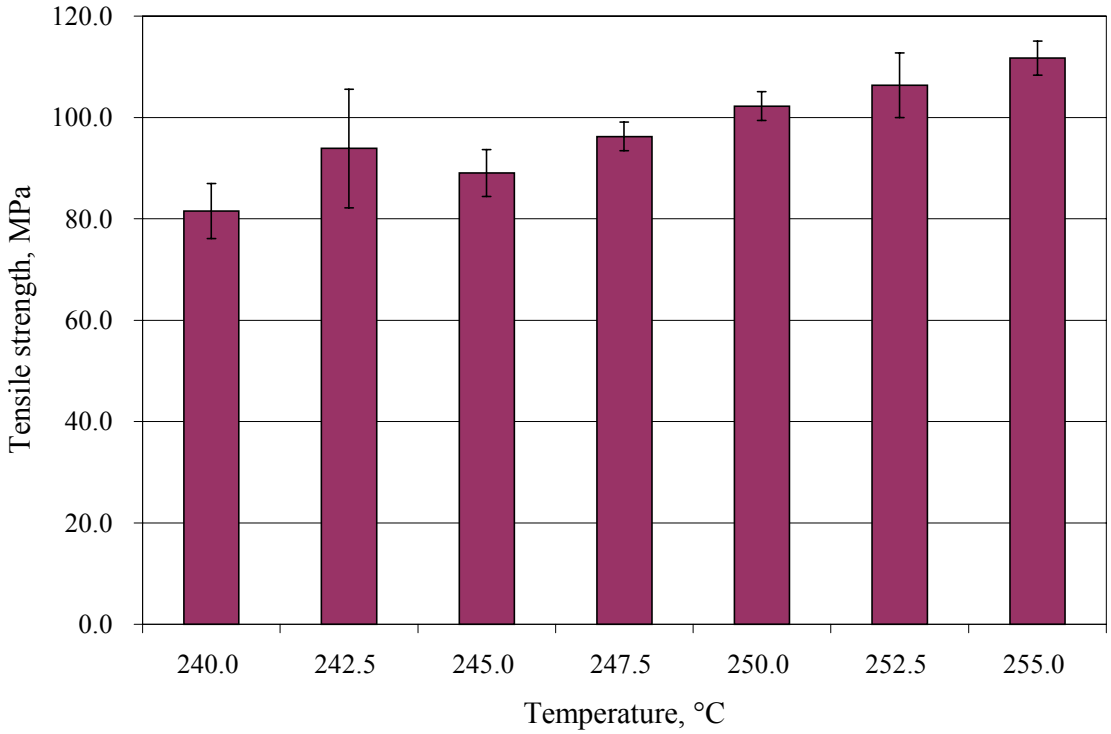

Figure 6.7 Tensile strength vs. set-point mold temperature

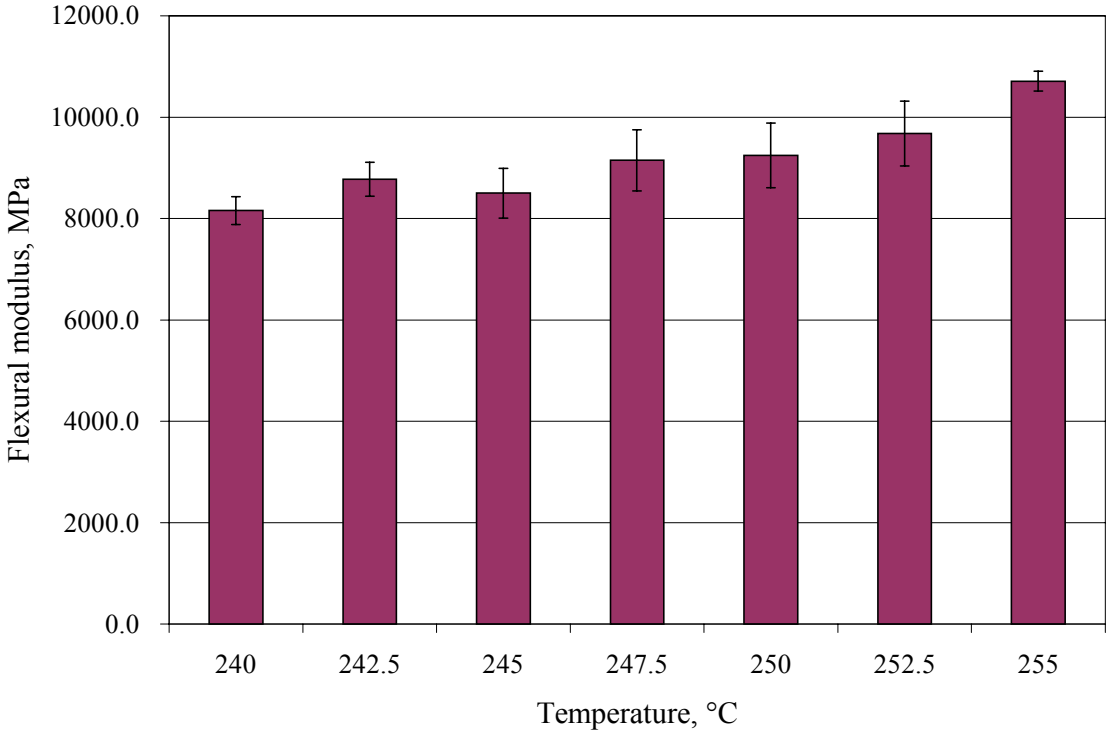

Figure 6.8 Flexural modulus vs. set-point mold temperature

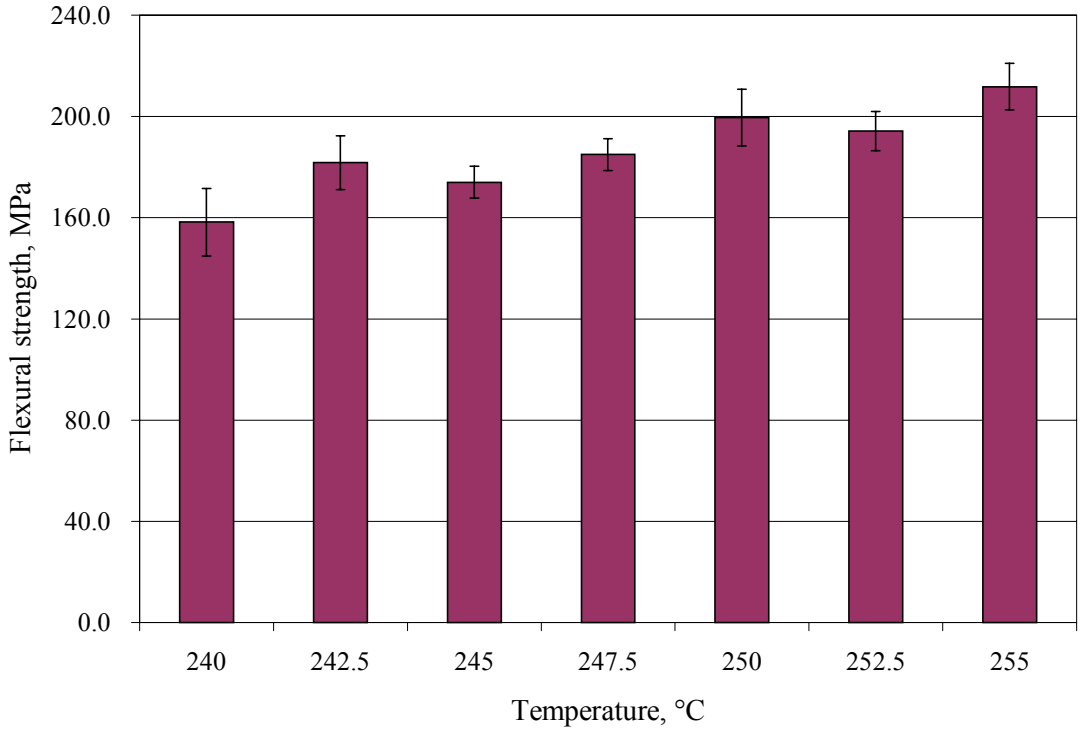

Figure 6.9 Flexural strength vs. set-point mold temperature

Both the tensile modulus and tensile strength increase as the set-point mold temperature increases. However, 255°C is not necessarily the best set-point mold temperature. The data in Table 6.1 show that at set-point mold temperatures of 252.5°C and 255°C, the weight yield percents of molded plaques are only 82.39% and 78.08%, respectively. Therefore, 252.5°C and 255°C may be too high to be used as set-point mold temperatures since there is too much weight loss due to the excessive resin flow. The resin loss will result in an increase in fiber volume fraction. So, eventually it is the increase of fiber volume fraction rather than the set-point mold temperature that causes the increase of the tensile modulus or strength of the composite.

Table 6.1 Weight yield percent under different set-point mold temperatures

Weight yield percent	Temperature, °C
98.12%	240
94.25%	242.5
91.09%	245
90.95%	247.5
94.84%	250
82.39%	252.5
78.08%	255

A set-point mold temperature of 250°C gives a very high weight yield percent of 94.84%. The maximum tensile strength is achieved at a set-point mold temperature of 250°C within the range of 240°C to 250°C. A relatively high tensile modulus is also achieved. Hence, a molding temperature of 250°C is considered as the optimal set-point mold temperature for the SC125 material among the temperature range studied.

The results of flexural tests also strongly indicate that 250°C is the optimal set-point mold temperature. As seen in Figure 6.8 and Figure 6.9, maximum values of both flexural modulus and flexural strength are achieved at a set-point mold temperature of

250°C without causing excessive resin loss. Again, it is reasonable to attribute the high modulus and strength at 252.5°C and 255°C to the actual increase of fiber volume fractions.

In summary, we conclude that 250°C is the optimal set-point mold temperature for the SC125 thermoplastic sheets.

6.3 Effects of Cooling Method

In Section 3.4 a typical molding process was presented. After the molding pressure is applied at the desired molding temperature, the heater is turned off and the cooling air is turned on to cool the mold down to 100°C. The cooling air is then stopped and cooling water is turned on to cool the mold to room temperature. This type of cooling method is referred as “normal cooling method”.

A question arises about the cooling method. Can other methods be used to yield better tensile or flexural properties of the composite? In order to find out the effects of the cooling method on the properties of the molded composite plaques, three other types of cooling were tried. These included water cooling, air cooling and natural cooling. For water cooling, the mold is cooled from the molding temperature to room temperature using only cooling water. For air cooling, only air is used to cool the mold to room temperature. As for the natural cooling, the mold is cooled slowly in ambient air. It requires about 9 hours for the mold temperature to drop down to room temperature. The mold and platen temperatures during a process cycle using the natural cooling method is shown in Figure 6.10, where “Platen-T”, “Platen-B” and “MoldTemp” have the same meaning as they do in Figure 6.2. Figure 6.11 displays the change of the mold pressure during a natural cooling process.

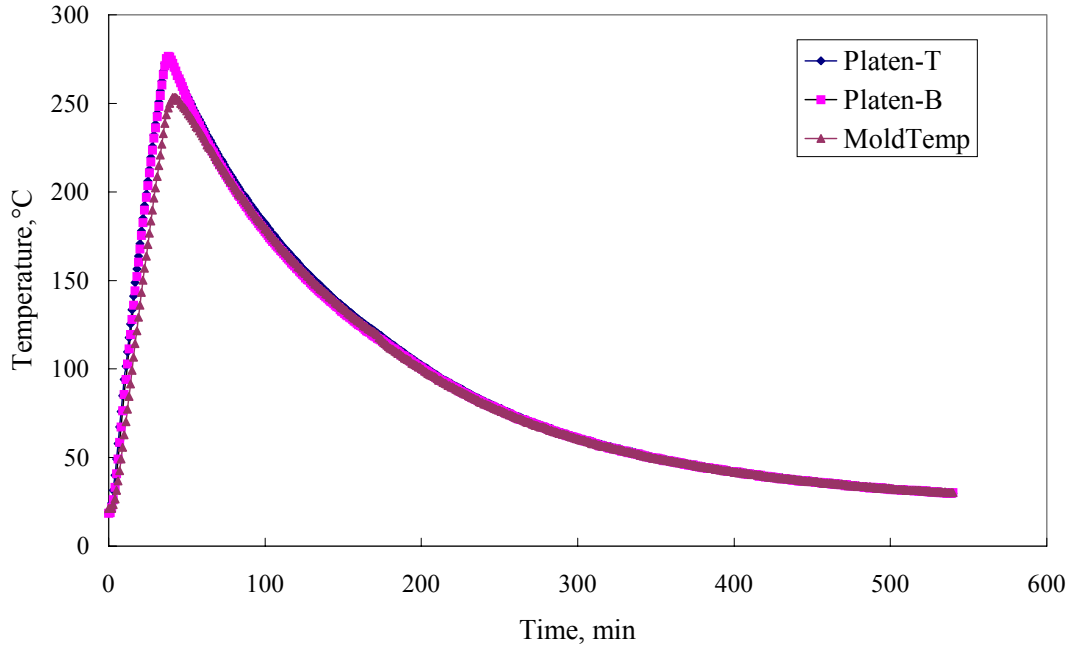

Figure 6.10 Mold temperatures vs. time during a natural cooling process

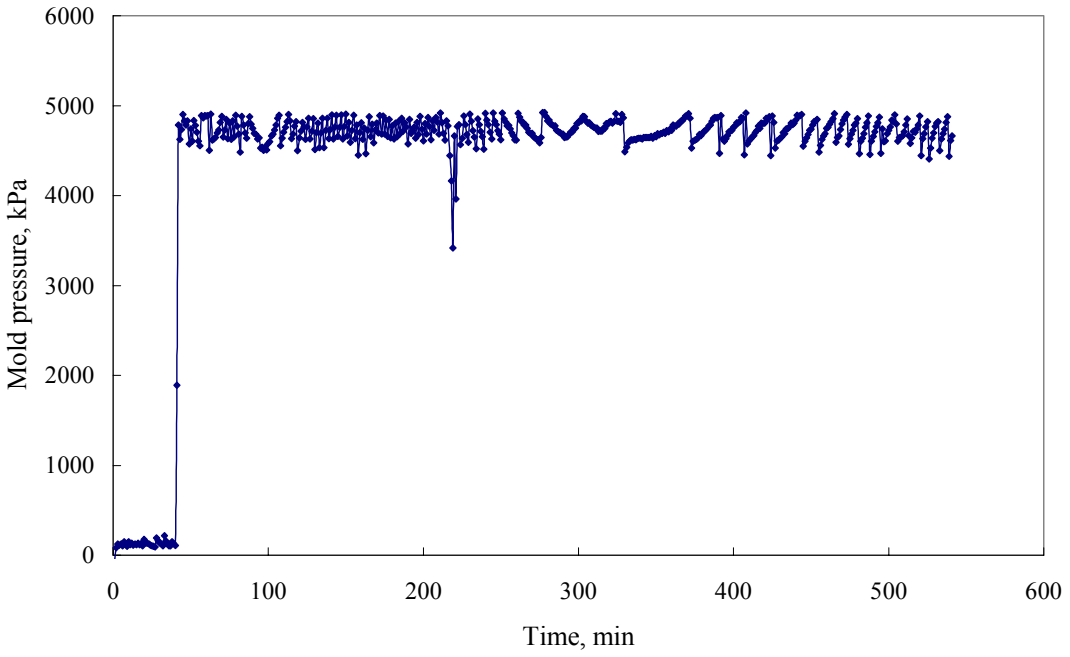

Figure 6.11 Mold pressure vs. time during a natural cooling process

Plaques were made under 5.06 MPa set-point mold pressure using these three different cooling methods. Specimens were cut from these plaques and tested. Six

specimens were tested in tensile and six in flexure. A set-point mold temperature of 250°C was used for all the cooling methods.

The tensile test results are shown in Figure 6.12 and Figure 6.13. Results of flexural tests are shown in Figure 6.14 and Figure 6.15.

From Figure 6.12 and Figure 6.13, it appears that water cooling gives the highest average tensile properties. However, there is a relatively high standard deviation in tensile modulus data of plaque molded using this cooling method.

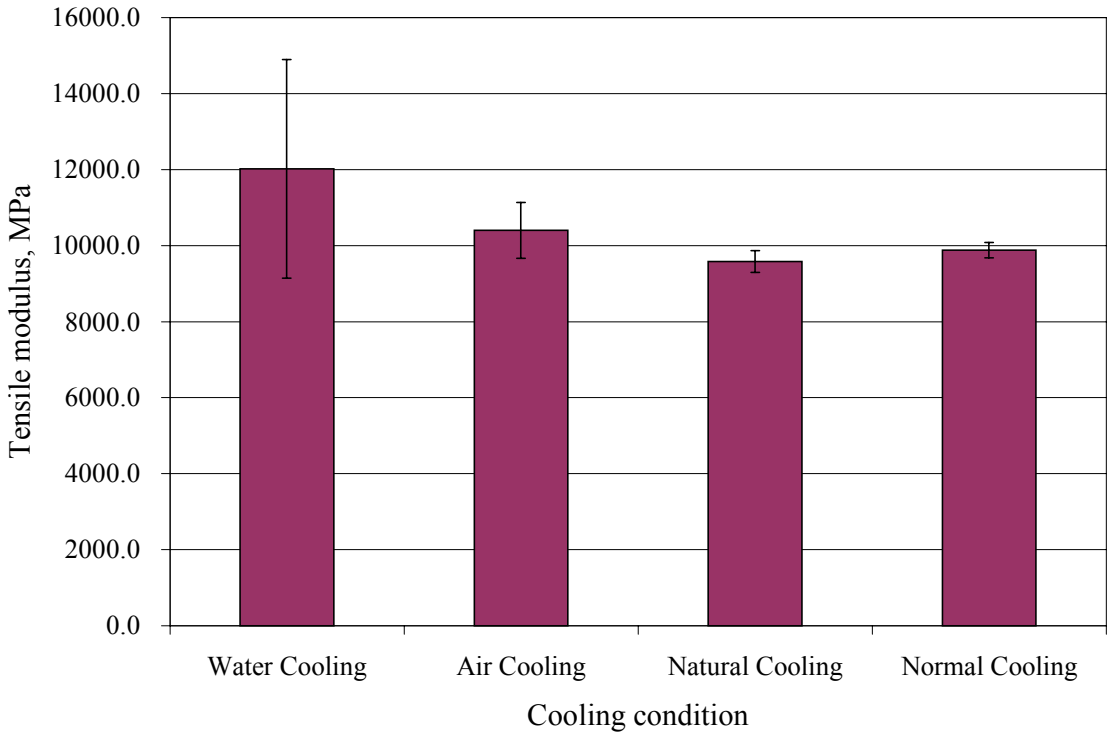

Figure 6.12 Tensile modulus vs. cooling methods

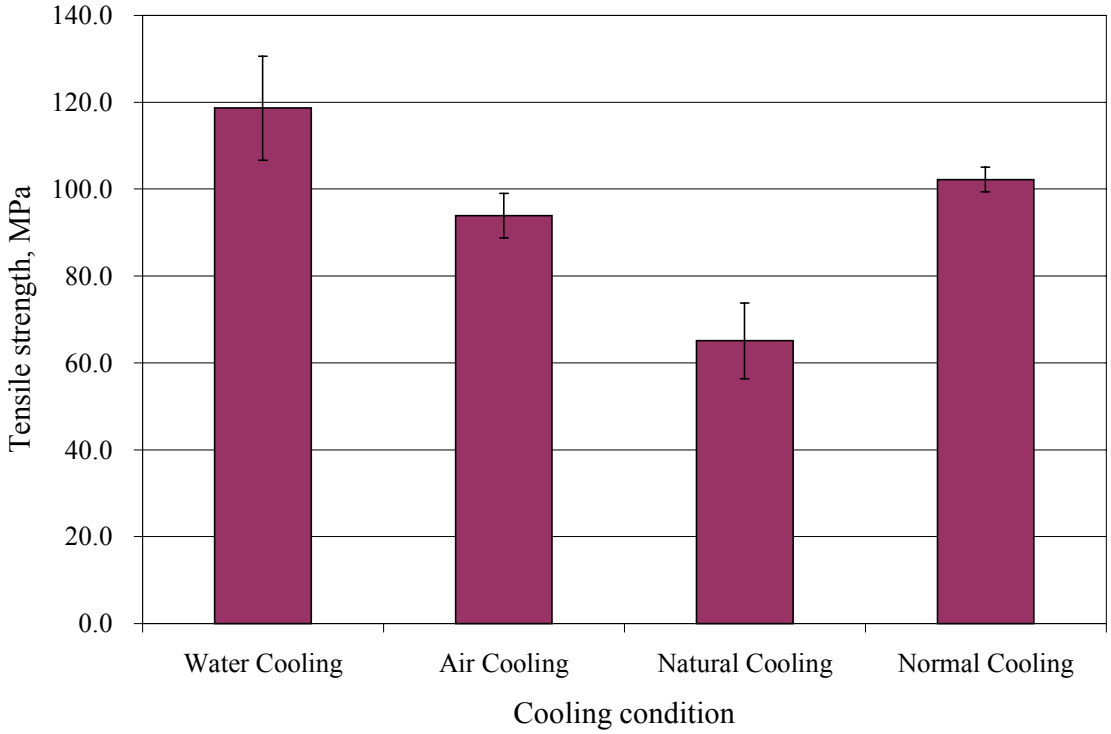

Figure 6.13 Tensile strength vs. cooling methods

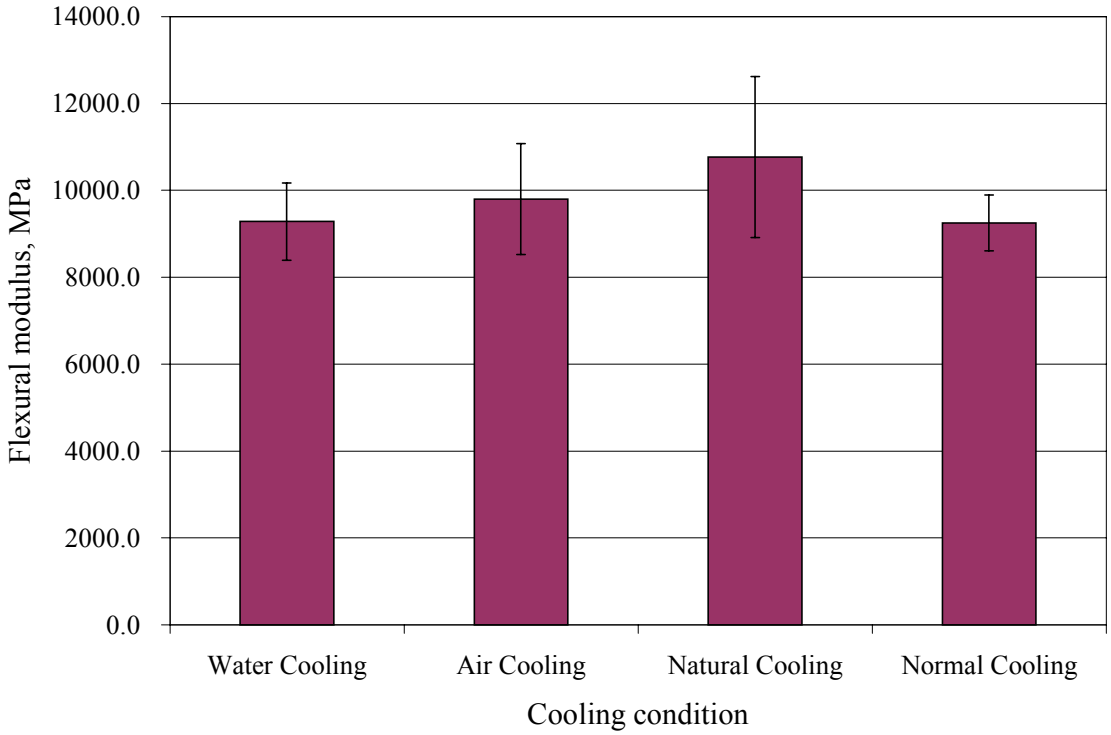

Figure 6.14 Flexural modulus vs. cooling method

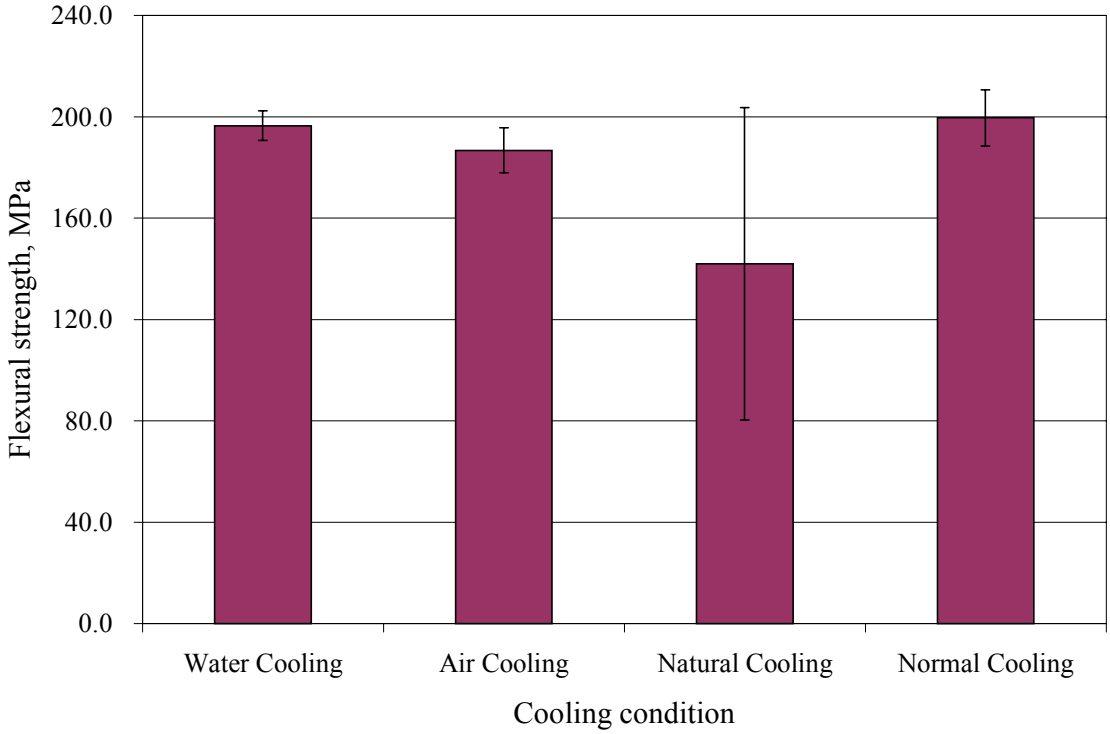

Figure 6.15 Flexural strength vs. cooling method

From Figure 6.12-Figure 6.15, it can be seen that the natural cooling method produces plaques that have the lowest properties (except for flexural modulus) among the four cooling methods. Also, it takes about five times longer time than the normal cooling method. Hence, natural cooling is not a good cooling method.

Water cooling yields the best tensile strength and modulus among these four cooling methods. However, there are some problems associated with this cooling method. Above 100°C, water exists in the form of vapor. When the cooling water is turned on to cool down the mold, the high temperature of the mold, as well as, the top and bottom platens (usually between 250 °C to 270°C) will quickly turn the water into vapor.

In summary, water cooling and air cooling can both be used as alternative methods to the normal cooling. However, the normal cooling method gives better dimensional consistency of the plaques than the other three cooling methods. Also, the properties

of plaques molded with normal cooling are very close to the properties of plaques molded using water or air cooling. Hence, unless the dimensional distortions associated with the water cooling or air cooling methods can be solved, normal cooling is still recommended for the molding process.

Chapter 7. Conclusions and Recommendations for Future Work

7.1 Conclusions from Present Work

The mechanical properties of the random fiber composites manufactured from the wetlay process were studied. The procedure of the wetlay process was introduced. Wetlay process is an efficient way to make preform random fiber composite sheets.

The molding parameters were investigated to find the optimal molding conditions. Set-point mold pressures of 5.06 MPa, 6.75 MPa, 8.43 MPa and 10.12 MPa were used. The flexural test results indicated that set-point mold pressure did not significantly affect the flexural modulus and strength of the composite. Any set-point mold pressure between 5.06 MPa and 10.12 MPa could make fully consolidated plaques. It was also found that set-point mold pressure higher than 11.81 MPa would cause excessive resin flow.

Set-point mold temperatures from 240°C to 255°C at an increment of 2.5°C were investigated. The tensile and flexural test results showed that 250°C was the optimal set-point mold temperature for the Dupont SC125 material. Plaques molded with 252.5°C and 255°C set-point mold temperatures had very low weight yield percentages due to resin loss.

Three other cooling methods in addition to the normal cooling method, namely, water cooling, air cooling and natural cooling were tried. It was found that the natural cooling was the worst cooling method. Plaques molded using water cooling method had the best tensile properties. Both water cooling and air cooling could be used as alternative methods to the normal cooling.

The tensile and flexural test results of both Glass/PP and Glass/PET composites were summarized in Appendix A-D and Chapter 4. For Glass/PP composite, the optimal fiber volume fraction at which the composite has the highest strength or stiffness was found to be 0.2 for both tensile and flexural strength, 0.3 for tensile modulus and 0.35 for flexural modulus. For Glass/PET composite, this value was about 0.3 for both tensile and flexural modulus, about 0.25 for tensile strength and about 0.2 for flexural strength.

Plaques of Carbon/PET composites were also molded and tested. The test results were much higher compared with Glass/PET composite at similar fiber volume fractions. Tensile and flexural tests were done on the PET resin. It was found that the strength of the PET was lower than data reported in the literature, which was an indication of possible degradation of the resin. Micrographs of selected Glass/PET specimens showed the existence of voids. The void content had a tendency to increase with the increasing of fiber volume fraction. A possible explanation for this is that the surface treatment of the glass fiber used in this study made it difficult to achieve good bonding between the glass fiber and PET resin.

Some micromechanics models that predict the modulus or strength of random fiber composite were reviewed in chapter 2. Evaluation of these models was done in Chapter 5. Predictions from some of the models were compared with test data. The models that predict the strength of random fiber composites usually can not be applied readily because extra data such as longitudinal strength of the corresponding

unidirectional composites and the shear and tensile strength of the resin must be known. For random fiber composites, these data are not available. In this sense the strength models are restricted to the theoretical lever.

For the tensile modulus, although some theories gave good predictions at low fiber volume fractions, no theory could fit the test data well at high fiber volume fractions. None of the models could predict that the properties of the random fiber composites decrease after reaching a maximum, which may be due to the interactions between fibers at high fiber volume fractions that resulted in the poor dispersion of the fibers or the development of voids in the composites.

7.2 Future Work

In the present study only two types of fiber, namely, glass fiber and carbon fiber and two types of resin, namely, PP and PET were used. Many other fibers and matrix materials are suitable for the wetly process. Better mechanical properties can be obtained when new combination of fiber/resin is used. For the same type of fiber, different fiber length can be tried to investigate the effect of fiber length on the properties of the random fiber composites.

The mold used in this study had problem of resin leakage when high pressure is applied, as discussed in Chapter 6. Therefore, work can be carried out toward the new design of the mold so that higher pressure can be applied, which may result in the improvement in properties of plaques molded. Since the crystallinity of the resin affects the properties of the composite, the cooling rates associated with the normal, water and air cooling methods need to be investigated to see how the cooling rate affects the crystallinity of the resin.

More work need to be done to find a micromechanics model for the random fiber reinforced composites. Successful models were not found in the literature. Some initiatory study is expected to construct a model that can predict the decrease of modulus or strength of random fiber composites made from wetlay process at high fiber volume fractions.

Adjustments can be made to the headbox of the wetlay machine to produce oriented rather than random prepreg sheet. This will be a big extension for the types of material that can be manufactured from the wetlay process.

References

[1] Ashbee, K. H. G, “Fundamental principles of fiber reinforced composites”, Technomic Pub. Co., 1993.

[2] Peters, S. T., “Handbook of composites, 2nd edition”, Chapman & Hall, London; New York, 1998.

[3] Lubin, G., “Handbook of composites”, Van Nostrand Reinhold, New York, 1982.

[4] Weeks, G. P. and Geary, J. E., “Fiber reinforced porous sheets”, US patent 5,134,016, 1992.

[5] ASTM D 3039/D 3039M-95a: Standard test method for tensile properties of polymer matrix composite materials.

[6] ASTM D 790-98: Standard test method for flexural properties of unreinforced and reinforced plastics and electrical insulating materials.

[7] Ashton, J. E., Halpin, J. C. and Petit, P. H., “Primer on Composite Materials: Analysis”, Technomic Stamford, Conn. 1969.

[8] Halpin, J. C., “Stiffness and Expansion Estimates for Oriented Short Fiber Composites”, *Journal of Composite Materials*, vol. 3, 1969, p.732-734.

[9] Tucker III, C. L., and Liang, E., “Stiffness prediction for unidirectional short-fiber composites: Review and evaluation”, *Composites Science and Technology*, No. 59, 1999, p.655-671.

[10] Nielson, L. E., “Mechanical properties of polymer and composites”, vol. 2, New

York: Marcel Dekker, 1974.

[11] Cox, H. L., “The elasticity and strength of paper and other fibrous materials”, *British Journal of Applied Physics*, No. 3, 1952, p.72-79.

[12] Starink, M. J. and Syngellakis, S., “Shear lag model for discontinuous composite: fiber end stressed and weak interface layers”, *Material Science and Engineering*, A270, 1999, p.270-277.

[13] Loewenstein, K. L., “Composite Materials”, Holliday and Elsevier, New York, 1966.

[14] Tsai, S. W. and Pagano, J. J., “Composite Materials Workshop”, Technomic Stamford, Conn. 1968.

[15] Blumentritt, B. F., VU, B. T. and Cooper, S. L., “Mechanical properties of Discontinuous Fiber Reinforced Thermoplastics. II. Random-in-Plane Fiber Orientation”, *Polymer Engineering and Science*, Vol. 15, No. 6, 1975, p.428-436.

[16] Blumentritt, B. F., VU, B. T. and Cooper, S. L., “Mechanical properties of Oriented Discontinuous Fiber Reinforced Thermoplastics. I. Unidirectional Fiber Orientation”, *Polymer Engineering and Science*, Vol. 14, No. 9, 1974, p.633-640.

[17] Christensen, R. M. and Waals, F. M., “Effective Stiffness of Randomly Oriented Fiber Composites”, *Journal of Composite Materials*, Vol. 6, 1972, p. 518-532.

[18] Lee, L. H., “Strength-Composition Relationships of Random Short Glass Fiber-Thermoplastics Composites”, *Polymer Engineering and Science*, Vol. 9, 1969, p. 213-219.

[19] Manera, M., “Elastic properties of randomly oriented short fiber-glass composites”, *Journal of Composite Materials*, Vol. 11, 1977, p. 235-247.

[20] Tsai, S. W. and Pagano, N. J., “Invariant properties of composite materials”, Composite Materials Workshop, Technomic Publishing Co., Stamford, Conn. 1968, p.233-238.

[21] Pan, N., “The elastic constants of randomly oriented fiber composite: A new approach to prediction”, *Science and Engineering of composite materials*, Vol. 5, No.

2, 1996, p.63-72.

[22] Crutis, P. T., Bader, M. G. and Bailey, J. E., “The stiffness and strength of a polyamide thermoplastic reinforced with glass and carbon fibers”, *Journal of Material Science*, Vol. 13, 1978, p.377-390.

[23] Kelly, A. and Tyson, W. R., *Journal of Mechanics and Physics of Solids*, Vol. 13, 1965, p.329-336

[24] Peijs, T., Garkhail, S., Heijenrath, R., Oever, M. and Bos, H., “Thermoplastic composites based on flax fibers and polypropylene: Influence of fiber length and fiber volume fraction on mechanical properties”, Macromol. Symp. 127, 1998, p.193-203.

[25] Thompson, J. L., Vlug, M. A., Schipper, G. and Krikort, H.G.L.T., “Influence of fiber length and concentration on the properties of glass fiber-reinforced polypropylene: Part 3. Strength and strain at failure”, *Composites Part A*, Vol. 27A, 1996, p.1075-1084.

[26] Chen, P. E., “Strength Properties of Discontinuous Fiber Composites”, *Polymer Engineering and Science*, Vol. 11, No. 1, 1971, p.51-56.

[27] Baxter, W. J., “The strength of metal matrix composites reinforced with randomly oriented discontinuous fibers”, *Metallurgical Transactions A*, Vol. 23A, 1992, p.3045-3053.

[28] Hahn, H. T., “On Approximations for Strength of Random Fiber Composites”, *Journal of Composite Materials*, Vol. 9, 1975, p. 316-326.

[29] Kuriger, R. J. and Alam, M. K., “Strength Prediction of Partially Aligned Discontinuous Fiber-reinforced Composites”, *Journal of Material Response*, Vol. 16, No.1, 2001, p.226-232.

[30] Li, Y., Mai, Y. and Ye, L., “Sisal fiber and its composites: a review of recent developments”, *Composites science and technology*, Vol. 60, 2000, p. 2037-2055.

[31] Balasuriya, P. W., Ye, L. and Mai, Y., “Mechanical properties of wood flake-polyethylene composites. Part I: effects of processing methods and matrix melt flow behavior”, *Composites Part A*, Vol. 32, 2001, p. 619-629.

[32] Thomason, J. L. and Vlug, M. A., “Influence of fiber length and concentration on the properties of glass fiber-reinforced polypropylene: Part 1. Tensile and flexural modulus”, *Composites Part A*, Vol. 27A, 1996, p. 477-484.

[33] More information is available at URL: http://www.wetlay.vt.edu. Most of the pictures in this chapter are provided by the web master Joe Price-O'Brien.

[34] Scheinberg, S. P., “Wetlay process for manufacture of highly-oriented fibrous mats”, US patent 6,066,235, 1998.

[35] Published by Boedeker Plastics, Inc., the data is available at URL: http://www.boedeker.com/polyp_p.htm

[36] Published by Eastpoint Co., the data is available at URL: http://www.plasticsusa.com/pet.html

[37] “Modern plastics world encyclopedia 2000”, a Mcgraw-Hill Publication, 1999, p.A196-A200.

Appendix A

Tensile test results of Glass/PP composite

5V% Glass/PP Tensile test

Plaque No.	1071701300			1071701400		
Specimen No.	1	2	3	4	5	6
Width, mm	0.502	0.503	0.502	0.494	0.505	0.521
Depth, mm	0.163	0.164	0.165	0.160	0.162	0.162
Ultimate Strain, %	2.21	2.27	1.81	2.33	1.78	1.85
Ultimate Strength, MPa	35.82	39.47	37.48	42.20	34.67	37.62
Modulus of Elasticity, MPa	2968.40	3180.53	3216.48	2942.03	2906.91	3230.93

10V% Glass/PP Tensile test

Plaque No.	1071702300			1071702400		
Specimen No.	1	2	3	4	5	6
Width, mm	0.494	0.500	0.511	0.503	0.494	0.512
Depth, mm	0.139	0.141	0.138	0.143	0.146	0.146
Ultimate Strain, %	2.58	2.82	2.66	2.50	2.51	3.21
Ultimate Strength, MPa	52.91	52.01	53.17	54.33	55.02	57.70
Modulus of Elasticity, MPa	3645.67	3368.64	3347.02	3795.19	3793.46	3460.37

15V% Glass/PP Tensile test

Plaque No.	1071807100			1071807200		
Specimen No.	1	2	3	4	5	6
Width, mm	0.496	0.502	0.497	0.497	0.508	0.495
Depth, mm	0.132	0.130	0.130	0.131	0.133	0.133
Ultimate Strain, %	1.44	1.63	1.55	2.16	2.14	2.06
Ultimate Strength, MPa	45.86	48.81	45.51	62.49	61.22	60.14
Modulus of Elasticity, MPa	4539.69	4322.04	4222.08	4464.70	4406.21	4408.26

20V% Glass/PP Tensile test

Plaque No.	1071704100			1071704200		
Specimen No.	1	2	3	4	5	6
Width, mm	0.498	0.497	0.497	0.506	0.503	0.503
Depth, mm	0.125	0.126	0.127	0.120	0.122	0.122
Ultimate Strain, %	2.55	1.96	2.31	1.80	1.95	2.23
Ultimate Strength, MPa	79.50	79.48	84.01	88.69	86.65	88.50
Modulus of Elasticity, MPa	5014.00	5801.98	5607.77	6686.15	6233.33	6119.58

25V% Glass/PP Tensile test

Plaque No.	1071705100			1071705200		
Specimen No.	1	2	3	4	5	6
Width, mm	0.503	0.505	0.503	0.505	0.505	0.504
Depth, mm	0.117	0.118	0.117	0.116	0.118	0.119
Ultimate Strain, %	1.91	2.02	2.06	1.42	1.72	1.83
Ultimate Strength, MPa	76.30	78.00	82.32	83.48	86.16	84.15
Modulus of Elasticity, MPa	6471.75	6546.71	6451.97	8029.66	7355.10	7148.63

30V% Glass/PP Tensile test

Plaque No.	1071801100			1071801200		
Specimen No.	1	2	3	4	5	6
Width, mm	0.504	0.502	0.501	0.497	0.499	0.507
Depth, mm	0.116	0.120	0.117	0.125	0.126	0.126
Ultimate Strain, %	1.71	1.43	1.82	1.75	1.53	1.85
Ultimate Strength, MPa	82.60	77.02	83.84	71.56	68.83	71.24
Modulus of Elasticity, MPa	7815.12	7851.01	7650.83	6847.69	6900.94	6902.63

35V% Glass/PP Tensile test

Plaque No.	1071802100			1071802200		
Specimen No.	1	2	3	4	5	6
Width, mm	0.503	0.499	0.503	0.503	0.500	0.500
Depth, mm	0.121	0.122	0.124	0.128	0.128	0.130
Ultimate Strain, %	1.81	1.60	2.37	1.32	1.91	2.076
Ultimate Strength, MPa	67.08	67.22	71.79	57.38	65.27	66.96
Modulus of Elasticity, MPa	6650.39	7153.76	6781.62	6840.06	6692.16	6763.38

40V% Glass/PP Tensile test

Plaque No.	1071803100			1071803200		
Specimen No.	1	2	3	4	5	6
Width, mm	0.502	0.501	0.504	0.501	0.503	0.504
Depth, mm	0.127	0.129	0.130	0.128	0.128	0.130
Ultimate Strain, %	1.83	1.83	2.21	1.21	1.50	1.45
Ultimate Strength, MPa	62.92	64.02	71.37	56.24	59.43	53.96
Modulus of Elasticity, MPa	7001.79	6802.30	6930.90	6991.95	6863.60	6322.36

45V% Glass/PP Tensile test

Plaque No.	1071804100			1071804200		
Specimen No.	1	2	3	4	5	6
Width, mm	0.502	0.502	0.504	0.502	0.503	0.502
Depth, mm	0.128	0.130	0.130	0.129	0.130	0.132
Ultimate Strain, %	1.63	1.40	1.35	2.00	1.51	1.49
Ultimate Strength, MPa	51.54	52.76	52.96	44.47	44.21	41.71
Modulus of Elasticity, MPa	6353.41	6611.20	6372.96	5516.81	5610.20	5691.46

50V% Glass/PP Tensile test

Plaque No.	1071805100			1071805200		
Specimen No.	1	2	3	4	5	6
Width, mm	0.501	0.503	0.502	0.501	0.503	0.502
Depth, mm	0.132	0.132	0.134	0.127	0.127	0.127
Ultimate Strain, %	1.43	1.17	1.37	1.35	1.03	0.93
Ultimate Strength, MPa	48.87	48.33	49.13	52.96	51.34	47.87
Modulus of Elasticity, MPa	6251.71	6322.98	6085.27	6708.09	6965.34	6611.14

Summary of tensile test results of Glass/PP

		Strength, MPa		Modulus, MPa	
Object VF	Actual VF	Average	Standard Deviation	Average	Standard Deviation
0.05	0.05	37.88	2.68	3074.21	150.17
0.1	0.10	54.19	2.02	3568.39	204.28
0.15	0.15	54.01	8.09	4393.83	110.73
0.2	0.20	84.47	4.21	5910.47	575.62
0.25	0.26	81.73	3.80	7000.64	631.39
0.3	0.30	75.85	6.32	7328.04	491.74
0.35	0.36	65.95	4.73	6813.56	179.63
0.4	0.39	61.32	6.24	6818.82	254.86
0.45	0.44	47.94	5.03	6026.01	472.04
0.5	0.49	49.75	1.98	6490.76	327.62

Appendix B

Tensile test results of Glass/PET composite

5V% **Glass/PET** **Tensile test**

Plaque No.	1052301100			1052301400		
Specimen No.	1	2	3	4	5	6
Width, mm	0.503	0.502	0.503	0.503	0.503	0.502
Depth, mm	0.100	0.100	0.097	0.138	0.137	0.143
Ultimate Strain, %	0.75	0.55	0.60	0.47	0.42	0.46
Ultimate Strength, MPa	34.88	30.59	28.33	24.63	22.28	23.49
Modulus of Elasticity, MPa	6669.00	6722.85	6539.31	5288.08	5418.63	5090.69

10V% **Glass/PET** **Tensile test**

Plaque No.	1052302100			1052302200		
Specimen No.	1	2	3	4	5	6
Width, mm	0.501	0.502	0.504	0.502	0.502	0.504
Depth, mm	0.126	0.125	0.120	0.117	0.115	0.118
Ultimate Strain, %	2.48	2.51	2.46	2.52	2.58	2.64
Ultimate Strength, MPa	54.31	53.49	54.97	59.63	57.00	56.22
Modulus of Elasticity, MPa	6177.21	5913.76	6210.23	6279.13	6246.25	6055.34

15V% Glass/PET Tensile test

Plaque No.	1052303100			1052303200		
Specimen No.	1	2	3	4	5	6
Width, mm	0.502	0.503	0.504	0.502	0.502	0.502
Depth, mm	0.107	0.108	0.107	0.124	0.124	0.124
Ultimate Strain, %	2.15	2.26	2.15	1.95	2.46	2.51
Ultimate Strength, MPa	72.43	73.73	72.91	75.40	82.58	81.28
Modulus of Elasticity, MPa	7685.67	7554.76	7737.20	7897.83	7552.52	7327.96

20V% Glass/PET Tensile test

Plaque No.	1052304100			1052304200		
Specimen No.	1	2	3	4	5	6
Width, mm	0.502	0.507	0.503	0.502	0.504	0.504
Depth, mm	0.118	0.116	0.117	0.127	0.128	0.115
Ultimate Strain, %	1.60	1.84	1.66	1.23	1.56	1.73
Ultimate Strength, MPa	91.63	97.05	88.74	68.95	73.86	83.68
Modulus of Elasticity, MPa	9313.73	8899.58	8821.19	7693.21	7735.06	8373.17

25V% Glass/PET Tensile test

Plaque No.	1052305100			1052305200		
Specimen No.	1	2	3	4	5	6
Width, mm	0.503	0.502	0.502	0.504	0.504	0.503
Depth, mm	0.106	0.112	0.106	0.121	0.121	0.119
Ultimate Strain, %	1.59	1.62	1.70	1.54	1.44	1.42
Ultimate Strength, MPa	89.23	87.75	94.00	87.86	82.60	82.49
Modulus of Elasticity, MPa	8297.21	8077.69	8475.41	8491.85	8314.6	8176.15

30V% **Glass/PET** **Tensile test**

Plaque No.	1052306100			1052306200		
Specimen No.	1	2	3	4	5	6
Width, mm	0.503	0.502	0.503	0.503	0.503	0.504
Depth, mm	0.120	0.116	0.117	0.118	0.118	0.117
Ultimate Strain, %	1.35	1.47	1.29	1.17	1.28	1.22
Ultimate Strength, MPa	88.40	89.68	83.47	76.67	83.64	83.04
Modulus of Elasticity, MPa	8860.36	8879.73	8598.38	8477.54	8882.52	8898.67

35V% **Glass/PET** **Tensile test**

Plaque No.	1052307100			1052307200		
Specimen No.	1	2	3	4	5	6
Width, mm	0.502	0.502	0.503	0.502	0.502	0.504
Depth, mm	0.122	0.122	0.121	0.130	0.132	0.134
Ultimate Strain, %	1.19	1.06	0.76	0.95	0.85	1.06
Ultimate Strength, MPa	65.63	63.59	54.50	58.52	59.06	65.41
Modulus of Elasticity, MPa	8534.70	7941.13	8706.45	7932.97	8869.65	8547.84

40V% **Glass/PET** **Tensile test**

Plaque No.	1052308100			1052308200		
Specimen No.	1	2	3	4	5	6
Width, mm	0.503	0.500	0.502	0.502	0.501	0.503
Depth, mm	0.139	0.133	0.133	0.132	0.132	0.133
Ultimate Strain, %	0.81	0.86	0.75	0.63	0.82	0.83
Ultimate Strength, MPa	44.72	47.34	44.20	38.08	46.54	44.16
Modulus of Elasticity, MPa	7263.10	7469.12	7356.36	7122.84	7361.72	6981.80

45V% **Glass/PET** **Tensile test**

Plaque No.	1052309100			1052309200		
Specimen No.	1	2	3	4	5	6
Width, mm	0.502	0.502	0.502	0.502	0.502	0.503
Depth, mm	0.140	0.140	0.140	0.138	0.138	0.139
Ultimate Strain, %	1.09	0.83	0.68	0.78	0.65	0.78
Ultimate Strength, MPa	43.36	39.80	35.62	41.95	40.54	45.58
Modulus of Elasticity, MPa	5934.87	6358.26	6283.05	6897.50	7208.15	7208.08

50V% **Glass/PET** **Tensile test**

Plaque No.	1052310100			1052310200		
Specimen No.	1	2	3	4	5	6
Width, mm	0.503	0.502	0.503	0.502	0.502	0.504
Depth, mm	0.150	0.149	0.147	0.142	0.140	0.142
Ultimate Strain, %	0.53	0.59	0.60	0.58	0.58	0.57
Ultimate Strength, MPa	21.63	27.04	27.97	22.32	25.78	23.28
Modulus of Elasticity, MPa	7261.96	4947.99	5212.67	4319.11	4806.01	4565.73

Summary of tensile test results of Glass/PET

		Strength, MPa		Modulus, MPa	
Object VF	Actual VF	Average	Standard Deviation	Average	Standard Deviation
0.05	0.05	27.37	4.82	5976.16	723.46
0.1	0.10	55.94	2.21	6123.54	134.60
0.15	0.14	76.39	4.43	7620.74	192.84
0.2	0.17	83.99	10.78	8472.66	659.18
0.25	0.24	87.32	4.34	8305.49	162.71
0.3	0.29	84.15	4.61	8766.20	181.28
0.35	0.35	61.12	4.46	8422.12	395.03
0.4	0.39	44.17	3.26	7259.16	178.65
0.45	0.45	41.14	3.40	6648.32	532.05
0.5	0.49	24.67	2.62	4692.37	318.21

Appendix C

Flexural test results of Glass/PP composite

5V% **Glass/PP** **Flexural test**

Plaque No.	1071701300				1071701400			
Specimen No.	1	2	3	4	5	6	7	8
Width, mm	0.502	0.497	0.501	0.499	0.528	0.512	0.497	0.497
Depth, mm	0.166	0.166	0.167	0.167	0.153	0.158	0.155	0.159
Ultimate Strain, %	3.25	4.71	2.65	4.19	6.44	3.56	7.09	3.55
Ultimate Strength, MPa	59.58	80.59	53.02	79.26	76.15	68.76	73.06	70.94
Modulus of Elasticity, MPa	2931.49	2739.97	2869.25	3026.63	2613.03	2996.67	2393.99	2935.70

10V% **Glass/PP** **Flexural test**

Plaque No.	1071702300				1071702400			
Specimen No.	1	2	3	4	5	6	7	8
Width, mm	0.498	0.500	0.503	0.493	0.512	0.504	0.499	0.503
Depth, mm	0.138	0.142	0.139	0.142	0.149	0.149	0.149	0.149
Ultimate Strain, %	6.20	5.58	5.70	5.56	5.39	5.40	5.09	5.11
Ultimate Strength, MPa	85.33	90.26	85.69	94.96	96.58	91.26	100.46	99.16
Modulus of Elasticity, MPa	2994.33	2924.99	3125.68	3030.45	3178.28	2932.48	3223.12	3361.00

15V% Glass/PP Flexural test

Plaque No.	1071807100				1071807200			
Specimen No.	1	2	3	4	5	6	7	8
Width, mm	0.501	0.501	0.504	0.503	0.504	0.501	0.504	0.500
Depth, mm	0.130	0.132	0.133	0.131	0.130	0.132	0.132	0.130
Ultimate Strain, %	3.65	4.08	3.54	3.85	3.45	4.18	4.07	4.33
Ultimate Strength, MPa	93.64	101.58	98.69	96.18	103.84	100.75	97.48	101.43
Modulus of Elasticity, MPa	4023.08	3982.88	4336.69	3906.70	4227.86	3889.37	3841.24	3981.63

20V% Glass/PP Flexural test

Plaque No.	1071704100				1071704200			
Specimen No.	1	2	3	4	5	6	7	8
Width, mm	0.502	0.505	0.505	0.504	0.505	0.503	0.505	0.500
Depth, mm	0.123	0.126	0.126	0.120	0.122	0.120	0.122	0.119
Ultimate Strain, %	3.58	3.59	3.76	3.44	3.52	3.42	3.67	3.43
Ultimate Strength, MPa	139.89	138.17	143.73	142.34	128.25	138.80	129.24	138.22
Modulus of Elasticity, MPa	5536.23	5550.28	5771.22	6091.99	5470.23	5980.10	5631.27	5588.02

25V% Glass/PP Flexural test

Plaque No.	1071705100				1071705200			
Specimen No.	1	2	3	4	5	6	7	8
Width, mm	0.504	0.506	0.499	0.502	0.508	0.505	0.503	0.499
Depth, mm	0.116	0.116	0.116	0.115	0.116	0.119	0.116	0.118
Ultimate Strain, %	3.30	3.38	2.90	2.92	3.02	3.06	3.26	3.16
Ultimate Strength, MPa	141.11	148.48	132.86	136.23	126.99	130.75	130.83	124.75
Modulus of Elasticity, MPa	6756.09	7132.84	6378.79	6352.08	6185.39	6169.16	6545.77	6059.22

30V% Glass/PP Flexural test

Plaque No.	1071801100				1071801200			
Specimen No.	1	2	3	4	5	6	7	8
Width, mm	0.503	0.505	0.501	0.502	0.501	0.497	0.497	0.501
Depth, mm	0.120	0.121	0.121	0.120	0.127	0.127	0.127	0.127
Ultimate Strain, %	2.83	3.00	3.18	2.76	2.71	2.38	2.73	2.98
Ultimate Strength, MPa	118.38	129.12	124.38	116.35	114.51	104.94	117.35	117.74
Modulus of Elasticity, MPa	6604.51	6871.85	6335.14	6252.95	6371.20	6125.07	6366.22	6369.16

35V% Glass/PP Flexural test

Plaque No.	1071802100				1071802200			
Specimen No.	1	2	3	4	5	6	7	8
Width, mm	0.502	0.503	0.503	0.505	0.502	0.504	0.505	0.502
Depth, mm	0.126	0.124	0.124	0.126	0.127	0.130	0.127	0.130
Ultimate Strain, %	3.55	2.65	2.87	2.69	2.81	2.62	2.80	3.27
Ultimate Strength, MPa	110.39	116.92	125.72	112.22	122.27	114.49	113.43	123.23
Modulus of Elasticity, MPa	6237.30	6995.93	7161.69	6940.51	6362.60	6643.60	6556.36	6424.68

40V% Glass/PP Flexural test

Plaque No.	1071803100				1071803200			
Specimen No.	1	2	3	4	5	6	7	8
Width, mm	0.504	0.505	0.501	0.503	0.504	0.506	0.503	0.502
Depth, mm	0.129	0.129	0.128	0.129	0.128	0.131	0.130	0.130
Ultimate Strain, %	2.33	2.58	2.65	2.56	2.39	2.78	2.70	2.07
Ultimate Strength, MPa	88.85	97.85	103.03	100.49	89.12	76.33	72.42	82.77
Modulus of Elasticity, MPa	6185.29	6203.33	6069.59	6016.15	5834.25	5163.64	5255.70	5461.66

45V% **Glass/PP** **Flexural test**

Plaque No.	1071804100				1071804200			
Specimen No.	1	2	3	4	5	6	7	8
Width, mm	0.501	0.501	0.504	0.503	0.504	0.503	0.500	0.498
Depth, mm	0.126	0.132	0.124	0.130	0.131	0.131	0.130	0.130
Ultimate Strain, %	2.12	2.55	4.14	3.00	2.13	2.86	2.67	2.92
Ultimate Strength, MPa	74.95	68.60	82.29	72.11	60.63	66.28	63.00	61.36
Modulus of Elasticity, MPa	5281.93	4797.31	6311.81	4966.68	4353.12	4418.28	4744.43	4950.70

50V% **Glass/PP** **Flexural test**

Plaque No.	1071805100				1071805200			
Specimen No.	1	2	3	4	5	6	7	8
Width, mm	0.502	0.502	0.502	0.502	0.503	0.502	0.503	0.503
Depth, mm	0.135	0.132	0.130	0.129	0.126	0.127	0.125	0.127
Ultimate Strain, %	2.03	3.77	2.20	2.41	2.62	2.51	1.86	2.72
Ultimate Strength, MPa	54.79	63.16	64.51	66.63	64.69	72.41	57.62	54.07
Modulus of Elasticity, MPa	4590.12	4881.02	5429.35	4636.46	5202.15	5911.04	5386.79	4352.57

Summary of flexural test results of Glass/PP

		Strength, MPa		Modulus, MPa	
Object VF	Actual VF	Average	Standard Deviation	Average	Standard Deviation
0.05	0.05	70.17	9.59	2822.13	224.71
0.1	0.10	92.96	5.77	3096.29	153.37
0.15	0.15	99.20	3.33	4023.68	172.42
0.2	0.20	137.33	5.66	5702.42	225.65
0.25	0.26	134.00	7.76	6447.42	355.64
0.3	0.30	117.85	7.07	6412.01	229.18
0.35	0.36	117.33	5.70	6665.33	333.06
0.4	0.39	88.86	11.22	5773.70	421.20
0.45	0.44	68.65	7.49	4978.03	616.82
0.5	0.49	62.24	6.31	5048.69	523.63

Appendix D

Flexural test results of Glass/PET composite

5V% **Glass/PET** **Flexural test**

Plaque No.	1052301100				1052301400			
Specimen No.	1	2	3	4	5	6	7	8
Width, mm	0.500	0.496	0.501	0.499	0.500	0.499	0.503	0.501
Depth, mm	0.097	0.130	0.098	0.131	0.138	0.144	0.137	0.146
Ultimate Strain, %	2.73	2.49	2.80	2.67	2.02	2.01	2.09	1.91
Ultimate Strength, MPa	78.89	68.09	77.01	70.49	61.42	59.88	57.81	59.99
Modulus of Elasticity, MPa	5122.47	5048.12	4763.63	5307.95	5495.33	5051.16	5029.32	2528.11

10V% **Glass/PET** **Flexural test**

Plaque No.	1052302100				1052302200			
Specimen No.	1	2	3	4	5	6	7	8
Width, mm	0.506	0.504	0.502	0.502	0.504	0.505	0.502	0.504
Depth, mm	0.124	0.121	0.120	0.123	0.115	0.109	0.115	0.109
Ultimate Strain, %	2.80	2.95	3.07	3.01	2.47	2.89	2.57	2.74
Ultimate Strength, MPa	98.05	104.28	108.90	109.04	92.02	104.89	98.85	106.14
Modulus of Elasticity, MPa	5298.62	5498.33	5569.03	5631.14	5458.63	5923.93	5484.32	6113.89

15V% **Glass/PET** **Flexural test**

Plaque No.	1052303100				1052303200			
Specimen No.	1	2	3	4	5	6	7	8
Width, mm	0.505	0.508	0.504	0.503	0.503	0.503	0.502	0.500
Depth, mm	0.108	0.120	0.118	0.105	0.120	0.127	0.120	0.127
Ultimate Strain, %	2.96	2.79	3.06	3.01	3.11	2.96	3.19	3.16
Ultimate Strength, MPa	150.78	132.44	136.79	140.70	139.50	142.84	138.84	150.75
Modulus of Elasticity, MPa	7997.21	8493.35	8914.26	7598.02	6264.82	7427.83	6359.38	6433.80

20V% **Glass/PET** **Flexural test**

Plaque No.	1052304100				1052304200			
Specimen No.	1	2	3	4	5	6	7	8
Width, mm	0.504	0.504	0.503	0.503	0.503	0.503	0.502	0.503
Depth, mm	0.126	0.114	0.126	0.113	0.127	0.117	0.117	0.127
Ultimate Strain, %	2.74	2.84	2.76	2.78	3.06	2.69	2.35	2.94
Ultimate Strength, MPa	151.33	163.14	150.28	166.19	163.01	170.33	154.53	143.28
Modulus of Elasticity, MPa	7868.95	6884.17	6570.44	7382.50	7359.06	6965.81	6481.32	6172.67

25V% **Glass/PET** **Flexural test**

Plaque No.	1052305100				1052305200			
Specimen No.	1	2	3	4	5	6	7	8
Width, mm	0.503	0.503	0.502	0.504	0.502	0.502	0.502	0.503
Depth, mm	0.117	0.106	0.117	0.107	0.113	0.120	0.113	0.120
Ultimate Strain, %	2.70	2.50	2.61	2.50	3.19	2.93	2.81	3.10
Ultimate Strength, MPa	160.12	162.52	172.76	164.19	139.79	135.72	146.01	153.52
Modulus of Elasticity, MPa	7916.16	7354.11	7710.72	8497.61	7438.38	7485.19	6606.72	6493.92

30V% **Glass/PET** **Flexural test**

Plaque No.	1052306100				1052306200			
Specimen No.	1	2	3	4	5	6	7	8
Width, mm	0.504	0.503	0.503	0.503	0.502	0.502	0.502	0.503
Depth, mm	0.110	0.117	0.110	0.117	0.110	0.116	0.109	0.115
Ultimate Strain, %	2.35	2.53	2.29	2.73	2.61	2.54	2.43	2.55
Ultimate Strength, MPa	125.31	139.85	128.38	149.10	122.58	117.64	117.22	131.61
Modulus of Elasticity, MPa	6653.67	8133.19	7645.88	8096.11	8331.47	8154.27	7866.33	8018.82

35V% **Glass/PET** **Flexural test**

Plaque No.	1052307100				1052307200			
Specimen No.	1	2	3	4	5	6	7	8
Width, mm	0.503	0.502	0.502	0.503	0.502	0.502	0.502	0.502
Depth, mm	0.135	0.119	0.120	0.132	0.125	0.131	0.124	0.131
Ultimate Strain, %	2.82	2.18	2.00	2.38	2.17	1.96	2.32	2.25
Ultimate Strength, MPa	91.57	108.08	93.90	95.05	96.57	97.71	123.53	108.82
Modulus of Elasticity, MPa	6093.50	7770.77	7954.83	6510.91	7849.66	7544.16	7854.03	7909.43

40V% **Glass/PET** **Flexural test**

Plaque No.	1052308100				1052308200			
Specimen No.	1	2	3	4	5	6	7	8
Width, mm	0.502	0.501	0.503	0.502	0.505	0.506	0.502	0.502
Depth, mm	0.131	0.136	0.134	0.136	0.136	0.133	0.138	0.135
Ultimate Strain, %	1.90	2.01	2.08	1.86	1.96	2.41	2.24	2.29
Ultimate Strength, MPa	69.86	62.11	68.60	63.90	58.50	76.96	49.86	71.17
Modulus of Elasticity, MPa	7588.82	6062.78	7365.68	7155.80	6657.21	6753.37	5311.91	6227.34

45V% **Glass/PET** **Flexural test**

Plaque No.	1052309100				1052309200			
Specimen No.	1	2	3	4	5	6	7	8
Width, mm	0.503	0.502	0.502	0.502	0.503	0.500	0.502	0.502
Depth, mm	0.141	0.140	0.138	0.140	0.127	0.137	0.137	0.124
Ultimate Strain, %	2.26	2.24	2.21	2.14	2.31	2.06	2.35	2.31
Ultimate Strength, MPa	55.02	57.39	55.62	52.96	83.96	60.79	61.40	89.72
Modulus of Elasticity, MPa	4988.14	6114.13	7716.00	4587.49	8664.47	6411.16	6602.32	8529.16

50V% **Glass/PET** **Flexural test**

Plaque No.	1052310100				1052310200			
Specimen No.	1	2	3	4	5	6	7	8
Width, mm	0.503	0.503	0.504	0.503	0.502	0.502	0.505	0.504
Depth, mm	0.139	0.152	0.138	0.154	0.139	0.160	0.141	0.155
Ultimate Strain, %	2.00	2.48	2.25	2.41	2.44	2.69	2.12	2.81
Ultimate Strength, MPa	52.26	36.04	59.48	41.00	54.71	26.03	44.45	26.31
Modulus of Elasticity, MPa	5527.14	3830.73	6730.40	4643.13	5593.04	3093.41	5387.91	3059.86

Summary of flexural test results of Glass/PET

		Strength, MPa		Modulus, MPa	
Object VF	Actual VF	Average	Standard Deviation	Average	Standard Deviation
0.05	0.05	66.70	8.19	4793.26	940.00
0.1	0.10	102.77	5.96	5622.24	267.67
0.15	0.14	141.58	6.43	7436.08	1012.75
0.2	0.17	157.76	9.28	6960.62	556.84
0.25	0.24	154.33	12.90	7437.85	656.55
0.3	0.29	128.96	11.03	7862.47	529.90
0.35	0.35	101.90	10.81	7435.91	719.23
0.4	0.39	65.12	8.44	6640.36	753.41
0.45	0.45	64.61	14.09	6701.61	1515.00
0.5	0.49	42.54	12.61	4733.20	1314.68

Appendix E

Tensile and flexural test results of PET resin

Tensile test

Specimen No.	1	2	3	4	5
Width, mm	13.040	13.110	13.040	12.990	13.030
Depth, mm	3.270	3.250	3.250	3.180	3.300
Ultimate Strain, %	0.17	0.26	0.37	0.28	0.57
Ultimate Strength, MPa	7.08	10.36	15.68	10.79	22.44
Modulus of Elasticity, MPa	3956.76	3833.08	4207.03	3714.24	3972.03

Flexural test

Specimen No.	1	2	3	4	5	6
Width, mm	13.49	12.93	12.87	12.75	12.64	13.10
Depth, mm	3.24	3.23	3.30	3.25	3.29	3.32
Ultimate Strain, %	1.59	1.57	1.55	1.60	1.78	1.61
Ultimate Strength, MPa	42.76	43.23	30.70	45.40	51.94	46.18
Modulus of Elasticity, MPa	3723.64	3607.41	3398.46	4059.64	3947.41	3563.93

Vita

Yunkai Lu was born in Shenyang, a city in the northeastern part of China, on September 15, 1975. After high school, he entered Tsinghua University, Beijing, China. He completed his B.S. degree majoring in Engineering Mechanics in July 1999. Upon graduation, he enrolled in the M.S. program in department of Engineering Science & Mechanics at Virginia Tech. He completed his master degree in August 2002.